

ISSN 1881-7815 Online ISSN 1881-7823

BST

BioScience Trends

Volume 7, Number 3
June, 2013



www.biosciencetrends.com

BST

BioScience Trends



ISSN: 1881-7815
Online ISSN: 1881-7823
CODEN: BTIRCZ
Issues/Year: 6
Language: English
Publisher: IACMHR Co., Ltd.

BioScience Trends is one of a series of peer-reviewed journals of the International Research and Cooperation Association for Bio & Socio-Sciences Advancement (IRCA-BSSA) Group and is published bimonthly by the International Advancement Center for Medicine & Health Research Co., Ltd. (IACMHR Co., Ltd.) and supported by the IRCA-BSSA and Shandong University China-Japan Cooperation Center for Drug Discovery & Screening (SDU-DDSC).

BioScience Trends devotes to publishing the latest and most exciting advances in scientific research. Articles cover fields of life science such as biochemistry, molecular biology, clinical research, public health, medical care system, and social science in order to encourage cooperation and exchange among scientists and clinical researchers.

BioScience Trends publishes Original Articles, Brief Reports, Reviews, Policy Forum articles, Case Reports, News, and Letters on all aspects of the field of life science. All contributions should seek to promote international collaboration.

Editorial Board

Editor-in-Chief:

Masatoshi MAKUUCHI
Japanese Red Cross Medical Center, Tokyo, Japan

Co-Editors-in-Chief:

Xue-Tao CAO
Chinese Academy of Medical Sciences, Beijing, China
Rajendra PRASAD
UP Rural Institute of Medical Sciences & Research, Uttar Pradesh, India
Arthur D. RIGGS
Beckman Research Institute of the City of Hope, Duarte, CA, USA

Chief Director & Executive Editor:

Wei TANG
The University of Tokyo, Tokyo, Japan

Managing Editor:

Munehiro NAKATA
Tokai University, Hiratsuka, Japan

Senior Editors:

Xunjia CHENG
Fudan University, Shanghai, China
Yoko FUJITA-YAMAGUCHI
Tokai University, Hiratsuka, Japan
Na HE
Fudan University, Shanghai, China
Kiyoshi KITAMURA
The University of Tokyo, Tokyo, Japan

Misao MATSUSHITA
Tokai University, Hiratsuka, Japan
Takashi SEKINE
The University of Tokyo, Tokyo, Japan
Yasuhiko SUGAWARA
The University of Tokyo, Tokyo, Japan

Web Editor:

Yu CHEN
The University of Tokyo, Tokyo, Japan

Proofreaders:

Curtis BENTLEY
Roswell, GA, USA
Christopher HOLMES
The University of Tokyo, Tokyo, Japan
Thomas R. LEBON
Los Angeles Trade Technical College, Los Angeles, CA, USA

Editorial Office

Pearl City Koishikawa 603,
2-4-5 Kasuga, Bunkyo-ku,
Tokyo 112-0003, Japan
Tel: +81-3-5840-8764
Fax: +81-3-5840-8765
E-mail: office@biosciencetrends.com

BioScience Trends

Editorial and Head Office

Pearl City Koishikawa 603, 2-4-5 Kasuga, Bunkyo-ku,
Tokyo 112-0003, Japan

Tel: +81-3-5840-8764, Fax: +81-3-5840-8765
E-mail: office@biosciencetrends.com
URL: www.biosciencetrends.com

Editorial Board Members

Girdhar G. AGARWAL (Lucknow, India)	Takahiro HIGASHI (Tokyo, Japan)	Miho OBA (Odawara, Japan)	John TERMINI (Duarte, CA, USA)
Hirotsugu AIGA (Geneva, Switzerland)	De-Xing HOU (Kagoshima, Japan)	Xianjun QU (Ji'nan, China)	Usa C. THISYAKORN (Bangkok, Thailand)
Hidechika AKASHI (Tokyo, Japan)	Sheng-Tao HOU (Ottawa, Canada)	John J. ROSSI (Duarte, CA, USA)	Toshifumi TSUKAHARA (Nomi, Japan)
Moazzam ALI (Geneva, Switzerland)	Yong HUANG (Ji'ning, China)	Carlos SAINZ-FERNANDEZ (Santander, Spain)	Kohjiro UEKI (Tokyo, Japan)
Ping AO (Shanghai, China)	Hirofumi INAGAKI (Tokyo, Japan)	Yoshihiro SAKAMOTO (Tokyo, Japan)	Masahiro UMEZAKI (Tokyo, Japan)
Michael E. BARISH (Duarte, CA, USA)	Masamine JIMBA (Tokyo, Japan)	Erin SATO (Shizuoka, Japan)	Junming WANG (Jackson, MS, USA)
Boon-Huat BAY (Singapore, Singapore)	Kimitaka KAGA (Tokyo, Japan)	Takehito SATO (Isehara, Japan)	Ling WANG (Shanghai, China)
Yasumasa BESSHO (Nara, Japan)	Ichiro KAI (Tokyo, Japan)	Akihito SHIMAZU (Tokyo, Japan)	Xiang-Dong Wang (Boston, MA, USA)
Generoso BEVILACQUA (Pisa, Italy)	Kazuhiro KAKIMOTO (Osaka, Japan)	Zhifeng SHAO (Shanghai, China)	Hisashi WATANABE (Tokyo, Japan)
Shiuan CHEN (Duarte, CA, USA)	Kiyoko KAMIBEPPU (Tokyo, Japan)	Ri SHO (Yamagata, Japan)	Lingzhong XU (Ji'nan, China)
Yuan CHEN (Duarte, CA, USA)	Haidong KAN (Shanghai, China)	Judith SINGER-SAM (Duarte, CA, USA)	Masatake YAMAUCHI (Chiba, Japan)
Naoshi DOHMAE (Wako, Japan)	Bok-Luel LEE (Busan, Korea)	Raj K. SINGH (Dehradun, India)	George W-C. YIP (Singapore, Singapore)
Zhen FAN (Houston, TX, USA)	Mingjie LI (St. Louis, MO, USA)	Junko SUGAMA (Kanazawa, Japan)	Benny C-Y ZEE (Hong Kong, China)
Ding-Zhi FANG (Chengdu, China)	Ren-Jang LIN (Duarte, CA, USA)	Hiroshi TACHIBANA (Isehara, Japan)	Xiaomei ZHU (Seattle, WA, USA)
Yoshiharu FUKUDA (Ube, Japan)	Daru LU (Shanghai, China)	Tomoko TAKAMURA (Tokyo, Japan)	(as of June 2013)
Rajiv GARG (Lucknow, India)	Duan MA (Shanghai, China)	Tadatoshi TAKAYAMA (Tokyo, Japan)	
Ravindra K. GARG (Lucknow, India)	Yutaka MATSUYAMA (Tokyo, Japan)	Shin'ichi TAKEDA (Tokyo, Japan)	
Makoto GOTO (Tokyo, Japan)	Qingyue MENG (Beijing, China)	Sumihito TAMURA (Tokyo, Japan)	
Demin HAN (Beijing, China)	Mark MEUTH (Sheffield, UK)	Puay Hoon TAN (Singapore, Singapore)	
David M. HELFMAN (Daejeon, Korea)	Satoko NAGATA (Tokyo, Japan)	Koji TANAKA (Tsu, Japan)	

Review

- 113 - 121 **Methicillin-resistant *Staphylococcus aureus* antibiotic resistance and virulence.**
Jufeng Xia, Jianjun Gao, Norihiro Kokudo, Kiyoshi Hasegawa, Wei Tang

Original Articles

- 122 - 128 **Factors affecting patient delay of diagnosis and completion of Direct Observation Therapy, Short-course (DOTS) among the migrant population in Shandong, China.**
Ruoyan Gai Tobe, Lingzhong Xu, Chengchao Zhou, Qing Yuan, Hong Geng, Xingzhou Wang
- 129 - 137 **A recombinant protein containing highly conserved hemagglutinin residues 81-122 of influenza H5N1 induces strong humoral and mucosal immune responses.**
Ye Li, Lanying Du, Hongjie Qiu, Guangyu Zhao, Lili Wang, Yusen Zhou, Shibo Jiang, Jimin Gao
- 138 - 143 **Glucose administration during volume resuscitation using dextran-40 from hemorrhagic shock ameliorates acid/base-imbalance in fasted rats under sevoflurane anesthesia.**
Gaku Kawamura, Takayuki Kitamura, Kanako Sato, Rui Sato, Yoshiteru Mori, Yuko Araki, Yoshitsugu Yamada
- 144 - 151 **Label-free quantification proteomics reveals novel calcium binding proteins in matrix vesicles isolated from mineralizing Saos-2 cells.**
Xiaoying Zhou, Yazhou Cui, Jing Luan, Xiaoyan Zhou, Genglin Zhang, Xiumei Zhang, Jinxiang Han
- 152 - 156 **Aberrant expression of Notch3 predicts poor survival for hepatocellular carcinomas.**
Lei Hu, Feng Xue, Minhua Shao, Anmei Deng, Gongtian Wei

Commentary

- 157 - 158 **Perspectives on human clinical trials of therapies using iPS cells in Japan: Reaching the forefront of stem-cell therapies.**
Peipei Song, Yoshinori Inagaki, Yasuhiko Sugawara, Norihiro Kokudo

CONTENTS

(Continued)

Guide for Authors

Copyright

Review

DOI: 10.5582/bst.2013.v7.3.113

Methicillin-resistant *Staphylococcus aureus* antibiotic resistance and virulence

Jufeng Xia, Jianjun Gao, Norihiro Kokudo, Kiyoshi Hasegawa, Wei Tang*

Hepato-Biliary-Pancreatic Surgery Division, Department of Surgery, Graduate School of Medicine, The University of Tokyo, Tokyo, Japan.

Summary

Methicillin-resistant *Staphylococcus aureus* (MRSA) is one of the most critical causes of healthcare-related or community-related infections. Resistance to most β -lactam antibiotics makes MRSA a big threat to clinical treatment. Utilization of low efficiency antibiotics such as vancomycin and teicoplanin makes new choices for therapies. Recently, much research has shed light on relevance between genetic mutations of MRSA and clinical characteristics such as antibiotic resistance, and virulence. These findings could contribute to development of novel antibiotics and vaccines.

Keywords: *Staphylococcus aureus*, antibiotic resistance, virulence, mutation, biofilm

1. Introduction

It has been fifty two years since the first methicillin-resistant *Staphylococcus aureus* (MRSA) was isolated by Patricia Jevons, only two years after the premier clinical utility of the antibiotic methicillin (1). MRSA is one of the most parlous pathogens, responsible for a great number of human infections all around the world (2-5) (Figure 1). From the 1980s, new strains of MRSA emerged which led to continuous pandemic infections of MRSA around the world. At present, many countries report that MRSA strains account for about 25-50% of infectious *Staphylococcus aureus* in hospitals (6). In contrast, some other countries such as some northern European countries have lower MRSA infection rate (often < 1%), most probably due to strict search-and-destroy and surveillance measures, as well as control in antibiotic prescriptions. Recently, a Japanese study suggests that antibiotic consumption without restraint leads to increased MRSA virulence with time (7).

MRSA can produce a series of toxins and present multiple resistance to antibiotics. Most of these functions

are derived from mobile genetic elements (MGEs) on the genome (8,9). Resistance to methicillin primarily stems from acquisition of the *mecA* gene, not inherently existent in this strain, which produces a modified penicillin-binding protein (PBP2a) with lower affinity to β -lactams (10). Lately, MRSA which is negative for *mecA* has been discovered in human populations in the UK. The new diverse *mecA* was about 70% homologous to *Staphylococcus aureus mecA* (11). The continuous emergence of mutations of key genes makes it more difficult to prevent and control MRSA.

While for a long time MRSA infections were detected in hospitals (healthcare-acquired/associated-MRSA, HA-MRSA), however, in the recent decade infections have appeared in community (community-acquired/associated-MRSA, CA-MRSA) and also derived from livestock (livestock-associated-MRSA, LA-MRSA). Thus, MRSA can not only be taken as a hospital-associated problem, but also a society wide problem. This review will give an overview over the genome structure, pathogen and molecular biological characteristics of MRSA, and vaccines. Through this analysis, a light may be shed on the future prevention and control of MRSA.

2. Genome structure of MRSA

The *Staphylococcus aureus* genome was sequenced in detail recently (12). In the last period of time, there have been many related sequencing results released on

*Address correspondence to:

Dr. Wei Tang, Hepato-Biliary-Pancreatic Surgery Division, Department of Surgery, Graduate School of Medicine, The University of Tokyo, 7-3-1 Hongo, Bunkyo-ku, Tokyo 113-8655, Japan.
E-mail: tang-sur@h.u-tokyo.ac.jp

Ratio	East Asia	Southeast Asia	Middle East	West Europe	North Europe	North America	South America	Australia	Africa
>50%									
25-50%									
10-25%									
5-10%									
<5%									

Figure 1. Worldwide prevalence of hospital-acquired methicillin-resistant *Staphylococcus aureus*. Epidemiological data from various health agencies and medical laboratories of different countries showed that the epidemiological situations of MRSA were much different in different countries and regions. The situation was rather severe in East Asia, Southeast Asia, North America, and South America. In the same region, different countries have different situations. In East Asia, prevalence rates in Japan and Korea are more than 50%, while those in the rest countries are about 25-50%. In Southeast Asia, prevalence rates in Indonesia and Singapore are 25-50% and those in the rest countries are more than 50%. In West Europe, Great Britain, Spain, Portugal, and Italy have a prevalence of 25-50%, and the rest are 10-25%. In North America, Canada is 5-10%, Mexico is 10-25%, Alaska of America is 25-50%, and the other states of America are more than 50%. In South America, Paraguay, Panama, and Columbia have a prevalence of 25-50%, while the rest countries are more than 50%. In Africa, data only represents the prevalence in North Africa and South Africa since the epidemiological data of Middle Africa is absent.

the NCBI website. Making a comprehensive survey of the great amount of sequencing data, three major points were revealed: *i*) there is a backbone of core genes which comprises about 97% of all the genes and is highly conserved; *ii*) except for backbone genes, there is a set of over 700 genes, named core variable (CV) genes which defines the *Staphylococcus aureus* lineage by various distribution patterns in the genome; *iii*) a group of mobile genetic elements (MGEs) genes exist discretely in the genome which can move around within the genome and play a critical role in the spread of virulence factors (13-16) (Table 1). CV genes have a major function in encoding surface proteins and structures which can interact with human genes and their regulators (14).

At present, *Staphylococcus aureus* is classified based on clonal complexes (CCs) via multilocus sequence typing (MLST), for example, CC1, CC5, and CC10. The MLST method is used to sequence seven conserved genes and allocate a sequence type (ST) number to a validated strain (17). One CC type can be subtyped into several different STs by single nucleotide polymorphisms (SNPs) on the seven house-keeping genes.

MGEs can be defined as a kind of fragments of DNA which transfer into the host cell to replicate or integrate into host DNA. The antibiotic resistance and virulence of *Staphylococcus aureus* are acquired from MGEs (18). Horizontal gene transfer (HGT) of these MGEs leads to higher invasiveness, virulence, anti-microbial resistance and host adaptation, but each MGE can only transfer into certain lineages not all lineages.

Various types of MGEs have been identified in *Staphylococcus aureus*: plasmids, *Staphylococcus aureus* pathogenicity islands, bacteriophages, transposons,

staphylococcal cassette chromosome mec (SCCmec), and genomic islands (19). Among these, the most important MGEs for *Staphylococcus aureus* are the methicillin resistance gene *mecA* on the different SCCmec, the bacteriophages produced Pantone-Valentine leukocidin (PVL) toxin, and many resistance elements encoded by plasmids and transposons (20). MGEs in *Staphylococcus aureus* can largely strengthen the pathogenic and resistance ability of this strain. It has been reported that MGEs are able to transfer, lose, and/or acquisition among different strains (14).

HGT is limited among various lineages by the *hsdS* gene. Different lineages have different *hsdS* genes which have different DNA modification and digestion sites. As a result, the lineage can recognize domestic DNA and destroy alien DNA (21). The *hsdS* genes could play a role of biomarker to differentiate different lineages (22).

3. Present pathogenic characteristic of MRSA

3.1. HA-MRSA

3.1.1. Antibiotic resistance

From a clinical standpoint, a critical situation that surgeons have to confront when treating *Staphylococcus aureus* infections is antibiotic resistance. Resistance to the first antibiotic, penicillin, occurred in the 1940s (23). In 1942, a penicillin-resistant *Staphylococcus aureus* strain was successfully found (24). Intrinsically, an enzyme called penicillinase caused the resistance to penicillin (25). Penicillinase cuts the β -lactam ring which is a core of β -lactam antibiotics such as penicillin and its derivatives. At present, most

Table 1. Mobile genetic elements (MGEs) validated in *Staphylococcus aureus*

MGE	Description	Instances	Reference
Bacteriophages toxins	Lysogenic phage carry toxin genes that can enhance the virulence of the bacterial host	<i>Staphylococcal</i> enterotoxin A (SEA), chemotaxis inhibitory protein (CHIP) staphylokinase , PVL Staphylococcal complement inhibitor (SCIN)	(13,15,19)
Pathogenicity islands	A distinct class of genomic islands acquired by microorganisms through horizontal gene transfer	Encode TSST, MDR transporters, superantigens (SEB, SEC), fusidic acid-resistant genes	(13,15,19)
Plasmids and transposons	Plasmids and transposons carry antibiotic, heavy metal and disinfectant resistance determinants, toxins, arginine metabolism	Plasmids: several resistance determinants such as resistance of <i>blaZ</i> , <i>blaI</i> , and <i>blaR1</i> toβ-lactam antibiotics Transposons: Tn552 carries <i>bla</i> for penicillinase	(13,15,18,20)
Staphylococcal cassette chromosome <i>mec</i> (<i>SCCmec</i>)	A mobile genetic element that carries the central determinant for broad-spectrum beta-lactam resistance encoded by the <i>mecA</i> gene	<i>SCCmec</i> types I–XI	(13,15,16,19)
genoms	A part of a genome that has evidence of horizontal origins, involving in pathogenesis	Three families: vSAα, vSAβ, vSAγ. Containing genes encoding phenol-soluble modulins (PSMs), responsible for pro-inflammatory activity, enterotoxins and bacteriocin production	(13,15,17,19)

infectious *Staphylococcus aureus* strains own resistance to penicillin and its derivatives. To resolve the dilemma with penicillin-resistant *Staphylococcus aureus*, methicillin was developed which stemmed from penicillin but can avoid penicillinase cleavage. Methicillin was used in the clinic in 1959; but just one year later, a methicillin-resistant strain was detected in the UK (26). Unfortunately, the mechanism of methicillin resistance protects *Staphylococcus aureus* from the whole group of β-lactam antibiotics including penicillins, cephalosporins and carbapenems. In recent times, many MRSA strains have acquired resistance to multiple antibiotics, such as ciprofloxacin, clindamycin, tetracycline, erythromycin, and so on. (27). A recent research result from the CDC of the US confirms this and shows resistance to tetracycline and clindamycin in 9% and 6.2% of strains respectively among 823 infectious strains lately isolated (28). Furthermore, these strains contain transferable antibiotic-resistant plasmids.

Until now, the clinical therapy of MRSA infection mainly depends on utility of the glycopeptides vancomycin and teicoplanin, although at the same time many others are also employed, such as co-trimoxazole, tetracyclines, clindamycin, fusidic acid, linezolid, daptomycin, tigecycline, telavancin, and ceftaroline. For decades, glycopeptides, especially vancomycin, have been considered as the gold standard for therapy of MRSA infections until the appearance of resistance to these antibiotics in enterococci and subsequently in *Staphylococcus aureus* were found (29,30). In enterococci, glycopeptide resistance is due to mutation of the terminal alanine in the operons which promote the transferable cell wall-producing gene transcript and

causes the glycopeptides to be off target. In the recent decade, the so-called VISA (vancomycin-intermediate *Staphylococcus aureus*) strains have attracted more attention in which minimum inhibitory concentrations (MICs) of vancomycin are ≥ 4 mg/L, and the strains, so-called hVISA strains, with vancomycin MICs are ≤ 2 mg/L that show heteroresistance. These strains always lead to a large amount of glycopeptide treatment failure in the clinic (31,32). van Hal *et al.* summarizes that the treatment failure rate of hVISA infection is 2.5-fold higher than vancomycin-susceptible *Staphylococcus aureus* (33). These strains can cause prolonged bacteraemia for the mutations in the *agr* system which show decreased toxin generation and slow down virulence being examined in animal models (34,35). Moreover, a mutation in *stp1* which encodes a serine/threonine phosphatase was reported to increase vancomycin resistance and decrease virulence (36). However, the relevance between vancomycin treatment failure and *agr* dysfunction is still in the dark, although a study indicated that *agr* dysfunction was related to a worse clinical treatment effect (37).

A number of substitutions in genes including *vraSR* and *graSR* have been reported to enable susceptible MRSA strains to transform to hVISA and hVISA to VISA (38). The *rpoB* mutations selected by rifampicin were found to have multiple resistance to both vancomycin and daptomycin by a possible mechanism of increased cell wall thickness and these mutations always were found in VISA strains (39). Meanwhile, rifampicin-resistant strains were found to contain vancomycin resistance (40), and the researchers suggest the *rpoB* mutations play an important role in vancomycin resistance. These results may give a reason

for the worse outcomes in treatment of patients showing bacteraemia and endocarditis with both vancomycin and rifampicin (41-43). Some case reports suggested that employment of rifampicin in combination with other antibiotics can heal biofilm-related infections (44,45). Thus, rifampicin combination therapies can be utilized to treat biofilm-related infections although not for bacteraemia and endocarditis. The mechanisms of MRSA resistance to daptomycin are still poorly understood. There are certain possible explanations including an increased positive surface charge caused by mutations of *mprF* and *dltABCD*, increased cell wall thickness caused by mutations of *rpoB* and mutations in *cls* and *pgsA* which change membrane lipids. Sometimes these factors work together (46-48).

Linezolid is another effective antibiotic and up until now has not encountered much resistance. Most existing resistance is derived from mutations on the target site on the 23S rRNA of the ribosome (49). However, MRSA has multiple (commonly 4 to 6) copies of the 23S rRNA genes, and resistance can just be induced by multiple mutations (50). Furthermore, MRSA strains with multiple mutations always show lower activity (51,52). As a result, linezolid-related MRSA infections are not a significant problem for healthcare although it has been utilized for more than one decade (53).

3.1.2. Colonization

Medical waste, contaminated devices, and patients or medical staffs who carry MRSA play a role as an infectious source of MRSA in hospitals. Nostrils are a major site for carrying MRSA, and the relativity between nasal carriage and infectious diseases has been reported eighty years ago (54). Then a theory emerged which suggested the nose colonization of MRSA led to infectious diseases (55,56). Besides the nose, perineum and throat are also colonization sites of MRSA, but there are few research studies on these sites. Obviously, prevention of MRSA carriage could decrease the infection probability. A recent study revealed that mupirocin is efficacious in short-term prevention of MRSA, such as administration before surgery in hospitals (57). It is reported that about 20% of people in the population are persistent nasal carriers of *Staphylococcus aureus* (54), and carriage rates differentiate in different ethnic groups and are higher in patients with certain underlying medical conditions. These indicate that host factors are important for colonization of *Staphylococcus aureus*. However, the molecular mechanisms of these phenomena are still unknown. Thus, focusing on molecular mechanism research will be a key to understand MRSA colonization.

Surface-anchored *Staphylococcus aureus*-binding proteins which can bind to exposed human matrix

molecules improve the nasal colonization of MRSA. Clumping factor B and *Staphylococcus aureus* surface proteins G and X (SasG, SasX) have been shown to combine to nasal epithelial cells (58-60). Among them, SasX lately has attracted more attention because it was found to play an important role in an MRSA epidemic (60). SasX existed in a MGE mainly belonging to the ST239 MRSA strain which was a major ringleader of MRSA infections in Asia areas. It was discovered that SasX played a wide role in nasal colonization, biofilm generation, immune evasion and virulence in animal infection models. Thus, SasX may be a critical element promoting ST239 spread in Asia. The way SasX functions may provide reference for doctors and researchers to understand how the spread of colonization and virulence elements through HGT drives an MRSA epidemic. Teichoic acids, a kind of surface polymer of *Staphylococcus aureus*, helped make MRSA able to colonize the human nose (54). Moreover, MRSA has some mechanisms resistant to antibacterial peptides which cause the subsequent innate immune reaction (61).

3.1.3. Biofilm

Biofilms are a group of microorganisms in which cells stick to each other on a surface. These adherent cells are frequently embedded within a self-produced matrix of extracellular polymeric substance (EPS). Biofilm EPS is a polymeric conglomeration generally composed of extracellular DNA, proteins, and polysaccharides. Biofilms can form on living or non-living surfaces, such as medical settings (62,63). Biofilms protect MRSA from antibiotics and host immune defenses and then MRSA remains adherent on biotic or abiotic surfaces. Thus, biofilms can play a role in prolonging the duration of infection and promoting colonization. Whether *Staphylococcus aureus* clones in the nose form biofilms is still an argument, but comparison of physiological situations between nasal colonization and in biofilms can bring certain hints. Nasal colonization and biofilms of *Staphylococcus aureus* share the same trait of keeping relatively calm compared to the invasive situation of toxin-producing acute *Staphylococcus aureus* disease. It was reported that many colonizing strains are deficient in global virulence regulator *Agr* (64). Of note, there is a study which indicates that biofilm formation has been associated with the spread of some clones such as the Brazilian MRSA ST239 strain which is considered an ancestor of the Chinese SasX positive ST239 strains (65).

3.1.4. Virulence

Virulence of MRSA includes multiple elements such as toxins, immune system invasion and other factors. In different *Staphylococcus aureus* strains, there are various toxin pools due to the reason that toxins are

encoded on MGEs which are variable in different strains. These MGE-derived toxins have various types including superantigens such as toxic shock syndrome toxin (TSST), some leukotoxins such as Panton-Valentine leukocidin which is typical factor in CA-MRSA, and exfoliative toxins. However, α -toxin, β -toxin, some leukotoxins and phenol-soluble modulins (PSMs) are synthesized in almost all strains. Different expression levels of toxin genes lead to different pathogenic activities. For example, obvious pathogenic differences are observed between *Agr*-positive strains and *Agr*-negative ones, and *Agr* is able to manage many toxin genes (66).

Surface proteins play many critical roles in MRSA pathogenesis. They have many functions including cell wall metabolism, immune evasion, bacterial aggregation and biofilm formation (67). Most surface genes are located on the core genome, so the virulence of MRSA may not be directly related to surface proteins. SasX on MGE promotes MRSA colonization by boosting bacterial aggregation which shares similar characteristics compared to aggregation caused by surface proteins (60).

Regulator systems, such as *Agr*, *SaeRS*, *SarA*, and so on, contribute to strengthen the virulence of MRSA. *Agr*, having been long acknowledged as a regulator of virulence, plays an important part in toxin production (68). Recent research suggested that *Agr* may increase surface protein expression in a strain-dependant way (69). Based on official guidelines, methicillin resistance of MRSA is generated by *mecA* but the mechanism is poorly understood. Lately, some studies indicated that core genome-encoded regulators and the *mec* locus both can affect *Agr* (69,70).

3.2. CA-MRSA

3.2.1. Epidemiology

Before the 1990s MRSA was only known as a healthcare-associated disease in hospitals. At that time MRSA infection cases appeared in communities without any records of hospitalization. CA-MRSA is a moderately severe infection of the human skin and soft tissues. At present, CA-MRSA has emerged in most areas of the world. All of the *Staphylococcus aureus* species have appeared in CA-MRSA strains (71). The terrible spread of CA-MRSA is thought to be associated with strengthened virulence and increased transmissibility compared to former HA-MRSA. In the last decade, much research was performed to illuminate the molecular mechanism of virulence, but research on transmissibility did not make much progress (72).

3.2.2. Transmissibility

Spread of CA-MRSA was attributed to direct

transmission from patients and/or hospital staff. But, in fact, CA-MRSA also showed transmissibility activity. CA-MRSA commonly contains SCCmec elements of type 4 or type 5 which have stronger transmissibility as a result of a smaller size than other elements. The arginine catabolic mobile genetic element (ACME) of certain strains contains a spermidin acetyltransferase gene (*speG*) which transfers resistance to spermidin and other polyamines (73). Furthermore, there is an arginine deiminase and an oligopeptide gene cluster located on ACME, which can promote colonization of CA-MRSA, but there are still no unimpugnable experimental results to support this theory (72). Meanwhile, CA-MRSA utilizes surface adhesions in a different way from other strains and mechanism studies are still in progress (69).

3.2.3. Virulence

The hypothesis that CA-MRSA has higher virulence than HA-MRSA to infect humans has been validated in animal infection models and has gradually become common sense. Evidence of increased virulence of CA-MRSA is that strains show considerable ability to evade attack from neutrophils which are the frontline defense against bacteria in the human body. There are two hypotheses to explain this evasion capacity of CA-MRSA. One is that CA-MRSA acquired MGEs containing Panton-Valentine leukocidin (PVL) (74). The other is that CA-MRSA promotes expression of core genome-encoded virulence genes, such as PSM cytolytins, α -toxin and so on (75). Actually, these two hypotheses can work together to increase the virulence of CA-MRSA.

Panton-Valentine leukocidin (PVL), which is associated with *staphylococcal* skin and pulmonary infections, is a member of the bi-component family of *staphylococcal* leukocidins. In the CA-MRSA epidemic, PVL genes *lukS* and *lukF* were discovered in CA-MRSA strains, and interestingly, PVL is typically absent in HA-MRSA (74). Thus, PVL is supposed to play an important role in CA-MRSA virulence. However, two experimental results cast a damper over the assumption. The first is that even in strains without PVL genes, virulence is still strong (76). The second is that isogenic PVL gene deletion mutants did not decrease the CA-MRSA virulence in a few animal models (77,78).

Phenol-soluble modulins (PSMs) are amphipathic peptides produced by staphylococci that have multiple functions in pathogenesis (79). PSMs have showed virulence increasing capacity in several animal models. Although PSMs exist in all *Staphylococcus aureus* strains, the expression level in CA-MRSA is obviously higher than HA-MRSA (75).

Cytolysin α -toxin greatly increases virulence of CA-MRSA in some animal models (76,80). The α -toxin was proven to significantly increase virulence

by lysing a series of cells, such as macrophages and erythrocytes, and cause collapse of the epithelial barrier (81). Recently, a core genome-encoded toxin, SEIX, was reported to lead to CA-MRSA pneumonia in a lung infection animal model (82).

4. Vaccines

In consideration of research results until now, a vaccine strategy would be an economical measure to prevent and control MRSA infections, but this will be a serious challenge for researchers to develop effective vaccines. A vaccine which targets two surface antigen clusters of MRSA was reported to fail in a Phase III trial (83). A few vaccines are still in their early stage of development, and no one has gotten close to authorization (84). This is a long road for investigators to walk.

5. Conclusion

For decades, doctors and researchers have been fighting with MRSA continuously and every time when new antibiotic weapons were developed MRSA could raise novel shields of resistance accordingly. In the war with MRSA, although humans have obtained partial success, the challenges from antibiotic-resistant *Staphylococcus aureus* are still severe. Especially during recent years, the appearance of CA-MRSA brought humans to a novel battle field. The hard work of many laboratories shed a light on the relevance between genetic mutations and MRSA phenomena, such as antibiotic resistance, virulence, and biofilms. The mutations of MRSA could be ideal targets for sequential development of novel antibiotics and vaccines.

Acknowledgements

This study was supported by Grants-in-Aid from the Ministry of Education, Science, Sports, and Culture of Japan.

References

- Jevons MP, Rolinson GN, Knox R. Celbenin-Resistant *Staphylococci*. *BMJ*. 1961; 1:b124-b125.
- Lowy FD. Medical progress - *Staphylococcus aureus* infections. *N Engl J Med*. 1998; 339:520-532.
- Grundmann H, Aanensen DM, van den Wijngaard CC, Spratt BG, Harmsen D, Friedrich AW, Reference ES. Geographic Distribution of *Staphylococcus aureus* Causing Invasive Infections in Europe: A Molecular-Epidemiological Analysis. *PLoS Med*. 2010; 7:e1000215.
- Song JH, Hsueh PR, Chung DR, *et al*. Spread of methicillin-resistant *Staphylococcus aureus* between the community and the hospitals in Asian countries: an ANSORP study. *J Antimicrob Chemother*. 2011; 66: 1061-1069.
- Mejia C, Zurita J, Guzman-Blanco M, Gram LAWG. Epidemiology and surveillance of methicillin-resistant *Staphylococcus aureus* in Latin America. *Braz J Infect Dis*. 2010; 14:S79-S86.
- Diekema DJ, Pfaller MA, Schmitz FJ, Smayevsky J, Bell J, Jones RN, Beach M, Grp SP. Survey of infections due to *Staphylococcus* species: Frequency of occurrence and antimicrobial susceptibility of isolates collected in the United States, Canada, Latin America, Europe, and the Western Pacific region for the SENTRY Antimicrobial Surveillance Program, 1997-1999. *Clin Infect Dis*. 2001; 32:S114-S132.
- Nakamura A, Miyake K, Misawa S, Kuno Y, Horii T, Hori S, Kondo S, Tabe Y, Ohsaka A. Association between antimicrobial consumption and clinical isolates of methicillin-resistant *Staphylococcus aureus*: a 14-year study. *J Infect Chemother*. 2012; 18:90-95.
- Monecke S, Coombs G, Shore AC, *et al*. A Field Guide to Pandemic, Epidemic and Sporadic Clones of Methicillin-Resistant *Staphylococcus aureus*. *PLoS One*. 2011; 6:e17936.
- Sanchini A, Campanile F, Monaco M, Cafiso V, Rasigade JP, Laurent F, Etienne J, Stefani S, Pantosti A. DNA microarray-based characterisation of Pantone-Valentine leukocidin-positive community-acquired methicillin-resistant *Staphylococcus aureus* from Italy. *Eur J Clin Microbiol Infect Dis*. 2011; 30:1399-1408.
- Pinho MG, de Lencastre H, Tomasz A. An acquired and a native penicillin-binding protein cooperate in building the cell wall of drug-resistant staphylococci. *Proc Natl Acad Sci U S A*. 2001; 98:10886-10891.
- García-Álvarez L, Holden MT, Lindsay H, *et al*. Methicillin-resistant *Staphylococcus aureus* with a novel *mecA* homologue in human and bovine populations in the UK and Denmark: a descriptive study. *Lancet Infect Dis*. 2011; 11:595-603.
- Harris SR, Cartwright EJP, Torok ME, Holden MTG, Brown NM, Ogilvy-Stuart AL, Ellington MJ, Quail MA, Bentley SD, Parkhill J, Peacock SJ. Whole-genome sequencing for analysis of an outbreak of methicillin-resistant *Staphylococcus aureus*: a descriptive study. *Lancet Infect Dis*. 2013; 13:130-136.
- Firth N SR. Gram-positive pathogens. ASM Press, Washington, DC, USA, 2006.
- Lindsay JA, Moore CE, Day NP, Peacock SJ, Witney AA, Stabler RA, Husain SE, Butcher PD, Hinds J. Microarrays reveal that each of the ten dominant lineages of *Staphylococcus aureus* has a unique combination of surface-associated and regulatory genes. *J Bacteriol*. 2006; 188:669-676.
- Lindsay JA. Genomic variation and evolution of *Staphylococcus aureus*. *Int J Med Microbiol*. 2010; 300:98-103.
- Malachowa N, DeLeo FR. Mobile genetic elements of *Staphylococcus aureus*. *Cell Mol Life Sci*. 2010; 67:3057-3071.
- Enright MC, Day NPJ, Davies CE, Peacock SJ, Spratt BG. Multilocus sequence typing for characterization of methicillin-resistant and methicillin-susceptible clones of *Staphylococcus aureus*. *J Clin Microbiol*. 2000; 38:1008-1015.
- Stefani S, Goglio A. Methicillin-resistant *Staphylococcus aureus*: related infections and antibiotic resistance. *Int J Infect Dis*. 2010; 14:S19-S22.
- Novick RP. *Staphylococcal* Plasmids and Their Replication. *Annu Rev Microbiol*. 1989; 43:537-565.

20. Campanile F BD, Borbone S, Stefani S. Methicillin-resistant *Staphylococcus aureus* evolution: the multiple facets of an old pathogen. *Eur Infect Dis.* 2010; 4:70-76.
21. Waldron DE, Lindsay JA. SauI: a novel line age-specific type I restriction-modification system that blocks horizontal gene transfer into *Staphylococcus aureus* and between S-aureus isolates of different lineages. *J Bacteriol.* 2006; 188:5578-5585.
22. Cockfield JD, Pathak S, Edgeworth JD, Lindsay JA. Rapid determination of hospital-acquired methicillin-resistant *Staphylococcus aureus* lineages. *J Med Microbiol.* 2007; 56:614-619.
23. Barber M, Rozwadowskadowzenko M. Infection by Penicillin-Resistant Staphylococci. *Lancet.* 1948; 255:641-644.
24. Rammelkamp CH, Maxon T. Resistance of *Staphylococcus aureus* to the action of penicillin. *Proc Soc Exp Biol Med.* 1942; 51: 386-389.
25. Abraham EP, Chain E. An Enzyme from Bacteria Able to Destroy Penicillin. 1940. (Reprinted from *Nature*, Vol 146, Pg 837, 1940). *Rev Infect Dis.* 1988; 10: 677-678.
26. Jevons MP, Coe AW, Parker MT. Methicillin Resistance in *Staphylococci*. *Lancet.* 1963; 1:904-907.
27. Shorr AF. Epidemiology of *staphylococcal* resistance. *Clin Infect Dis.* 2007; 45: S171-S176.
28. McDougal LK, Fosheim GE, Nicholson A, Bulens SN, Limbago BM, Shearer JES, Summers AO, Patel JB. Emergence of Resistance among USA300 Methicillin-Resistant *Staphylococcus aureus* Isolates Causing Invasive Disease in the United States. *Antimicrob Agents Chemother.* 2010; 54:3804-3811.
29. Moellering RC, Jr., Linden PK. The specter of glycopeptide resistance: current trends and future considerations. Introduction. *Am J Med.* 1998; 104:1S-2S.
30. Sakoulas G MRJ. Increasing antibiotic resistance among methicillin-resistant *Staphylococcus aureus* strains. *Clin Infect Dis.* 2008; Suppl 5: S360-S367.
31. Howden BP, Ward PB, Charles PGP, *et al.* Treatment outcomes for serious infections caused by methicillin-resistant *Staphylococcus aureus* with reduced vancomycin susceptibility. *Clin Infect Dis.* 2004; 38:521-528.
32. Tenover FC, Moellering RC. The rationale for revising the Clinical and Laboratory Standards Institute vancomycin minimal inhibitory concentration interpretive criteria for *Staphylococcus aureus*. *Clin Infect Dis.* 2007; 44:1208-1215.
33. van Hal SJ, Paterson DL. Systematic Review and Meta-Analysis of the Significance of Heterogeneous Vancomycin-Intermediate *Staphylococcus aureus* Isolates. *Antimicrob Agents Chemother.* 2011; 55:405-410.
34. Peleg AY, Monga D, Pillai S, Mylonakis E, Moellering RC, Eliopoulos GM. Reduced Susceptibility to Vancomycin Influences Pathogenicity in *Staphylococcus aureus* Infection. *J Infect Dis.* 2009; 199:532-536.
35. Kennedy AD, Otto M, Braughton KR, Whitney AR, Chen L, Mathema B, Mediavilla JR, Byrne KA, Parkins LD, Tenover FC, Kreiswirth BN, Musser JM, DeLeo FR. Epidemic community-associated methicillin-resistant *Staphylococcus aureus*: Recent clonal expansion and diversification. *Proc Natl Acad Sci U S A.* 2008; 105:1327-1332.
36. Peleg AY CD, Ward D. A novel mechanism of reduced susceptibility to vancomycin in *Staphylococcus aureus*. The Twenty-first European Congress of Clinical Microbiology and Infectious Diseases/Twenty-seventh International Congress of Chemotherapy. Milan, Italy, 2011.
37. Schweizer ML, Furuno JP, Sakoulas G, Johnson JK, Harris AD, Shardell MD, McGregor JC, Thom KA, Perencevich EN. Increased Mortality with Accessory Gene Regulator (*agr*) Dysfunction in *Staphylococcus aureus* among Bacteremic Patients. *Antimicrob Agents Chemother.* 2011; 55:1082-1087.
38. Neoh HM, Cui L, Yuzawa H, Takeuchi F, Matsuo M, Hiramatsu K. Mutated response regulator *graR* is responsible for phenotypic conversion of *Staphylococcus aureus* from heterogeneous vancomycin-intermediate resistance to vancomycin-intermediate resistance. *Antimicrob Agents Chemother.* 2008; 52:45-53.
39. Cui LZ, Isii T, Fukuda M, Ochiai T, Neoh HM, Camargo ILBD, Watanabe Y, Shoji M, Hishinuma T, Hiramatsu K. An RpoB Mutation Confers Dual Heteroresistance to Daptomycin and Vancomycin in *Staphylococcus aureus*. *Antimicrob Agents Chemother.* 2010; 54:5222-5233.
40. Watanabe Y, Cui LZ, Katayama Y, Kozue K, Hiramatsu K. Impact of *rpoB* Mutations on Reduced Vancomycin Susceptibility in *Staphylococcus aureus*. *J Clin Microbiol.* 2011; 49:2680-2684.
41. Levine DP, Fromm BS, Reddy BR. Slow Response to Vancomycin or Vancomycin Plus Rifampin in Methicillin-Resistant *Staphylococcus aureus* Endocarditis. *Ann Intern Med.* 1991; 115:674-680.
42. Riedel DJ, Weekes E, Forrest GN. Addition of rifampin to standard therapy for treatment of native valve infective endocarditis caused by *Staphylococcus aureus*. *Antimicrob Agents Chemother.* 2008; 52:2463-2467.
43. Jang HC, Kim SH, Kim KH, Kim CJ, Lee S, Song KH, Jeon JH, Park WB, Bin Kim H, Park SW, Kim NJ, Kim EC, Oh M, Choe KW. Salvage Treatment for Persistent Methicillin-Resistant *Staphylococcus aureus* Bacteremia: Efficacy of Linezolid With or Without Carbapenem. *Clin Infect Dis.* 2009; 49:395-401.
44. Garrigos C, Murillo O, Euba G, Verdaguer R, Tubau F, Cabellos C, Cabo J, Ariza J. Efficacy of Usual and High Doses of Daptomycin in Combination with Rifampin versus Alternative Therapies in Experimental Foreign-Body Infection by Methicillin-Resistant *Staphylococcus aureus*. *Antimicrob Agents Chemother.* 2010; 54:5251-5256.
45. Vergidis P, Rouse MS, Euba G, Karau MJ, Schmidt SM, Mandrekar JN, Steckelberg JM, Patel R. Treatment with Linezolid or Vancomycin in Combination with Rifampin Is Effective in an Animal Model of Methicillin-Resistant *Staphylococcus aureus* Foreign Body Osteomyelitis. *Antimicrob Agents Chemother.* 2011; 55:1182-1186.
46. Friedman L, Alder JD, Silverman JA. Genetic changes that correlate with reduced susceptibility to daptomycin in *Staphylococcus aureus*. *Antimicrob Agents Chemother.* 2006; 50:2137-2145.
47. Peleg AY MA, Miyakis S. Genetic evolution of resistance to daptomycin in *Staphylococcus aureus*. The Fiftieth Interscience Conference on Antimicrobial Agents and Chemotherapy. American Society for Microbiology. Washington, DC, USA, 2010.
48. Yang SJ, Kreiswirth BN, Sakoulas G, Yeaman MR, Xiong YQ, Sawa A, Bayer AS. Enhanced Expression of *dltABCD* Is Associated with the Development of Daptomycin Nonsusceptibility in a Clinical Endocarditis Isolate of *Staphylococcus aureus*. *J Infect Dis.* 2009;

- 200:1916-1920.
49. Prystowsky J, Siddiqui F, Chosay J, Shinabarger DL, Millichap J, Peterson LR, Noskin GA. Resistance to linezolid: Characterization of mutations in rRNA and comparison of their occurrences in vancomycin-resistant enterococci. *Antimicrob Agents Chemother.* 2001; 45:2154-2156.
 50. Marshall SH, Donskey CJ, Hutton-Thomas R, Salata RA, Rice LB. Gene dosage and linezolid resistance in *Enterococcus faecium* and *Enterococcus faecalis*. *Antimicrob Agents Chemother.* 2002; 46:3334-3336.
 51. Besier S, Ludwig A, Zander J, Brade V, Wichelhaus TA. Linezolid resistance in *Staphylococcus aureus*: Gene dosage effect, stability, fitness costs, and cross-resistances. *Antimicrob Agents Chemother.* 2008; 52:1570-1572.
 52. Meka VG, Pillai SK, Sakoulas G, Wennersten C, Venkataraman L, DeGirolami PC, Eliopoulos GM, Moellering RC, Gold HS. Linezolid resistance in sequential *Staphylococcus aureus* isolates associated with a T2500A mutation in the 23S rRNA gene and loss of a single copy of rRNA. *J Infect Dis.* 2004; 190:311-317.
 53. Meka VG, Gold HS, Cooke A, Venkataraman L, Eliopoulos GM, Moellering RC, Jenkins SG. Reversion to susceptibility in a linezolid-resistant clinical isolate of *Staphylococcus aureus*. *J Antimicrob Chemother.* 2004; 54:818-820.
 54. Wertheim HFL, Melles DC, Vos MC, van Leeuwen W, van Belkum A, Verbrugh HA, Nouwen JL. The role of nasal carriage in *Staphylococcus aureus* infections. *Lancet Infect Dis.* 2005; 5:751-762.
 55. Smyth DS, Kafer JM, Wasserman GA, Velickovic L, Mathema B, Holzman RS, Knipe TA, Becker K, von Eiff C, Peters G, Chen L, Kreiswirth BN, Novick RP, Shopsin B. Nasal Carriage as a Source of agr-Defective *Staphylococcus aureus* Bacteremia. *J Infect Dis.* 2012; 206:1168-1177.
 56. Wertheim HFL, Vos MC, Ott A, van Belkum A, Voss A, Kluytmans JAJW, van Keulen PHJ, Vandembroucke-Grauls CMJE, Meester MHM, Verbrugh HA. Risk and outcome of nosocomial *Staphylococcus aureus* bacteraemia in nasal carriers versus non-carriers. *Lancet.* 2004; 364:703-705.
 57. Ammerlaan HSM, Kluytmans JAJW, Berkhout H, *et al.* Eradication of carriage with methicillin-resistant *Staphylococcus aureus*: effectiveness of a national guideline. *J Antimicrob Chemother.* 2011; 66:2409-2417.
 58. Mulcahy ME, Geoghegan JA, Monk IR, O'Keefe KM, Walsh EJ, Foster TJ, McLoughlin RM. Nasal Colonisation by *Staphylococcus aureus* Depends upon Clumping Factor B Binding to the Squamous Epithelial Cell Envelope Protein Loricrin. *PLoS Pathog.* 2012; 8:e1003092.
 59. Roche FM, Meehan M, Foster TJ. The *Staphylococcus aureus* surface protein SasG and its homologues promote bacterial adherence to human desquamated nasal epithelial cells. *Microbiology.* 2003; 149:2759-2767.
 60. Li M, Du X, Villaruz AE, Diep BA, Wang DC, Song Y, Tian YR, Hu JH, Yu FY, Lu Y, Otto M. MRSA epidemic linked to a quickly spreading colonization and virulence determinant. *Nat Med.* 2012; 18:816-217.
 61. Andra J, Goldmann T, Ernst CM, Peschel A, Gutschmann T. Multiple Peptide Resistance Factor (MprF)-mediated Resistance of *Staphylococcus aureus* against Antimicrobial Peptides Coincides with a Modulated Peptide Interaction with Artificial Membranes Comprising Lysyl-Phosphatidylglycerol. *J Biol Chem.* 2011; 286:18692-18700.
 62. Hall-Stoodley L, Costerton JW, Stoodley P. Bacterial biofilms: From the natural environment to infectious diseases. *Nat Rev Microbiol.* 2004; 2:95-108.
 63. Lear G. *Microbial Biofilms: Current Research and Applications.* Caister Academic Press, Norwich, UK, 2012.
 64. Shopsin B, Drlica-Wagner A, Mathema B, Adhikari RP, Kreiswirth BN, Novick RP. Prevalence of agr dysfunction among colonizing *Staphylococcus aureus* strains. *J Infect Dis.* 2008; 198:1171-1174.
 65. Amaral MM, Coelho LR, Flores RP, Souza RR, Silva-Carvalho MC, Teixeira LA, Ferrerira-Carvalho BT, Figueiredo AMS. The predominant variant of the Brazilian epidemic clonal complex of methicillin-resistant *Staphylococcus aureus* has an enhanced ability to produce biofilm and to adhere to and invade airway epithelial cells. *J Infect Dis.* 2005; 192:801-810.
 66. Novick RP, Ross HF, Projan SJ, Kornblum J, Kreiswirth B, Moghazeh S. Synthesis of *Staphylococcal* Virulence Factors Is Controlled by a Regulatory Rna Molecule. *Embo Journal.* 1993; 12:3967-3975.
 67. Conrady DG, Wilson JJ, Herr AB. Structural basis for Zn²⁺-dependent intercellular adhesion in *staphylococcal* biofilms. *Proc Natl Acad Sci U S A.* 2013; 110:E202-E211.
 68. Otto M. Mobile genetic element-encoded cytolysin connects virulence to methicillin resistance in MRSA. *Virulence.* 2010; 1:49-51.
 69. Cheung GYC, Wang R, Khan BA, Sturdevant DE, Otto M. Role of the Accessory Gene Regulator agr in Community-Associated Methicillin-Resistant *Staphylococcus aureus* Pathogenesis. *Infect Immun.* 2011; 79:1927-1935.
 70. Rudkin JK, Edwards AM, Bowden MG, Brown EL, Pozzi C, Waters EM, Chan WC, Williams P, O'Gara JP, Massey RC. Methicillin Resistance Reduces the Virulence of Healthcare-Associated Methicillin-Resistant *Staphylococcus aureus* by Interfering With the agr Quorum Sensing System. *J Infect Dis.* 2012; 205:798-806.
 71. Deleo FR, Chambers HF. Reemergence of antibiotic-resistant *Staphylococcus aureus* in the genomics era. *Journal of Clinical Investigation.* 2009; 119: 2464-2474.
 72. Otto M. Basis of Virulence in Community-Associated Methicillin-Resistant *Staphylococcus aureus*. *Annu Rev Microbiol.* 2010; 64:143-162.
 73. Thurlow LR, Joshi GS, Clark JR, Spontak JS, Neely CJ, Maile R, Richardson AR. Functional Modularity of the Arginine Catabolic Mobile Element Contributes to the Success of USA300 Methicillin-Resistant *Staphylococcus aureus*. *Cell Host Microbe.* 2013; 13:100-107.
 74. Vandenesch F, Naimi T, Enright MC, Lina G, Nimmo GR, Heffernan H, Liassine N, Bes M, Greenland T, Reverdy ME, Etienne J. Community-acquired methicillin-resistant *Staphylococcus aureus* carrying Panton-Valentine leukocidin genes: Worldwide emergence. *Emerg Infect Dis.* 2003; 9:978-984.
 75. Li M, Diep BA, Villaruz AE, Braughton KR, Jiang XF, Deleo FR, Chambers HF, Lu Y, Otto M. Evolution of virulence in epidemic community-associated methicillin-resistant *Staphylococcus aureus*. *Proc Natl Acad Sci U S A.* 2009; 106:5883-5888.
 76. Kobayashi SD, Malachowa N, Whitney AR, Braughton

- KR, Gardner DJ, Long D, Bubeck-Wardenburg J, Schneewind O, Otto M, DeLeo FR. Comparative Analysis of USA300 Virulence Determinants in a Rabbit Model of Skin and Soft Tissue Infection. *J Infect Dis.* 2011; 204:937-941.
77. Watkins RR, David MZ, Salata RA. Current concepts on the virulence mechanisms of methicillin-resistant *Staphylococcus aureus*. *J Med Microbiol.* 2012; 61:1179-1193.
78. Lipinska U, Hermans K, Meulemans L, Dumitrescu O, Badiou C, Duchateau L, Haesebrouck F, Etienne J, Lina G. Panton-Valentine Leukocidin Does Play a Role in the Early Stage of *Staphylococcus aureus* Skin Infections: A Rabbit Model. *PLoS One.* 2011; 6:e22864.
79. Periasamy S CS, Cheung GY, Otto M. Phenol-soluble modulins in staphylococci: What are they originally for? *Commun Integr Biol.* 2012; 5:275-277.
80. Bubeck-Wardenburg J, Bae T, Otto M, DeLeo FR, Schneewind O. Poring over pores: alpha-hemolysin and Panton-Valentine leukocidin in *Staphylococcus aureus* pneumonia. *Nat Med.* 2007; 13:1405-1406.
81. Hanberger H, Walther S, Leone M, Barie PS, Rello J, Lipman J, Marshall JC, Anzueto A, Sakr Y, Pickkers P, Felleiter P, Engoren M, Vincent JL, Investigators EIG. Increased mortality associated with methicillin-resistant *Staphylococcus aureus* (MRSA) infection in the Intensive Care Unit: results from the EPIC II study. *Int J Antimicrob Agents.* 2011; 38:331-335.
82. Wilson GJ, Seo KS, Cartwright RA, Connelley T, Chuang-Smith ON, Merriman JA, Guinane CM, Park JY, Bohach GA, Schlievert PM, Morrison WI, Fitzgerald JR. A Novel Core Genome-Encoded Superantigen Contributes to Lethality of Community-Associated MRSA Necrotizing Pneumonia. *PLoS Pathog.* 2011; 7:e1002271.
83. Shinefield H, Black S, Fattom A, Horwith G, Rasgon S, Ordonez J, Yeoh H, Law D, Robbins JB, Schneerson R, Muenz L, Naso R. Use of a *Staphylococcus aureus* conjugate vaccine in patients receiving hemodialysis. *N Engl J Med.* 2002; 346:491-496.
84. Anderson AS, Miller AA, Donald RGK, Scully IL, Nanra JS, Cooper D, Jansen KU. Development of a multicomponent *Staphylococcus aureus* vaccine designed to counter multiple bacterial virulence factors. *Hum Vaccin Immunother.* 2012; 8:1585-1594.

(Received May 6, 2013; Revised June 23, 2013; Accepted June 25, 2013)

Factors affecting patient delay of diagnosis and completion of Direct Observation Therapy, Short-course (DOTS) among the migrant population in Shandong, China

Ruoyan Gai Tobe¹, Lingzhong Xu^{1,*}, Chengchao Zhou¹, Qing Yuan¹, Hong Geng², Xingzhou Wang¹

¹Department of Health Management and Maternal and Child Healthcare, School of Public Health, Shandong University, Ji'nan, China;

²Shandong Province Tuberculosis Prevention and Control Center, Ji'nan, China.

Summary

In China, the epidemiological and socioeconomic status of the migrant population suggests that the vulnerable population should be prioritized for tuberculosis (TB) control. A face-to-face interview using a structured questionnaire was performed on a total of 314 smear-positive pulmonary TB patients among the migrant population of 12 randomly selected counties in Shandong Province, China. From the results, the cases of patient delay of diagnosis accounted for 40.8%, and the completion rate of Direct Observation Therapy, Short-course (DOTS) was as low as 67.2%. There were 47.1% missed cases in the first diagnosis. Factors affecting detection and treatment were present in their socioeconomic status, working style, and the accessibility to related TB care. The findings indicated that migrant TB patients suffer delayed diagnosis, a low case detection rate and a low completion DOTS rate. Improvement of migrants' working conditions and accessibility to specialized TB care is essential and is expected to lead to better case detection and treatment completion.

Keywords: Migrant population, tuberculosis, direct observation therapy, short-course (DOTS), China

1. Introduction

China has the world's second largest tuberculosis (TB) disease burden. The Chinese government has a political commitment for TB control, with an increased financing investment during the past ten years. As the results show, from 2000 to 2009, the prevalence of TB has declined from 466 per 100,000 to 459 per 100,000, and active cases decreased from 169 per 100,000 to 66 per 100,000 (1). Direct Observation Therapy, Short-course (DOTS) strategy has universally covered TB patients and the cure rate of active TB cases by DOTS reached over 90% at the county level, the global target for TB control (2).

*Address correspondence to:

Dr. Lingzhong Xu, Department of Health Services Management & Maternal and Child Healthcare, School of Public Health, Shandong University, Wen-hua-xi Road No.44, Ji'nan City, Shandong Province, 250012, China.
E-mail: lz Xu@sdu.edu.cn

In China, case management for the migrant population remains as one of the major challenges. With rapid economic growth and urbanization, the number of the rural-to-urban migrant population is estimated to reach to 211 million in 2010, and it will be continuously increasing in the up-coming several decades (3). After moving to the urban area, most of the rural-to-urban migrant population tends to be engaged in work with the poor environment, heavy loads, high risks, but low payment. They are exposed to a higher risk of TB infection due to the poor living and working environment, bad nutritional status and the characteristics of frequent migration. To the contrary, their accessibility to healthcare is often seriously restricted by their citizenship and their poor financial conditions (4). So far, due to civil registration status and temporary employment, most of the migrant population are not eligible for urban citizen medical insurance and has to pay out-of-pocket for healthcare services. The medical costs in the urban area are

much higher than those in the rural area, restricting their access to medical care when they become ill (5). Compared to urban residents they face longer delays in obtaining a TB diagnosis (6). Because the vulnerable population has brought a significant influence on the epidemiological status of TB control in the immigrated regions, particularly metropolitan areas, this suggests an urgent necessity for TB control strategies targeting them in the urban area (7-9).

China has recently implemented a free TB treatment policy that now covers the migrant population as well. The free service package includes diagnostic and treatment services, such as a free sputum smear test, a free X-ray examination upon one's initial visit, and free anti-TB drugs in accordance with the standard protocol (6 months for new patients and 8 months for re-treated patients). Nevertheless, barriers to TB detection, management and treatment among the migrant population continue to have both financial and non-financial aspects including poor health literature and social stigma in the working place, based on the review of previous qualitative studies (10). Due to their frequent moving, migrant TB cases are difficult to be managed and provided related healthcare services. Our previous study suggested a relevant number of rural-to-urban migrant workers defaulted or failed DOTS, leading to the actual gap between the surprisingly low success rate of DOTS in the rural field and that officially reported (11). Once the migrant workers default or fail treatment but leave for work, it potentially causes the spread of the disease and leads to a huge risk to public health. Moreover, deficient case management and irregular treatment leads to high-risk development and spread of drug-resistant tuberculosis (12), which is now another serious problem in TB control in China, paralleling the high burden among the migrant population. Once drug resistance occurs, it brings severe difficulties for treatment and case control, as current anti-TB drugs are limited in number (13). A study in eastern China also indicated that previously treated migrant patients were more likely to harbor drug-resistant TB and MDR-TB than new migrant cases (14). It is necessary to investigate case detection in patients and completion of DOTS among the migrant population, in order to find an effective way of case detection, management and treatment. Therefore, the objective of this study is to assess factors affecting delay of patient diagnosis and completion of TB treatment by DOTS among the migrant population.

2. Materials and Methods

2.1. Study design

This was a cross-sectional study conducted during the period from September to October 2009 in Shandong Province, the second largest province in China with a

population of 96.7 million. The amount of the migrant population in Shandong Province has increased, and in 2008 it reached 6,910,000 (15). A huge amount of funds from the national government and international organizations has been injected into the TB control program (16). In 2008, there were 38,885 newly-enrolled cases and 4,320 re-enrolled cases reported for the treatment regimen in total, and 76.55% of the cases were rural residents (17).

The study subject is smear-positive pulmonary TB patients in the migrant population registered in the local County TB dispensary (CTD). The inclusive criteria were *i*) non-permanent residents in the study sites, *ii*) continuously working or living in the study sites for more than 3 months, and *iii*) registered in the CTD of the study sites and closed DOTS during the period from September 2008 to August 2009. A multi-stage random sampling was performed to recruit participants. First, a total of 141 counties in the province were grouped into 12 clusters based on socioeconomic and demographical status, which indicators included GDP per capita in 2008, population number, population density, amount of migrant population, work status, maternal & infant mortality, and compulsory education receiving rate. One county from each cluster was randomly selected, and the total number of the study sites came to 12 counties. Then, all patients meeting the inclusive criteria were recruited. In total, there were 314 migrant TB patients enrolled in the study.

2.2. Data collection and quality control

Migrant TB patients were face-to-face interviewed in the local CTD using a structured questionnaire, which included demographic and socioeconomic characteristics of participants, working, living conditions and life style, accessibility to health services, seeking healthcare services including severity of onset symptoms and the time interval from the first onset of symptoms to visiting a formal health care facility, and implementation, compliance and results of treatment course by DOTS. For those who could not return to the study sites during the period, we implemented a telephone interview using the same questionnaire. For quality control, a pilot study was implemented at non-study sites in 2008, to check the technical and logistical aspects of the investigation, including deficiencies in study design, the questionnaire and guideline for investigators and potential bias in the field survey. The investigators consisted of researchers in the School of Public Health, experts in Shandong University, Shandong Province Tuberculosis Prevention Center, and staffs from CTD of the study sites.

2.3. Definitions

- The migrant population refers to those non-

registered residents currently living in the study sites for more than 3 months or expected to live there for more than 3 months.

- Patient delay of diagnosis refers to more than two weeks time interval from the first onset of tuberculosis symptoms until visiting a formal health care facility (health centers, CTD, hospitals).
- According to the national guideline, "completion of treatment" refers to patients that completed the concentrated course of six months and were recorded as having at least one negative smear specimen result; "default" is defined as a patient who definitely stopped medicine for more than two months before completion of the concentrated course; "failure" is a smear-positive patient that had a positive result at the end of the fifth month.
- Regarding types of registration, a new patient refers to those who were newly diagnosed and registered in a CTD; while a re-enrolled patient was one who was recorded as treatment default or failure and was re-registered for DOTS.
- Consulting with clinical experts, severities of the onset symptoms were categorized in three levels: mild symptoms such as coughing up of sputum, night sweats; moderate symptoms such as chest pain, low weight and low fever; and severe symptoms such as high fever and hemoptysis.

2.4. Data analysis

The data were entered and analyzed using SPSS 18.0 for Windows (SPSS, Inc., Chicago, USA). Descriptive and inferential analyses were performed as appropriate. χ^2 test was employed for univariate analysis. Moreover, a Multi-logistic regression model was developed to further assess the impact of variables on treatment outcomes.

2.5. Ethical consideration

The Ethical Committee of Shandong University approved this study. This investigation was conducted after the informed consent of all participants were obtained.

3. Results

3.1. Demographic and socioeconomic characteristics

Major demographic and socioeconomic characteristics of the surveyed patients are summarized in Table 1. There were 57.3% migrant patients working more than five days per week and 34.1% whose working time was over 8 hours. Regarding household economic status, 290 surveyed TB patients reported poor or moderate level in the study sites and 28.7% of their household bears debt. There were 64.6% of the surveyed TB patients

Table 1. Demographic and socioeconomic characteristics

Items	Frequency (%)
Gender	
Male	199 (63.4)
Female	115 (36.6)
Marital status	
Single	140 (44.6)
Married	163 (51.9)
Divorced/Widowed	11 (3.5)
Education	
Illiteracy and primary education	59 (18.8)
Middle school	126 (40.1)
High school and above	129 (41.1)
Type of household	
Rural residency	277 (88.2)
Urban residency	37 (11.8)
Household economic status in the study sites	
Good	24 (7.6)
Moderate	222 (70.7)
Poor	68 (21.7)
Household debt	
Yes	224 (71.3)
No	90 (28.7)
Working days per week	
≤ 5 days	134 (42.7)
> 5 days	180 (57.3)
Whether a welfare household	
Yes	17 (5.4)
No	297 (94.6)
Medical insurance	
Yes	111 (35.4)
No	203 (64.6)
Time spending on visiting the nearest health facilities	
less than 5 minutes	99 (31.5)
5 to 10 minutes	98 (31.2)
10 to 30 minutes	77 (24.5)
30 minutes or more	40 (12.7)
Severity of onset symptom	
Mild	120 (38.2)
Moderate	131 (41.7)
Severe	63 (20.1)

not covered by any medical insurance. Regarding their enrollment into DOTS, 94.6% were registered as new patients in CTD and the rest were re-enrolled patients. For the distance to the closest community healthcare centers, 31.5% spent less than five minutes from living or working place to the destination, 31.2% spent 5 to 10 minutes, 24.5% spent 10 to 30 minutes, and 12.7% spent more than 30 minutes.

3.2. Patient delay of diagnosis

The average and median time interval from the first onset of tuberculosis symptoms until visiting a formal health care facility were 18.8 days and 10 days, respectively. Among the surveyed TB patients, the cases of patient delay of diagnosis accounted for 40.8%. As shown in Figure 1, 59.2% of the TB patients had a time interval less than two weeks, 16.3% had a time interval between two to four weeks, and 24.5% had a time interval more than four weeks. Regarding the health care facility the TB patients first

visited, 31.8% went to village or community health centers and 40.8% selected county general hospitals. In their first visit to health care facilities, only 52.9% of the cases were initially diagnosed as TB while the rest were missed. Less than half of the participants knew about the national free TB treatment policy (41.7%).

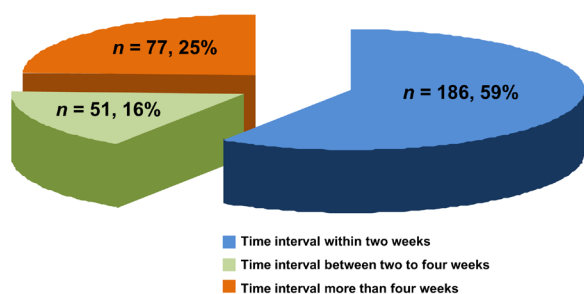


Figure 1. Proportion of patient delay of diagnosis.

We performed univariate and multivariate analysis for factors contributable to patient delay of diagnosis. Chi-square test, Fisher's exact test and Kruskal Wallis H test were employed for univariate analysis. As shown in Table 2, working days per week ($p < 0.001$), status of medical insurance ($p < 0.05$), time spent on visiting the closest health facilities ($p < 0.05$), status of a welfare household ($p < 0.05$), annual income ($p < 0.05$), and severity of onset symptoms ($p < 0.05$) significantly affected patient delay diagnosis. Variables associated with patient delay where $p < 0.05$ in the univariate analysis was subsequently included in the multivariate logistic regression model. As for the results, TB patients working more than five days every week, those that don't have any medical insurance, those spending more than 30 minutes on visiting the closest health facilities, those with a poorer annual income, those coming from a welfare household, and those with mild onset symptoms, were much more likely to have a delay of patient diagnosis.

Table 2. Multivariate analysis of factors affecting patient delay of TB diagnosis

Items	Not delayed % (n = 186)	Delayed% (n = 128)	p (univariate analysis)	OR (95% CI)	p (logistic regression model)
Gender					
Male	60.8	39.2	0.457		
Female	56.5	43.5			
Marital status					
Single	59.3	40.7	0.953		
Married	58.9	41.1			
Divorced/Widowed	63.6	36.4			
Education					
Illiteracy and primary education	57.6	40.1	0.924		
Middle school	58.7	41.3			
High school and above	60.5	36.5			
Type of household					
Rural residency	58.5	41.5	0.458		
Urban residency	64.9	35.1			
Household economic status in the study sites					
Good	62.5	37.5	0.127		
Moderate	62.2	37.8			
Poor	48.5	51.5			
Household debt					
Yes	60.0	40.0	0.861		
No	58.9	41.1			
Working days per week					
≤ 5 days	75.4	24.6	<0.001	1	
> 5 days	47.2	52.8		3.39 (1.98-5.79)	<0.001
Whether a welfare household					
Yes	35.3	64.7	0.039	1	
No	60.6	39.4		0.30 (0.10-0.94)	0.039
Medical insurance					
Yes	68.5	31.5	0.014	1	
No	54.2	45.8		1.97 (1.14-3.43)	0.016
Time spending on visiting the nearest health facilities					
less than 5 minutes	63.6	36.4	0.007	1	
5 to 10 minutes	59.2	40.8		1.36 (0.71-2.57)	0.354
10 to 30 minutes	66.2	33.8		0.80 (0.40-1.57)	0.511
30 minutes or more	35.0	65.0		2.52 (1.07-5.95)	0.035
Severity of onset symptom					
Severe	53.3	46.7	0.034	1	
Moderate	58.0	42.0		0.87 (0.49-1.52)	0.618
Mild	73.0	27.0		0.35 (0.16-0.75)	0.007

Table 3. Multivariate analysis of factors affecting DOTS completion

Items	Completed % (n = 211)	Not completed % (n = 103)	p (univariate analysis)	OR (95% CI)	p (logistic regression model)
Gender					
Male	65.4	34.6	0.587		
Female	70.0	30.0			
Marital status					
Single	68.5	31.5	0.919		
Married	66.7	33.3			
Divorced/Widowed	60.0	40.0			
Education					
Illiteracy and primary education	62.5	37.5	0.859		
Middle school	67.9	32.1			
High school and above	68.8	31.2			
Type of household					
Rural residency	65.5	34.5	0.402		
Urban residency	80.0	20.0			
Individual annual income					
Forth quartile	86.7	13.3		1	
Third quartile	78.3	21.7		2.03 (0.91-2.69)	0.067
Second quartile	70.8	29.2		4.25 (2.61-6.86)	0.034
First quartile	50.0	50.0	0.021	6.22 (3.33-9.36)	0.022
Household debt					
No	71.1	28.9	0.031	1	
≤ 10,000 RMB	68.4	31.6		0.28 (0.03-2.67)	0.267
> 10,000 RMB	433.3	66.7		33.01 (1.17-93.21)	0.04
Proportion of medical expenditure for TB treatment in the annual income					
< 30%	76.6	23.4	0.005	1	
≥ 30%	52.9	47.1		0.77 (0.07-8.97)	0.835
Working days per week					
≤ 5 days	61.0	39.0	0.169		
> 5 days	72.5	27.5			
Status of medical insurance					
No	60.7	39.3	0.018	1	
Yes	82.1	17.9		0.06 (0.004-0.69)	0.024
Severity of onset symptom					
Severe	46.2	53.8	0.014	1	
Moderate	66.7	33.3		1.21 (0.14-10.82)	0.864
Mild	80.0	20.0		0.14 (0.01-2.69)	0.193
Adherence to drug intake and health check					
Yes (n = 299)	69.7	30.3	0.024	1	
No (n = 15)	16.7	83.3		6.14 (4.29-9.17)	0.011
Full-course supervision by community health staffs					
Yes (n = 211)	75.6	24.4	0.011	1	
No (n = 103)	51.2	48.8		12.79 (3.21-51.01)	0.019

3.3. Completion of DOTS

Among the 314 cases, the completion rate was 67.2% (211/314). During the duration of treatment, patients self-reported good adherence to daily drug intake and regular health checks accounted for 95.2% (299/314) and the proportion of participants that received full-course supervision by community health staffs was 59.2% (211/314).

Besides univariate analysis, we performed a multivariate logistic regression to control possible confounding of the influence on treatment outcomes. Individual annual income, household debt, status of medical insurance, proportion of medical expenditure for TB treatment in the annual income, adherence to drug intake and health checks, and full-course supervision by

community health staffs were identified as independent factors affecting health completion of DOTS (Table 3).

4. Discussion

Among migrant TB patients registered in twelve counties of Shandong Province, our study identified a relevant amount of migrant TB patients with delayed diagnosis (40.8%) and who did not complete DOTS (32.8%). Delayed TB diagnosis and treatment outcomes of migrant TB patients were reported poor elsewhere in urban China as well. The cure rate of smear-positive TB patients was 55% in migrants in Shanghai (18). Similar results were reported in Beijing that the cure rate among the smear-positive migrant population was 49% (19). The delayed diagnosis in our study was lower

than in a previous study, reporting that 68% of migrants delayed for more than two weeks before seeking care for symptoms suggestive of TB, in Chongqing (6).

The study results confirmed there is an economic barrier to accessing TB diagnosis, even though recently the free TB treatment policy has been widely provided to those registered migrant patients as well in TB dispensaries. Poor financial and insured status is closely related to the migrant population's seeking diagnosis and completion of DOTS, as indicated in several previous studies (6,20-21). The free treatment covered drug use, healthcare and medical tests during DOTS; but not additional treatment for side effects such as liver protection drugs. On the other hand, the costs of seeking health care and referral from general hospitals still represented a heavy financial burden. Our survey suggests the limited impact of such a free treatment policy on their financial burden, finding that medical expenditure for TB treatment still accounted for a relevant proportion of their annual income. Therefore, substantially, besides the basic package of TB treatment, the range of reimbursement should be extended and cover those additional but necessary costs in the process of case detection and treatment. Improvement in medical insurance and social security for migrants is crucial for the effective control of TB in China (22-23).

Moreover, we found the initial case detection rate among the participants was 52.9%, which did not meet the goal of 70% case detection made by the World Health Organization (WHO) (24). Delayed case detection leads to not only potential risk to public health, but also an increased financial burden for the patients due to the prolonged treatment process. Our study found that a relevant number of participants sought diagnosis at community health centers and general hospitals, rather than TB dispensaries, which provide a free TB treatment course and are recommended as the best one compared to other healthcare facilities such as community health centers and general hospitals. Community health centers tend to respond to basic healthcare and public health services, and the technical capacity for case detection is limited; while general hospitals provide advanced healthcare services and has less specialization for TB. The costs attending general hospitals are much more expensive than that in TB dispensaries, leading to the heavy financial burden for the patients (25). Deficient knowledge about the free treatment provided by TB dispensaries among migrant patients contributes to the low initial case detection rate and needs to be addressed.

We found that those working more than five days per week tended to have a higher proportion of patient delay. Recently in China, most migrant populations are working in a poor environment, such as prolonged working hours and lack of vacation.

Relevant workers are working overtime forcibly or for economic incentives. Therefore, working conditions profoundly affect health care seeking behavior and TB detection. Moreover, the fact indicated in this study that knowledge of TB and the current free treatment policy are deficient among the migrant population and may further make the barrier difficult to seek diagnosis. Delay of TB diagnosis has not only a negative impact on treatment outcomes, but also potential to spread the disease in the working place. Strategies need to focus on strengthening their labor, medical security and health education (23).

Full-course supervision by health workers with regular follow-up and patient's adherence significantly improved DOTS completion, as it has been reported significant among other populations as well (11,26). On the other hand, due to various reasons, for example, long working times and irregular living places on the patient's side and lack of human resources and budgets on the health worker's side, recently it is often difficult to implement full-course supervision for migrant TB patients. Therefore, measures to ensure full-course supervision for migrant patients remains an important issue in the local health system.

We admitted that there have been some limitations in this study. First, we targeted those TB patients registered in CTD, which was the only feasible way to access the population. Because a relevant proportion of migrant patients were unable to be accessed due to the characteristics of migration and the potential social stigma to such a vulnerable population, the sample may have a constrained representativeness. Moreover, due to a retrospective study design, migrant TB patients may have a recall bias as their answer. Nevertheless, the questionnaire focused on what happened during the year prior to the study, in order to reduce the bias.

In conclusion, the results of this study indicated that problems remain in the surveyed migrant TB patients such as delayed diagnosis, low case detection rate, lack of knowledge on the national free treatment policy and a low completion rate of DOTS. Factors affecting detection and treatment were present in their financial conditions, working condition, and accessibility of related TB care. Due to additional costs, the free treatment policy has a limited impact on reduction of their financial burden. Improvement of migrants' working conditions and accessibility of specialized TB care is essential and is expected to lead to better case detection and treatment completion.

Acknowledgements

This study is granted by Chinese Tuberculosis Control Program of the Global Fund to Fight AIDS, Tuberculosis and Malaria and China Center for Disease Control and Prevention (Fund ID: TB08-004) and Shandong Excellent Young Scientist Research Award

Fund (Fund ID: BS2012SF010). We wish to express our sincere thanks to the officers of local health agencies and all participants and staffs at the study sites for their cooperation.

References

1. The Central People's Government of the People's Republic of China. The National Tuberculosis Control and Prevention Plan 2011-2015. http://www.gov.cn/zwqk/2011-12/06/content_2012869.html (Accessed June 14, 2012).
2. Xianyi C, Fengzeng Z, Hongjin D, Liya W, Lixia W, Xin D, Chin DP. The DOTS strategy in China: Results and lessons after 10 years. *Bull World Health Organ.* 2002; 80: 430-436.
3. National Population and Family Planning Commission of P.R.China. Chinese migrant population development report 2011. China Population Press, Beijing, China, 2011.
4. Wilkinson G. Treating a hidden problem: Tuberculosis among China's 'floating people'. *J R Soc Promot Health.* 2000; 120:76-77.
5. Peng Y, Chang W, Zhou H, Hu H, Liang W. Factors associated with health-seeking behavior among migrant workers in Beijing, China. *BMC Health Serv Res.* 2010; 10:69.
6. Long Q, Li Y, Wang Y, Yue Y, Tang C, Tang S, Squire SB, Tolhurst R. Barriers to accessing TB diagnosis for rural-to-urban migrants with chronic cough in Chongqing, China: A mixed methods study. *BMC Health Serv Res.* 2008; 8:202.
7. Jia ZW, Jia XW, Liu YX, Dye C, Chen F, Chen CS, Zhang WY, Li XW, Cao WC, Liu HL. Spatial analysis of tuberculosis cases in migrants and permanent residents, Beijing, 2000-2006. *Emerg Infect Dis.* 2008; 14:1413-1419.
8. Li T, He XX, Chang ZR, Ren YH, Zhou JY, Ju LR, Jia ZW. Impact of new migrant populations on the spatial distribution of tuberculosis in Beijing. *Int J Tuberc Lung Dis.* 2011; 15:163-168.
9. Wang W, Wang J, Zhao Q, Darling ND, Yu M, Zhou B, Xu B. Contribution of rural-to-urban migration in the prevalence of drug resistant tuberculosis in China. *Eur J Microbiol Infect Dis.* 2011; 30:581-586.
10. Tobe R, Xu L, Song P, Huang Y. Migrant population, directly-observed treatment strategy (DOTS), tuberculosis control, China. *Biosci Trends.* 2011; 5:226-230.
11. Xu L, Gai R, Wang X, Liu Z, Cheng J, Zhou C, Liu J, Zhang H, Li H, Tang W. Socio-economic factors affecting the success of tuberculosis treatment in six counties of Shandong Province, China. *Int J Tuberc Lung Dis.* 2010; 14:440-446.
12. Xu L, Jian-Zhong X, Xue-Mei L, Bao-Feng G. Drug susceptibility testing guided treatment for drug-resistant spinal tuberculosis: A retrospective analysis of 19 patients. *Int Surg.* 2013; 98:175-180.
13. Hu Y, Hoffner S, Wu L, Zhao Q, Jiang W, Xu B. Prevalence and the genetic characterization of second-line and extensively drug resistant Mycobacterium tuberculosis in rural China. *Antimicrob Agents Chemother.* 2013. (doi: 10.1128/AAC.00102-13)
14. Wang W, Wang J, Zhao Q, Darling ND, Yu M, Zhou B, Xu B. Contribution of rural-to-urban migration in the prevalence of drug resistant tuberculosis in China. *Eur J Clin Microbiol Infect Dis.* 2011; 30:581-586.
15. Shandong Province Statistical Bureau. Analysis of current status, characteristics and employment of migrant population in Shandong Province. http://www.stats.gov.cn/tjfx/dfcx/t20090702_402569778.html (Accessed June 14, 2012).
16. Li R, Li H, Li Y, Li S, Fu G. Mid-evaluation on carrying out "TB control planning of China (2001-2010)" in Shandong Province. *Modern Prev Med.* 2007; 34:3939-3940.
17. Li Y, Wang Z. Analysis on tuberculosis incidence data in Shandong Province. *Prev Med Tribut.* 2011; 17:368-370.
18. Shen G, Xue Z, Shen X, Sun B, Gui X, Shen M, Mei J, Gao Q. The study recurrent tuberculosis and exogenous reinfection, Shanghai, China. *Emerg Infect Dis.* 2006; 12:1776-1778.
19. Zhang LX, Tu DH, An YS, Enarson DA. The impact of migrants on the epidemiology of tuberculosis in Beijing, China. *Int J Tuberc Lung Dis.* 2006; 10:959-962.
20. Wei X, Chen J, Chen P, Newell JN, Li H, Sun C, Mei J, Walley JD. Barriers to TB care for rural-to-urban migrant TB patients in Shanghai: A qualitative study. *Trop Med Int Health.* 2009; 14:754-760.
21. Wang W, Jiang Q, Abdullah ASM, Xu B. Barriers in accessing to tuberculosis care among non-residents in Shanghai: A descriptive study of delays in diagnosis. *Eur J Public Health.* 2007; 17:419-423.
22. Liang QF, Pang Y, Chen QY, Lin SF, Lin J, Zhao Y, Wei SZ, Zheng JF, Zheng SH. Genetic profile of tuberculosis among the migrant population in Fujian Province, China. *Int J Tuberc Lung Dis.* 2013; 17:655-661.
23. Li X, Jiang S, Li X, Mei J, Zhong Q, Xu W, Li J, Li W, Liu X, Zhang H, Wang L. Predictors on delay of initial health-seeking in new pulmonary tuberculosis cases among migrants population in East China. *PLoS One.* 2012; 7:e31995.
24. World Health Organization. Global Tuberculosis Control: Surveillance, Planning, and Financing. WHO, Geneva, Switzerland, 2008.
25. Gai R, Xu L, Wang X, Liu Z, Cheng J, Zhou C, Liu J, Zhang H, Li H, Kuroiwa C. The role of village doctors on tuberculosis control and the DOTS strategy in Shandong Province, China. *Biosci Trends.* 2008; 2:181-186.
26. Walley JD, Khan MA, Newell JN, Khan MH. Effectiveness of the direct observation component of DOTS for tuberculosis: A randomized controlled trial in Pakistan. *Lancet.* 2001; 357:664-669.

(Received February 11, 2013; Revised April 1, 2013; Re-revised June 5, 2013; Accepted June 10, 2013)

A recombinant protein containing highly conserved hemagglutinin residues 81-122 of influenza H5N1 induces strong humoral and mucosal immune responses

Ye Li^{1,2}, Lanying Du^{2,*}, Hongjie Qiu³, Guangyu Zhao³, Lili Wang², Yusen Zhou³, Shibo Jiang^{2,4}, Jimin Gao^{1,*}

¹ School of Medical Laboratory Science, Wenzhou Medical College, Wenzhou, Zhejiang, China;

² Lindsley F. Kimball Research Institute, New York Blood Center, New York, NY, USA;

³ State Key Laboratory of Pathogen and Biosecurity, Beijing Institute of Microbiology and Epidemiology, Beijing, China;

⁴ Key Laboratory of Medical Molecular Virology of Ministries of Education and Health, Shanghai Medical College and Institute of Medical Microbiology, Fudan University, Shanghai, China.

Summary

Influenza has long been considered a serious global health threat. The highly pathogenic avian influenza A virus (IAV) H5N1, particularly the currently identified IAV/H7N9 in humans in China, illustrates that influenza is still a significant public health problem. Due to the high mortality of H5N1, development of safe and effective vaccines against divergent strains of H5N1 influenza virus, especially the one capable of inducing both strong systemic and local immune responses in the vaccinated targets, is a challenge of immediate importance. In the present study, we designed two recombinant proteins containing highly conserved hemagglutinin (HA) residues 81-122 of H5N1 fused with Fc of human IgG (HA-81-122-Fc) and/or foldon (Fd) trimeric motif (HA-81-122-Fdc), and identified their immunogenicity in vaccinated mice. We found that HA-81-122-Fc and HA-81-122-Fdc proteins formed high molecular weight dimer and oligomer, respectively, and induced potent IgG antibodies in vaccinated mouse sera and lung wash. Stronger IgG1 (Th2-associated) and IgG2 (Th1-associated) antibody responses could be raised in the sera of mice following last vaccination of HA-81-122-Fdc than those raised by HA-81-122-Fc vaccination. Importantly, HA-81-122-Fdc is able to elicit high titers of IgA antibodies in vaccinated mouse lung wash and sera through the parenteral immunization pathway. Our data demonstrated that the recombinant protein containing highly conserved HA residues 81-122 of H5N1 fused with Fd and Fc could induce strong local mucosal and systemic humoral immune responses in the vaccinated animals, revealing the possibility of developing an effective Fc-mediated mucosal influenza vaccine.

Keywords: Influenza, H5N1 vaccine, hemagglutinin, conserved sequences, mucosal responses

1. Introduction

The highly pathogenic avian influenza A virus (IAV) H5N1, particularly the currently identified IAV/H7N9 in

humans in China (1), illustrates that influenza is still a significant public health problem. According to the WHO report, H7N9 maintains about 25% of death rate as of May 08, 2013 (http://www.who.int/csr/don/2013_05_08/en/), while H5N1 is more pathogenic, with the cumulative fatality rate approaching 60% (http://www.who.int/influenza/human_animal_interface/EN_GIP_20130426CumulativeNumberH5N1cases.pdf). Accordingly, the H5N1 virus remains a greater concern of influenza pandemic, although the possibility of efficient human-to-human transmission of the virus has been rare (2-4). Therefore, development of antiviral agents and efficient vaccines against highly pathogenic avian influenza

*Address correspondence to:

Dr. Lanying Du, Lindsley F. Kimball Research Institute, New York Blood Center, New York, NY 10065, USA.
E-mail: Ldu@NYBloodCenter.org

Dr. Jimin Gao, School of Medical Laboratory Science, Wenzhou Medical College, Wenzhou, Zhejiang 325035, China.

E-mail: jimingao64@163.com

(HPAI) H5N1 virus is an urgent task.

Recombinant subunit vaccines incorporating antigenic viral membrane glycoproteins, especially hemagglutinin (HA), are attractive vaccine candidates since they are able to induce virus-neutralizing antibodies (5-7). The HA subunit 1 (HA1) has been previously shown as an important antigen to induce neutralizing antibodies and protect against IAV challenge (5,8). The amino acids of HA1 tend to develop continuous mutation, but some conserved regions with limited changes are still found throughout the passage. Thus, development of novel vaccines based on these conserved sequences would be practicable against divergent virus strains. Using a broadly neutralizing antibody, we have identified a novel and highly conserved conformational epitope centered on residues 81-122 of HA1 of H5N1 virus (9), further providing important information to develop a universal vaccine based on the identified sequence. In this study, we fused the conserved HA sequences covering residues 81-122 of influenza H5N1 with Fc of human IgG and/or foldon (Fd) to express recombinant proteins, and detected their ability to induce systemic and local immune responses in vaccinated mice in order to develop an Fc-mediated, HA1 conserved sequence-based vaccine to prevent H5N1 influenza virus infection.

2. Materials and Methods

2.1. Ethics statement

The study of animals was approved by the Institutional Animal Care and Use Committee at the New York Blood Center (Approval #322.02). All animal studies were carried out in strict accordance with the recommendations of the American Veterinary Medical Association (AVMA) Guidelines and the approved protocols.

2.2. Construction, expression and purification of recombinant proteins

The construction, expression and purification of recombinant HA-81-122 proteins fused with Fc plus Fd (HA-81-122-Fdc) or without Fd (HA-81-122-Fc), were performed following our previously described protocols with some modifications (5,10). Briefly, the genes encoding HA1 residues 81-122 of A/Anhui/1/2005(H5N1) (AH/1) (GenBank:ABD28180) fused with Fd were amplified by polymerase chain reaction (PCR) using our previously constructed HA1-Fdc plasmid (5), and overlapping primers covering Fd as the template and inserted into Pfuse-hlgG1-Fc2 expression vector (hereinafter named Fc, InvivoGen, San Diego, CA, USA) to construct HA-81-122-Fdc recombinant. HA-81-122-Fc was constructed by directly digesting HA-81-122 PCR product and inserting into Fc vector. The sequence-confirmed recombinant

plasmids were transfected into 293T cells (ATCC, Manassas, VA, USA) seeded 24 h prior to transfection, using the calcium phosphate method. Culture medium was replaced by fresh Dulbecco's modified Eagle's medium (DMEM) (Invitrogen, Grand Island, NY, USA) 10 h later, and supernatant was collected 72 h post-transfection. The recombinant HA-81-122-Fdc and HA-81-122-Fc proteins in the supernatant were purified by Protein A affinity chromatography (GE Healthcare, Piscataway, NJ, USA) according to the manufacturer's instructions. Constructed recombinants were shown in Figure 1A.

2.3. SDS-PAGE, N-PAGE, Cross-linker and Western blot

Purified HA-81-122 proteins were analyzed by sodium dodecyl sulfate polyacrylamide gel electrophoresis (SDS-PAGE) and Western blot, as previously described (5) using our developed anti-HA HA-7 monoclonal antibody (mAb). Briefly, purified proteins were either non-boiled or boiled at 95°C for 5 min and separated by 10% Tris-Glycine SDS-PAGE gels, which were then stained with Coomassie Blue or transferred to nitrocellulose membranes. After blocking overnight at 4°C, the blots were incubated with HA-7 mAb (1:3,000) for 1 h at room temperature. After three washes, the blots were then incubated with horseradish peroxidase (HRP)-conjugated goat anti-mouse IgG (1:5,000, Invitrogen) for 1 h at room temperature. Signals were visualized with ECL Western blot substrate reagents and Amersham Hyperfilm (GE Healthcare).

Native PAGE (N-PAGE) and cross-linker analyses were done as before (10). For N-PAGE, the proteins were first separated by 6% N-PAGE gels using N-PAGE sample buffer and running buffer (Invitrogen), followed by the same protocols as above. For protein cross-linker detection, 4.5 µg of purified proteins were respectively mixed with 20 µl of 0.1% glutaraldehyde (final concentration 4 mM) and left at room temperature in the dark for 2 h before SDS-PAGE and Coomassie Blue staining as described above.

2.4. Vaccination protocol

Groups of five female BALB/c mice at 6-8 weeks were respectively subcutaneously (*s.c.*) primed-vaccinated with 20 µg/mouse of HA-81-122-Fdc and HA-81-122-Fc proteins resuspended in phosphate buffered saline (PBS) in the presence of Montanide ISA 51 adjuvant (SEPPIC, Fairfield, NJ, USA) and boosted twice with 10 µg/mouse of immunogen containing adjuvant ISA 51 at 3-week intervals. Control mice were *s.c.* injected with the same volume of PBS/Montanide ISA 51.

2.5. Sample collection

Sera were collected before immunization and 10 days

post-each vaccination to detect HA-specific antibodies by a rapid, simple, and humane submandibular bleeding method (11) with some modifications. Briefly, mice were anesthetized and held from the scruff of the neck in the air to establish the most relaxed situation. A sterile 18G1 needle was then poked to the cheek of mice with enough force to create a small stick hole so that drops of blood would exude from the point of penetration. This bleeding method may consistently yield a reasonable blood volume, and it is much more humane. Collected sera were retained for enzyme-linked immunosorbent assay (ELISA) analysis. For the collection of lung wash, after sacrifice of mice, a midline incision was made over the neck aspect of the ventral. A small hole was cut in the trachea with small surgical scissors. Around 800 μ L/mice of sterile PBS were slowly injected into the alveoli through tracheal lumen of mice and then drained from the alveoli by using a 1 mL syringe. This procedure was repeated 3 times.

2.6. ELISA

The IgG antibody responses and/or subtypes were evaluated by ELISA in the collected mouse sera and lung wash, as previously described (5) with some modifications. Briefly, 96-well ELISA plates were precoated, respectively, with recombinant HA-81-122-Fdc and HA-81-122-Fc fusion proteins at 4°C overnight and blocked with 2% non-fat milk at 37°C for 2 h. Serially diluted mouse sera and lung wash were added to the plates and incubated at 37°C for 1 h, followed by four washes. Bound antibodies were incubated with HRP-conjugated goat anti-mouse IgG (1:2,000, Invitrogen), anti-mouse IgG1 (1:2,000, Bethyl Laboratories, Montgomery, TX, USA) or anti-mouse IgG2a (1:2,000, Invitrogen), respectively, for 1 h at 37°C. The reaction was visualized by substrate 3,3',5,5'-Tetramethylbenzidine (TMB) (Invitrogen) and stopped by 1 N H₂SO₄. The absorbance at 450 nm (A450) was measured by ELISA plate reader (Tecan, San Jose, CA, USA).

Secretory anti-HA IgA antibody responses in lung wash were measured by ELISA using protocols similar to those described above, except for the addition of lung lavage fluid at 50 μ L/well or sera (1:50, 50 μ L/well) in duplicate wells of the plates. The HRP-conjugated goat anti-mouse IgA (Invitrogen) was added at a dilution of 1:2,000, followed by measuring the absorbance at A450.

2.7. Statistical analysis

Values were presented as mean with standard deviation (SD). Statistical significance among different groups was calculated by Student's *t*-test using *Stata* statistical software. *P* values less than 0.05 were considered significant.

3. Results

3.1. Recombinant HA-81-122-Fc and HA-81-122-Fdc proteins formed high molecular weight dimeric and oligomeric structures

The highly conserved sequences of HA-81-122 of A/Anhui/1/2005 (H5N1-HA) containing 44 amino acid residues were fused with or without Fd, followed by insertion in-frame to the Fc vector, generating recombinant HA-81-122-Fdc and HA-81-122-Fc, respectively, with IL2ss signal sequence of the Fc vector as the signal sequence (Figure 1B). The recombinant proteins were expressed in the culture supernatant of transfected 293T cells, followed by purification of the protein using protein A columns. The purified proteins were analyzed by SDS-PAGE, N-PAGE and Cross-linker, followed by Coomassie Blue staining, and the reactivity was determined by using an HA1-specific monoclonal antibody (HA-7 mAb) developed in our laboratory (9). As shown in Figure 1C, one clear band was observed in the corresponding samples of both non-boiled and boiled HA-81-122-Fc and HA-81-122-Fdc proteins analyzed by reducing SDS-PAGE, with the molecular weight of the non-boiled proteins (dimers) equaling almost 2-fold that of the boiled proteins (monomers), which contain influenza HA-81-122 with the Fc region (CH2 and CH3 domains) of the human IgG1 heavy chain and the hinge region and/or Fd. The above results demonstrated that highly purified proteins could be obtained from the transfected culture supernatant and that the expressed proteins fused with Fc and/or Fd formed conformational structures. These purified HA-81-122 proteins could be further recognized by the HA1-specific HA-7 mAb, as indicated by Western blot (Figure 1D), revealing their high specificity to the HA1 of H5N1.

Since the reducing SDS-PAGE could not reflect the actual size of the expressed protein, we used a crosslinking assay and N-PAGE for further detection of the molecular weight of these proteins. Results from the crosslinking analysis showed that the crosslinked HA-81-122-Fc and HA-81-122-Fdc formed high molecular weight dimer or oligomer, respectively, while non-crosslinked proteins retained their monomeric status (Figure 1E). N-PAGE analysis identified oligomeric structures of these proteins, with HA-81-122-Fdc showing the highest molecular weight (Figure 1F). The above results indicate that the expressed HA1 fused with Fc and/or Fd is able to polymerize into high molecular weight dimer or oligomer, maintaining conformational structures.

3.2. HA-81-122 protein fused with Fd and Fc induced strong humoral immune responses in both vaccinated mouse sera and lung wash

In order to evaluate the ability of HA-81-122-Fdc and

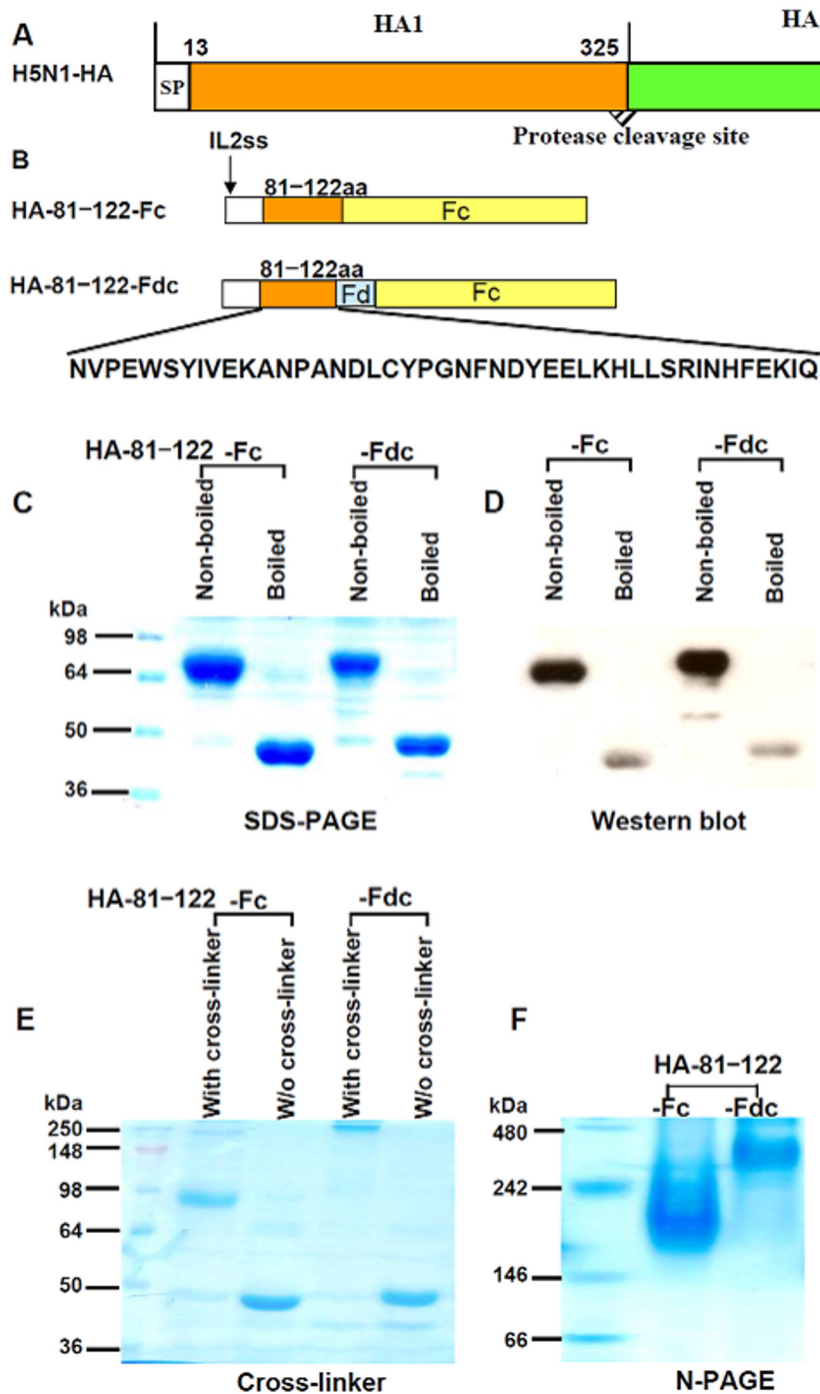


Figure 1. Construction of recombinant protein fragments and analysis of the expression of HA-81-122-Fc and HA-81-122-Fdc proteins. (A) Schematic outline of A/Anhui/2005(H5N1) HA protein (H5N1-HA). H5N1-HA is composed of signal peptide (SP) at the 5' terminus, HA1 subunit with protease cleavage site at its 3' terminus, and HA2 subunit with fusion peptide (FP) at its 5' terminus. (B) Construction of HA-81-122 recombinant fragments, respectively fused with Fc (HA-81-122-Fc) and Fd plus Fc (HA-81-122-Fdc). Signal peptide IL2ss was constructed at the 5' terminus of the recombinants to lead expressed proteins to the culture supernatant. Lower panel shows the amino acid residues of HA-81-122. The expression of the HA-81-122 proteins fused with Fc and/or Fd was detected by SDS-PAGE followed by Coomassie Blue staining (C), Western blot using an HA-specific HA-7 mAb (D), Cross-linker (E) and N-PAGE (F). The proteins without cross-linker (w/o cross-linker) were used as the controls. The protein molecular weight marker (kDa) is indicated on the left.

HA-81-122-Fc proteins with conformational structures in inducing specific immune responses, we vaccinated mice using these proteins and detected IgG antibody responses by ELISA in the collected mouse sera and lung wash. As shown in Figure 2A, recombinant HA proteins, particularly HA-81-122-Fdc, induced a high

level of serum IgG antibody response specific to HA-81-122 fusion proteins, with the antibody titer quickly reaching a high level after the first vaccination. The increase of the boost vaccination did not significantly improve the antibody titer, suggesting that one immunization dose could elicit sufficient antibody

response. The IgG antibody response raised by HA-81-122-Fdc was relatively higher than that raised by HA-81-122-Fc. An average end-point antibody titer of $1:5.2 \times 10^7$ was detected in the mouse sera collected at 10 days post-last boost (Figure 2B). In addition, HA-81-122-Fdc elicited a significantly higher level of HA-specific IgG than HA-81-122-Fc in the vaccinated

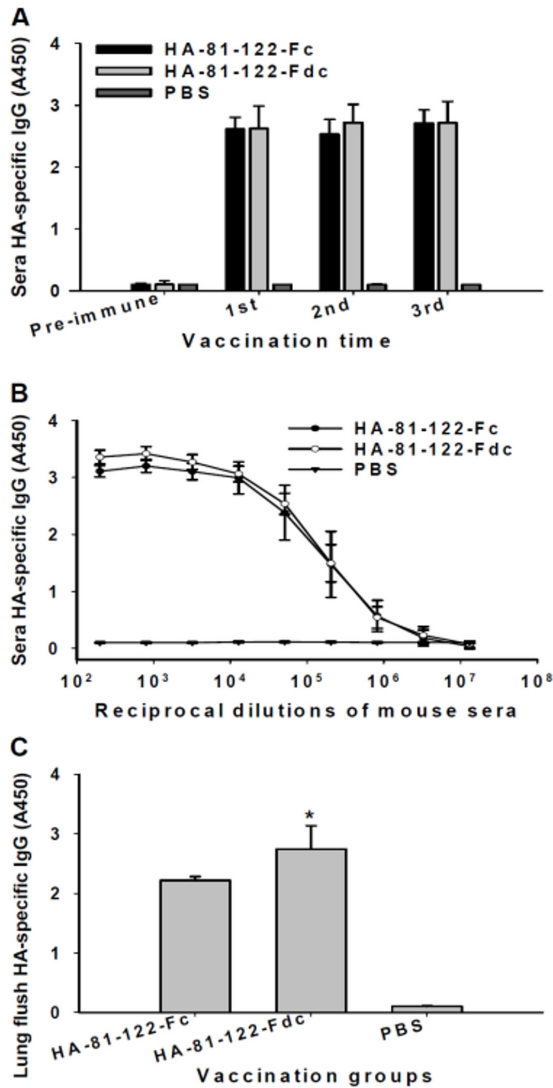


Figure 2. Detection of antigen-specific IgG antibody responses by ELISA in HA-81-122 fusion protein-vaccinated mouse sera and lung wash. PBS was used as the negative control. (A) Reactivity of antigen-specific IgG antibody response with HA-81-122-Fc or HA-81-122-Fdc protein in the vaccinated mouse sera. The ELISA plates were respectively coated with HA-81-122-Fc or HA-81-122-Fdc, and IgG was detected using sera (1:3,200) from mice before immunization (pre-immune) and 10 days after each boost. The data are presented as mean A450 \pm S.D. of five mice per group. (B) Ability of IgG to bind the recombinant proteins was detected using mouse sera from 10 days post-last vaccination. The data are presented as mean A450 \pm S.D. of five mice per group at various dilution points. (C) Reactivity of IgG with HA-81-122-Fc or HA-81-122-Fdc protein in the vaccinated mouse lung wash from 10 days post-last vaccination. The data are presented as mean A450 \pm S.D. of five mice per group. * indicates significant difference ($p < 0.05$) between HA-81-122-Fdc and other groups.

mouse lungs (Figure 2C). In contrast, no IgG antibody response was detectable in the sera and lungs of control mice injected with PBS plus adjuvant (Figure 2).

To further evaluate whether immunization with HA-81-122-Fdc and HA-81-122-Fc fusion proteins could activate and differentiate native T lymphocytes into either CD4+ T helper 1 (Th1) or T helper 2 (Th2) cells and identify which T helper cell subsets were more functional, IgG1 (Th2) and IgG2a (Th1) subtypes induced by HA-81-122-Fdc and HA-81-122-Fc proteins were detected in the mouse sera collected at 10 days post-last vaccination. The results showed that the expressed HA proteins could elicit HA-specific antibodies in the vaccinated mouse sera, respectively belonging to the IgG1 (Th2-associated, Figure 3A) and IgG2a (Th1-associated, Figure 3B) subclasses, reaching an end-point antibody titer of $1:5.2 \times 10^7$ and 2.1×10^8 , respectively. In particular, higher molecular weight HA-81-122 protein fused with Fd plus Fc (HA-81-122-Fdc) induced a higher level of IgG1 antibodies than lower molecular weight HA-81-122-Fc protein without Fd fusion. However, no HA-specific IgG1 or IgG2a antibody response was detected in the sera of PBS control mice (Figure 3).

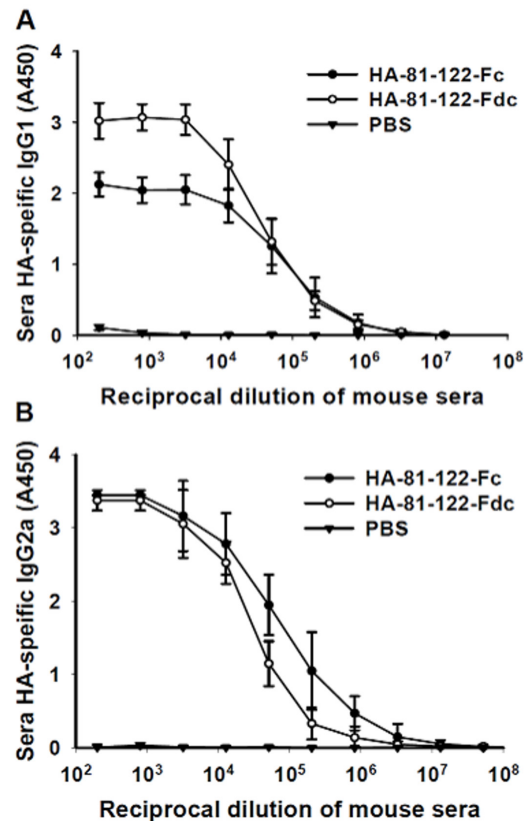


Figure 3. Measurement of IgG1 and IgG2a antibody titers by ELISA in HA-81-122 fusion protein-vaccinated mouse sera. PBS was used as the negative control. Ability of IgG1 (A) and IgG2a (B) antibodies to bind HA-81-122 proteins was detected using sera from 10 days post-last vaccination. The data are presented as mean A450 \pm S.D. of five mice per group at various dilution points.

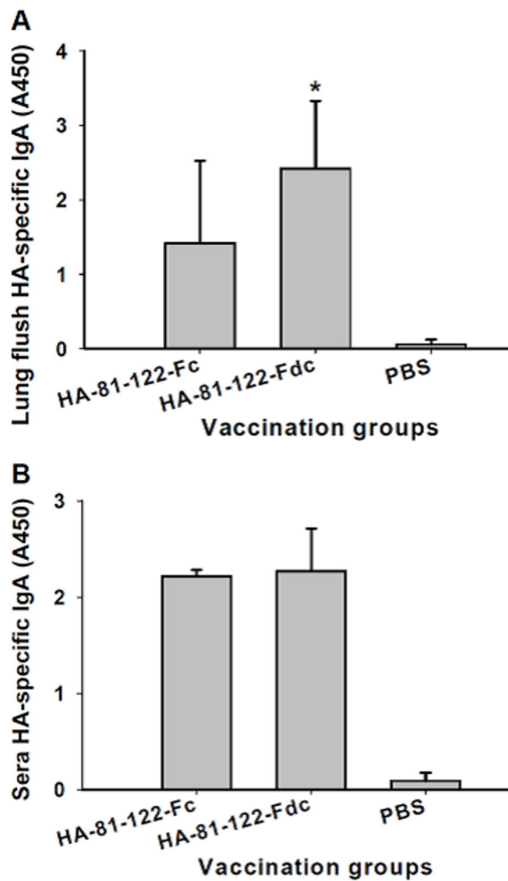


Figure 4. Detection of IgA antibody response by ELISA in HA-81-122 fusion protein-vaccinated mouse sera and lung wash. PBS was used as the negative control. Ability of IgA to bind HA-81-122 proteins was detected using lung wash (A) and sera (B) from 10 days post-last vaccination. The data are presented as mean A450 \pm S.D. of five mice per group. * indicates significant difference ($p < 0.05$) between HA-81-122-Fdc and other groups.

The above data demonstrate that expressed HA-81-122 proteins, particularly HA-81-122-Fdc, can elicit strong humoral antibody responses specific to the HA protein of H5N1 virus, implying the high immunogenicity of HA-81-122-Fdc containing oligomeric structure in stimulating elevated humoral systemic immune responses in the vaccinated mice.

3.3. HA-81-122 protein fused with Fd and Fc induced strong mucosal immune responses in both vaccinated mouse lung wash and sera

To evaluate the regional mucosal immunity potentially induced by HA-81-122 proteins, vaccinated mice were collected for lung wash 10 days post-last vaccine for the detection of mucosal IgA by ELISA. As a comparison, IgA was also evaluated in the vaccinated mouse sera. As shown in Figure 4A, the recombinant HA-81-122-Fdc protein induced a significantly higher titer of mucosal IgA responses specific to the HA protein of H5N1 in the lung wash of the vaccinated mice than HA-81-122-Fc. In addition, a higher level of IgA antibody response

could also be detected in the sera of mice vaccinated with HA-81-122-Fdc than with HA-81-122-Fc (Figure 4B). By comparison, no specific IgA was found in the lung wash or sera of the PBS control mice (Figure 4). The above data suggested that strong local immune responses could be specifically induced by HA-81-122-Fdc protein through the parenteral *s.c.* vaccination pathway.

4. Discussion

The HA of H5N1, the main surface protein of the virus, serves as an important target for inducing neutralization antibodies and/or protective immunity against HAPI H5N1 virus (12,13), and it makes a greater contribution toward the induction of neutralizing antibodies than other viral proteins, such as neuraminidase (NA), nucleoprotein (NP) and membrane protein (M2) (12,14). HA-based vaccines have been shown to elicit higher titers of neutralizing antibodies to prevent influenza virus infection in tested animals (15-18), as well as human clinical trials (19-22). The HA1 antigenic domain of HA has been demonstrated to induce an immune response equal to that of the full-size protein (23). Our previous studies have also indicated that recombinant vaccines containing the full-length HA1 fragment of H5N1 are able to induce strong immune responses in vaccinated mice, protecting against tested strains of H5N1 virus challenge (5), suggesting that the HA1 subunit of H5N1 virus is a major target for inducing protective immunity. Nevertheless, the frequent mutation of the HA1 protein makes it especially important to develop universal influenza vaccines based on the highly conserved epitopes of HA1 that potentially induce broad-spectrum protection against divergent strains of virus infections (24). It has been reported that the immunogenicity caused by direct expression of the major vaccine antigen HA protein is often low, requiring large doses of vaccines to generate a level of seroconversion consistent with protection (25,26). Because of the importance of structure-based antigen, oligomeric HA is more efficient than monomeric HA (27). However, oligomerization is usually ensured through the addition of an extraneous sequence of unknown risk for human immunization. Important to the present study, Fc fragment of human IgG is considered an important fusion tag for coexpression with several viral proteins in order to facilitate their purification and subsequent immunogenicity (25,28). Fc not only promotes correct folding of the fusion proteins following expression, but may also help to enhance binding of the antigen to antigen-presenting cells (APCs) and cell lines expressing Fc receptors (FcR) (29,30). As another antigen modification motif, the 27 amino acid-containing Fd derived from native T4 phage fibrin has been typically incorporated at the C-terminus of

collagen-like protein molecules to facilitate stabilization of protein trimers or oligomers (31-34), indicating that C-terminal Fd is essential for correct trimerization and folding of the protein.

Using a broadly neutralizing antibody, HA-7, we have previously identified a neutralizing epitope containing highly conserved sequences of residues 81-122 of H5N1 HA1, with residues 81^N, 82^V, 82A^P, 83^E, 117^H, 118^F, 119^E, 120^K, 121^I, and 122^Q as the core epitope. We showed that residues 81 to 83 exist as a loop, while residues 117 to 122 adopt a β -strand conformation, manifesting the conformational nature of the epitope (9). In the present study, we aimed to develop a novel H5N1 vaccine by fusing these conserved sequences of HA1 with Fc immunoenhancer and/or Fd trimeric motif to form native conformational structures and then detect the ability of this vaccine to induce humoral and mucosal immunity in vaccinated mice. As expected, the expressed HA-81-122-Fdc and HA-81-122-Fc proteins formed high molecular weight dimer or oligomer, respectively, being able to maintain conformational structures, and indeed induced strong H5N1 HA-specific IgG antibody responses in the vaccinated mouse sera following one dose of immunization. HA-specific IgG, IgG1 (Th2) or IgG2a (Th1) antibody responses were detected in the vaccinated mouse lung wash and sera collected at 10 days post-last immunization. These results suggest that conformational HA-81-122 proteins, particularly oligomeric HA-81-122-Fdc, could induce strong humoral immune responses against virus infection.

In addition to humoral immune responses, mucosal immunity characterized by secretory IgA antibody could also play an essential role in the protection against virus infection, especially those caused by influenza A virus, a mucosal pathogen infecting humans through the respiratory tract (35). Thus, an influenza vaccine potentially inducing ample mucosal immunity in the vaccinated hosts would be considered an important factor in developing effective influenza vaccines. It is reported that the induction of IgA can broaden the vaccine-induced immune response and introduce local cross-protective immune responses to reduce viral load, ensuring the best possible preparedness for the next influenza pandemic (36). IgA has also been shown to be very effective in inhibiting initial pathogen colonization without causing tissue damage (37,38). However, it is generally believed that local protective antibody responses at the respiratory tract are not easily induced by parenteral vaccine pathways (39), such as *s.c.*, intramuscular (*i.m.*) or intradermal (*i.d.*) administration.

In this study, we found that parenteral *s.c.* immunization of mice with HA-81-122-Fdc and HA-81-122-Fc proteins could, indeed, induce high level of IgA antibodies in both vaccinated mouse lung wash and sera, suggesting that HA-81-122 recombinant proteins fused with Fc and/or Fd could elicit sufficient mucosal

immunity, even when introduced parenterally, unlike some conventional inactivated vaccines which usually induce only limited local immunity *via* parenteral administration (40,41). This may partially result from the ability of FcR to transport FcR-targeted HA antigen to FcR-bearing APC cells within mucosal surfaces, enabling FcR-mediated transport of antigen across the mucosal barrier (42). The function of Fd in promoting the formation of oligomeric HA-81-122-Fdc protein could also play a role in increasing immunogenicity (10).

Antibody responses to virus HA provide essential immunity against IAV infection (26); thus, the antiviral effect of HA-81-122-based vaccines could be mediated by systemic and local antibodies to the HA antigen. Therefore, the induction of HA-81-122-specific antibody responses was necessary for HA-81-122-based vaccines in the prevention of H5N1 virus infection. Compared with the full-length HA1 protein, HA1 proteins containing residues 81-122 induced relatively lower level of HA-specific IgG antibodies in the vaccinated mouse sera (5). Although no data are currently available to compare the mucosal immunity induced by the full-length HA1 and the HA-81-122 protein, results from the present study indicated that HA-81-122, particularly HA-81-122-Fdc fused with Fd and Fc, was able to elicit high mucosal IgA antibody response which was detected in the vaccinated mouse lungs and sera (Figure 4). No side-effects were observed in the mice vaccinated with HA-81-122 proteins fused with Fc and/or Fd. Our study further confirms the ability of Fd trimeric motif and Fc immunoenhancer in the promotion of recombinant proteins forming correct conformational structures, thus enhancing immunogenicity (10). Further studies would be needed to test the efficacy of this vaccine in other vaccination pathways, as well as its cross-protective immunity against multiple strains of influenza virus infection.

To summarize, our data showed that highly conserved HA residues 81-122 of influenza H5N1 fused with Fd and Fc of human IgG induced strong local mucosal and humoral systemic immune responses in the vaccinated animals. This study provides a sound scientific platform for the development of an effective and safe mucosal H5N1 vaccine based on the highly conserved HA residues 81-122 of influenza H5N1 to prevent future influenza outbreaks caused by avian influenza virus.

Acknowledgements

This work was supported by the National Institutes of Health (R03AI088449 to LD), the National 973 Basic Research Program of China (2011CB504706 to YZ), and Chinese Ministry of Science & Technology, Hong Kong, Macau, Taiwan Collaborative Program (201200007673 to SJ).

References

1. Gao R, Cao B, Hu Y, *et al.* Human infection with a novel avian-origin influenza A (H7N9) virus. *N Engl J Med.* 2013; 68:1888-1897.
2. Papaioanou M. Highly pathogenic H5N1 avian influenza virus: Cause of the next pandemic? *Comp Immunol Microbiol Infect Dis.* 2009; 32:287-300.
3. Hunter P. H5N1 infects the biosecurity debate. Governments and life scientists are waking up to the problem of dual-use research. *EMBO Rep.* 2012; 13:604-607.
4. Peiris JS, de Jong MD, Guan Y. Avian influenza virus (H5N1): A threat to human health. *Clin Microbiol Rev.* 2007; 20:243-267.
5. Du L, Leung VH, Zhang X, *et al.* A recombinant vaccine of H5N1 HA1 fused with foldon and human IgG Fc induced complete cross-clade protection against divergent H5N1 viruses. *PLoS One.* 2011; 6:e16555.
6. Moon HJ, Lee JS, Talactac MR, Chowdhury MY, Kim JH, Park ME, Choi YK, Sung MH, Kim CJ. Mucosal immunization with recombinant influenza hemagglutinin protein and poly gamma-glutamate/chitosan nanoparticles induces protection against highly pathogenic influenza A virus. *Vet Microbiol.* 2012; 160:277-289.
7. Wang TT, Tan GS, Hai R, Pica N, Ngai L, Ekiert DC, Wilson IA, Garcia-Sastre A, Moran TM, Palese P. Vaccination with a synthetic peptide from the influenza virus hemagglutinin provides protection against distinct viral subtypes. *Proc Natl Acad Sci U S A.* 2010; 107:18979-18984.
8. Verma S, Dimitrova M, Munjal A, Fontana J, Crevar CJ, Carter DM, Ross TM, Khurana S, Golding H. Oligomeric recombinant H5 HA1 vaccine produced in bacteria protects ferrets from homologous and heterologous wild-type H5N1 influenza challenge and controls viral loads better than subunit H5N1 vaccine by eliciting high-affinity antibodies. *J Virol.* 2012; 86:12283-12293.
9. Du L, Jin L, Zhao G, Sun S, Li J, Yu H, Li Y, Zheng BJ, Liddington RC, Zhou Y, Jiang S. Identification and structural characterization of a broadly neutralizing antibody targeting a novel conserved epitope on the influenza virus H5N1 hemagglutinin. *J Virol.* 2013; 87:2215-2225.
10. Du L, Zhao G, Sun S, Zhang X, Zhou X, Guo Y, Li Y, Zhou Y, Jiang S. A critical HA1 neutralizing domain of H5N1 influenza in an optimal conformation induces strong cross-protection. *PLoS One.* 2013; 8:e53568.
11. Golde WT, Gollobin P, Rodriguez LL. A rapid, simple, and humane method for submandibular bleeding of mice using a lancet. *Lab Anim (NY).* 2005; 34:39-43.
12. Nayak B, Kumar S, DiNapoli JM, Paldurai A, Perez DR, Collins PL, Samal SK. Contributions of the avian influenza virus HA, NA, and M2 surface proteins to the induction of neutralizing antibodies and protective immunity. *J Virol.* 2010; 84:2408-2420.
13. Wei CJ, Xu L, Kong WP, Shi W, Canis K, Stevens J, Yang ZY, Dell A, Haslam SM, Wilson IA, Nabel GJ. Comparative efficacy of neutralizing antibodies elicited by recombinant hemagglutinin proteins from avian H5N1 influenza virus. *J Virol.* 2008; 82:6200-6208.
14. Patel A, Tran K, Gray M, Li Y, Ao Z, Yao X, Kobasa D, Kobinger GP. Evaluation of conserved and variable influenza antigens for immunization against different isolates of H5N1 viruses. *Vaccine.* 2009; 27:3083-3089.
15. Kreijtz JH, Suezer Y, de MG, van den Brand JM, van AG, Schnierle BS, Kuiken T, Fouchier RA, Lower J, Osterhaus AD, Sutter G, Rimmelzwaan GF. Preclinical evaluation of a modified vaccinia virus Ankara (MVA)-based vaccine against influenza A/H5N1 viruses. *Vaccine.* 2009; 27:6296-6299.
16. Prabakaran M, Madhan S, Prabhu N, Qiang J, Kwang J. Gastrointestinal delivery of baculovirus displaying influenza virus hemagglutinin protects mice against heterologous H5N1 infection. *J Virol.* 2010; 84:3201-3209.
17. Shoji Y, Bi H, Musiyuchuk K, *et al.* Plant-derived hemagglutinin protects ferrets against challenge infection with the A/Indonesia/05/05 strain of avian influenza. *Vaccine.* 2009; 27:1087-1092.
18. Schwartz JA, Buonocore L, Suguitan A, Jr., Hunter M, Marx PA, Subbarao K, Rose JK. Vesicular stomatitis virus-based H5N1 avian influenza vaccines induce potent cross-clade neutralizing antibodies in rhesus macaques. *J Virol.* 2011; 85:4602-4605.
19. Schwarz TF, Horacek T, Knuf M, Damman HG, Roman F, Drame M, Gillard P, Jilg W. Single dose vaccination with AS03-adjuvanted H5N1 vaccines in a randomized trial induces strong and broad immune responsiveness to booster vaccination in adults. *Vaccine.* 2009; 27:6284-6290.
20. Leroux-Roels I, Roman F, Forgas S, Maes C, De BF, Drame M, Gillard P, van der Most R, Van MM, Hanon E, Leroux-Roels G. Priming with AS03 A-adjuvanted H5N1 influenza vaccine improves the kinetics, magnitude and durability of the immune response after a heterologous booster vaccination: An open non-randomised extension of a double-blind randomised primary study. *Vaccine.* 2010; 28:849-857.
21. Lakey DL, Treanor JJ, Betts RF, Smith GE, Thompson J, Sannella E, Reed G, Wilkinson BE, Wright PF. Recombinant baculovirus influenza A hemagglutinin vaccines are well tolerated and immunogenic in healthy adults. *J Infect Dis.* 1996; 174:838-841.
22. Treanor JJ, Schiff GM, Couch RB, Cate TR, Brady RC, Hay CM, Wolff M, She D, Cox MM. Dose-related safety and immunogenicity of a trivalent baculovirus-expressed influenza-virus hemagglutinin vaccine in elderly adults. *J Infect Dis.* 2006; 193:1223-1228.
23. Tonegawa K, Nobusawa E, Nakajima K, Kato T, Kutsuna T, Kuroda K, Shibata T, Harada Y, Nakamura A, Itoh M. Analysis of epitope recognition of antibodies induced by DNA immunization against hemagglutinin protein of influenza A virus. *Vaccine.* 2003; 21:3118-3125.
24. Du L, Zhou Y, Jiang S. Research and development of universal influenza vaccines. *Microbes Infect.* 2010; 12:280-286.
25. Loureiro S, Ren J, Phapugrangkul P, Colaco CA, Bailey CR, Shelton H, Molesti E, Temperton NJ, Barclay WS, Jones IM. Adjuvant-free immunization with hemagglutinin-Fc fusion proteins as an approach to influenza vaccines. *J Virol.* 2011; 85:3010-3014.
26. Garcia JM, Pepin S, Lagarde N, Ma ES, Vogel FR, Chan KH, Chiu SS, Peiris JS. Heterosubtype neutralizing responses to influenza A (H5N1) viruses are mediated by antibodies to virus haemagglutinin. *PLoS One.* 2009; 4:e7918.
27. Weldon WC, Wang BZ, Martin MP, Koutsonanos DG, Skountzou I, Compans RW. Enhanced immunogenicity of stabilized trimeric soluble influenza hemagglutinin.

- PLoS One. 2010; 5:e12466.
28. He Y, Lu H, Siddiqui P, Zhou Y, Jiang S. Receptor-binding domain of severe acute respiratory syndrome coronavirus spike protein contains multiple conformation-dependent epitopes that induce highly potent neutralizing antibodies. *J Immunol.* 2005; 174:4908-4915.
 29. Chen H, Xu X, Jones IM. Immunogenicity of the outer domain of a HIV-1 clade C gp120. *Retrovirology.* 2007; 4:33.
 30. Martyn JC, Cardin AJ, Wines BD, Cendron A, Li S, Mackenzie J, Powell M, Gowans EJ. Surface display of IgG Fc on baculovirus vectors enhances binding to antigen-presenting cells and cell lines expressing Fc receptors. *Arch Virol.* 2009; 154:1129-1138.
 31. Du C, Wang M, Liu J, Pan M, Cai Y, Yao J. Improvement of thermostability of recombinant collagen-like protein by incorporating a foldon sequence. *Appl Microbiol Biotechnol.* 2008; 79:195-202.
 32. Pakkanen O, Hamalainen ER, Kivirikko KI, Myllyharju J. Assembly of stable human type I and III collagen molecules from hydroxylated recombinant chains in the yeast *Pichia pastoris*. Effect of an engineered C-terminal oligomerization domain foldon. *J Biol Chem.* 2003; 278:32478-32483.
 33. Letarov AV, Londer YY, Boudko SP, Mesyanzhinov VV. The carboxy-terminal domain initiates trimerization of bacteriophage T4 fibritin. *Biochemistry (Mosc).* 1999; 64:817-823.
 34. Boudko SP, Londer YY, Letarov AV, Sernova NV, Engel J, Mesyanzhinov VV. Domain organization, folding and stability of bacteriophage T4 fibritin, a segmented coiled-coil protein. *Eur J Biochem.* 2002; 269:833-841.
 35. Price GE, Soboleski MR, Lo CY, Misplon JA, Quirion MR, Houser KV, Pearce MB, Pappas C, Tumpey TM, Epstein SL. Single-dose mucosal immunization with a candidate universal influenza vaccine provides rapid protection from virulent H5N1, H3N2 and H1N1 viruses. *PLoS One.* 2010; 5:e13162.
 36. Cerutti A, Cols M, Gentile M, Cassis L, Barra CM, He B, Puga I, Chen K. Regulation of mucosal IgA responses: Lessons from primary immunodeficiencies. *Ann N Y Acad Sci.* 2011; 1238:132-144.
 37. Brandtzaeg P. Induction of secretory immunity and memory at mucosal surfaces. *Vaccine.* 2007; 25:5467-5484.
 38. Brandtzaeg P. Role of secretory antibodies in the defence against infections. *Int J Med Microbiol.* 2003; 293:3-15.
 39. de Haan A, Haijema BJ, Voorn P, Meijerhof T, van Roosmalen ML, Leenhouts K. Bacterium-like particles supplemented with inactivated influenza antigen induce cross-protective influenza-specific antibody responses through intranasal administration. *Vaccine.* 2012; 30:4884-4891.
 40. Ichinohe T, Ainal A, Tashiro M, Sata T, Hasegawa H. PolyI: PolyC12U adjuvant-combined intranasal vaccine protects mice against highly pathogenic H5N1 influenza virus variants. *Vaccine.* 2009; 27:6276-6279.
 41. Kreijtz JH, Osterhaus AD, Rimmelzwaan GF. Vaccination strategies and vaccine formulations for epidemic and pandemic influenza control. *Hum Vaccin.* 2009; 5:126-135.
 42. Gosselin EJ, Bitsaktsis C, Li Y, Iglesias BV. Fc receptor-targeted mucosal vaccination as a novel strategy for the generation of enhanced immunity against mucosal and non-mucosal pathogens. *Arch Immunol Ther Exp (Warsz).* 2009; 57:311-323.
- (Received May 1, 2013; Revised May 16, 2013; Accepted May 30, 2013)

Glucose administration during volume resuscitation using dextran-40 from hemorrhagic shock ameliorates acid/base-imbalance in fasted rats under sevoflurane anesthesia

Gaku Kawamura^{1,*}, Takayuki Kitamura², Kanako Sato¹, Rui Sato¹, Yoshiteru Mori¹, Yuko Araki¹, Yoshitsugu Yamada¹

¹Department of Anesthesiology, Faculty of Medicine, The University of Tokyo, Tokyo, Japan;

²Department of Anesthesiology, Toho University Sakura Medical Center, Sakura, Japan.

Summary

The hyperglycemic response is an important prognostic factor for survival after hemorrhage. In this study, we investigated the effects of glucose administration during volume resuscitation from hemorrhagic shock in fasted rats under sevoflurane anesthesia on hemodynamics, acid/base-balance and glucose metabolism. Hemorrhagic shock was induced in rats by withdrawing 25 mL/kg of blood. For volume resuscitation, rats in group-Dextran[saline] and group-Dextran[glucose] underwent infusion therapy using 10% dextran-40 dissolved in physiological saline and 10% dextran-40 dissolved in 5% glucose, respectively. Arterial blood was sampled just before blood withdrawal, immediately after blood withdrawal, immediately after volume resuscitation and at 30 min after volume resuscitation for arterial gas analyses and measurement of plasma insulin levels. After volume resuscitation, group-Dextran[glucose] showed similar arterial blood pressure, significantly lower heart rate, similar arterial PO₂ and similar hematocrit in comparison with group-Dextran[saline], suggesting that there was no particular difference in oxygen demand/supply-balance between the two groups. After volume resuscitation, group-Dextran[glucose] showed significantly higher arterial pH, similar arterial PCO₂, significantly higher bicarbonate levels and significantly higher base excess in comparison with group-Dextran[saline], suggesting that metabolic acidosis is a cause of the difference in acid/base-balance between the two groups. After volume resuscitation, group-Dextran[glucose] showed significantly higher glucose levels, significantly higher insulin levels and significantly lower lactate levels in comparison with group-Dextran[saline]. At 30 min after volume resuscitation, base excess correlated significantly with lactate levels. These results suggest that glucose administration during volume resuscitation using dextran-40 from hemorrhagic shock ameliorates acid/base-imbalance associated with hyperlactatemia in fasted rats under sevoflurane anesthesia.

Keywords: Hyperlactatemia, glucose metabolism, energy demand/supply-balance, fluid therapy, plasma substitute

1. Introduction

Restoring blood volume is essential for the treatment of hemorrhagic shock; use of a plasma substitute is

a practical tool for expanding blood volume. Several artificial molecules have been developed as plasma substitutes, and the efficiency of these molecules on volume resuscitation have been evaluated (1-5); however, the effects of the solvent for the molecules on volume resuscitation have not been elucidated. Two kinds of molecule, dextran-40 and hydroxyethyl starch 70/0.5/4, are clinically available in Japan; dextran-40 is dissolved in either lactated-Ringer's solution or 5% glucose, and hydroxyethyl starch 70/0.5/4 is dissolved

*Address correspondence to:

Dr. Gaku Kawamura, Department of Anesthesiology, Faculty of Medicine, The University of Tokyo, 7-3-1 Hongo, Bunkyo-ku, Tokyo 113-8655, Japan.
E-mail: gaku-kawa@umin.ac.jp

in either physiological saline or lactated-Ringer's solution containing 1% glucose. The hyperglycemic response is known to be an important prognostic factor for survival after hemorrhage (6,7), suggesting the possible advantageous effects of glucose administration on volume resuscitation from hemorrhagic shock. In this study, infusion therapy using two kinds of 10% dextran-40 solution (dextran-40 dissolved in physiological saline and dextran-40 dissolved in 5% glucose) was given to fasted rats with hemorrhagic shock under sevoflurane anesthesia, and hemodynamics, acid/base-balance and glucose metabolism were evaluated.

2. Materials and Methods

2.1. Subjects

All experimental protocols were approved by the animal care committee of The University of Tokyo (protocol number: P09-125). We used 9- to 11-week-old, male, Wistar rats (Nippon Bio-Supply Center, Tokyo, Japan). Rats were housed in a regulated environment with room temperature maintained at 25°C and a 12-h light-dark cycle (7 AM and 7 PM). A standard diet (Oriental Yeast Co., Ltd., Tokyo, Japan) and water were provided *ad libitum*. Each rat was fasted for 20 h prior to the experiment; however, water was provided until the experiment started. All experiments were performed between 1 PM and 5 PM. A heat lamp and a heating pad were used to prevent hypothermia during the experiments.

2.2. Experimental protocols

Anesthesia for surgical preparation was induced with sevoflurane (Maruishi Pharmaceutical Co., Ltd., Osaka, Japan) *via* a tightly fitting face mask. After tracheotomy and tracheal intubation, sevoflurane (2.5% in 1 L/min oxygen) was administered *via* the tracheal tube, and the lungs were mechanically ventilated; and the ventilator setting was not changed throughout the experimental period. A 19-gauge catheter was inserted into the right jugular vein. Another 19-gauge catheter was inserted into the right carotid artery.

After surgical preparation, all rats were administered 100 IU of heparin intravenously to maintain patency of the catheters. Sevoflurane administration was continued, and physiological saline was administered intravenously with a bolus dose of 4 mL/kg followed by continuous infusion at a rate of 4 mL/kg/h. The arterial catheter was connected to a low volume pressure transducer for monitoring mean arterial blood pressure (MAP) and heart rate (HR).

A 30-min stabilization period was allowed, followed by 25 mL/kg of arterial blood withdrawn at a rate of 1 mL/min to induce hemorrhagic shock. Volume resuscitation was then started. Rats in group-

Dextran[saline] ($n = 8$) underwent infusion therapy using 25 mL/kg of 10% dextran-40 dissolved in physiological saline at a rate of 1 mL/min *via* the venous catheter; dextran-40 (Sigma-Aldrich Japan, Tokyo, Japan) was sterilely dissolved in physiological saline just before administration. Rats in group-Dextran[glucose] ($n = 8$) underwent infusion therapy using 25 mL/kg of 10% dextran-40 dissolved in 5% glucose (Low Molecular Dextran D Injection; Otsuka Pharmaceutical Factory, Inc., Tokushima, Japan) at a rate of 1 mL/min *via* the venous catheter.

Arterial blood (1.5 mL) was sampled just before blood withdrawal (T-1), immediately after blood withdrawal (T-2), immediately after volume resuscitation (T-3) and at 30 min after volume resuscitation (T-4).

2.3. Arterial blood gas analyses and measurement of plasma insulin levels

Immediately after each blood sampling, arterial blood gas analyses were performed using an i-STAT 1 Analyzer (Fuso Pharmaceutical Industries, Ltd., Osaka, Japan). Each blood sample was spun in a pre-refrigerated centrifuge (4°C) at $1000 \times g$ for 15 min, and plasma was stored at -60°C. Plasma insulin levels were measured by enzyme-linked immunosorbent assay using AKRIN-010T (Shibayagi Co., Ltd., Gunma, Japan).

2.4. Statistical analysis

Data are shown as means \pm S.D. Statistical analyses were performed using JMP Pro version 9.0.2. (SAS Institute, Cary, NC). For overall comparisons of serial data between the two groups, 2-way repeated-measures of analysis of variance (ANOVA), with group and time points as the factors, were used; statistical significance was set at $p < 0.05$. Homogeneity of variance was examined using a Bartlett test; statistical significance was set at $p < 0.05$. For comparisons of data with homogeneity of variance between the two groups at each time point, an unpaired *t*-test was used; statistical significance was set at $p < 0.05$. For comparisons of data without homogeneity of variance between the two groups at each time point, a Welch test was used; statistical significance was set at $p < 0.05$. Simple linear regression analysis was used to examine the correlation between base excess and lactate levels in arterial blood.

3. Results

3.1. Hemodynamics, arterial PO_2 and hematocrit

Rats in group-Dextran[saline] and group-Dextran[glucose] weighed 298 ± 26 g and 304 ± 34 g, respectively; and there was no significant difference between the two groups. Thus, there was no significant difference in the time required for blood withdrawal and volume

resuscitation between the two groups.

The time course of hemodynamics, arterial PO₂ and hematocrit are shown in Table 1.

There was no significant difference in the time course of MAP between the two groups ($p = 0.6193$, 2-way repeated-measures ANOVA). There was a significant difference in the time course of HR between the two groups ($p = 0.0064$, 2-way repeated-measures ANOVA); group-Dextran[glucose] showed significantly lower HR than group-Dextran[saline] at T-4 ($p = 0.0002$, unpaired *t*-test). There was no significant difference in the time course of arterial PO₂ between the two groups ($p = 0.0706$, 2-way repeated-measures ANOVA). There was no significant difference in the time course of hematocrit between the two groups ($p = 0.6736$, 2-way repeated-measures ANOVA).

3.2. Acid/base-balance

The time course of arterial pH, arterial PCO₂, bicarbonate

levels and base excess are shown in Table 2.

There was a significant difference in the time course of arterial pH between the two groups ($p = 0.0098$, 2-way repeated-measures ANOVA); group-Dextran[glucose] showed significantly higher arterial pH than group-Dextran[saline] at T-4 ($p = 0.0080$, Welch test). There was no significant difference in the time course of arterial PCO₂ between the two groups ($p = 0.1592$, 2-way repeated-measures ANOVA). There was a significant difference in the time course of bicarbonate levels between the two groups ($p = 0.0014$, 2-way repeated-measures ANOVA); group-Dextran[glucose] showed significantly higher bicarbonate levels than group-Dextran[saline] at T-3 and T-4 ($p = 0.0052$ and $p = 0.0007$, respectively, unpaired *t*-test). There was a significant difference in the time course of base excess between the two groups ($p = 0.0008$, 2-way repeated-measures ANOVA); group-Dextran[glucose] showed significantly higher base excess than group-Dextran[saline] at T-3 ($p = 0.0202$, unpaired *t*-test) and T-4 ($p = 0.0004$, Welch test).

Table 1. The time course of hemodynamics, arterial PO₂ and hematocrit during the experiments

Groups	Time point			
	T-1	T-2	T-3	T-4
Mean arterial blood pressure (mmHg)				
Dextran[saline]	93 ± 22	22 ± 2	78 ± 13	37 ± 11
Dextran[glucose]	84 ± 15	22 ± 2	78 ± 13	38 ± 13
Heart rate (beats/min)				
Dextran[saline]	402 ± 38	334 ± 58	448 ± 25	441 ± 26
Dextran[glucose]	367 ± 53	361 ± 53	423 ± 38	354 ± 44*
Arterial PO ₂ (mmHg)				
Dextran[saline]	511 ± 12	420 ± 78	451 ± 39	477 ± 38
Dextran[glucose]	483 ± 23	412 ± 53	489 ± 48	387 ± 138
Hematocrit (%)				
Dextran[saline]	44 ± 3	35 ± 2	12 ± 1	15 ± 3
Dextran[glucose]	42 ± 2	33 ± 1	11 ± 1	15 ± 3

Data are shown as means ± S.D. There are no significant differences in the time course of mean arterial blood pressure, arterial PO₂ and hematocrit between the two groups ($p > 0.05$ in all comparisons, 2-way repeated-measures ANOVA); however, there is a significant difference in the time course of heart rate between the two groups ($p < 0.05$ in all comparisons, 2-way repeated-measures ANOVA). * $p < 0.05$ versus group-Dextran[saline] at each time point, unpaired *t*-test.

Table 2. The time course of acid/base-balance during the experiments

Groups	Time point			
	T-1	T-2	T-3	T-4
Arterial pH				
Dextran[saline]	7.505 ± 0.038	7.614 ± 0.032	7.332 ± 0.087	7.334 ± 0.035
Dextran[glucose]	7.505 ± 0.020	7.617 ± 0.050	7.381 ± 0.039	7.437 ± 0.080†
Arterial PCO ₂ (mmHg)				
Dextran[saline]	33.8 ± 0.9	13.4 ± 2.1	33.5 ± 4.4	25.9 ± 5.9
Dextran[glucose]	31.4 ± 2.3	14.7 ± 1.1	35.3 ± 2.5	31.4 ± 9.7
Bicarbonate levels (mmol/L)				
Dextran[saline]	26.7 ± 2.2	13.6 ± 2.0	17.7 ± 2.1	13.9 ± 3.7
Dextran[glucose]	24.8 ± 1.4	15.0 ± 1.6	20.9 ± 1.8*	20.5 ± 2.3*
Base excess (mmol/L)				
Dextran[saline]	4 ± 3	-8 ± 2	-8 ± 3	-12 ± 4
Dextran[glucose]	2 ± 1	-6 ± 3	-4 ± 2*	-4 ± 2†

Data are shown as means ± S.D. There are significant differences in the time course of arterial pH, bicarbonate levels and base excess between the two groups ($p < 0.05$ in all comparisons, 2-way repeated-measures ANOVA); however, there is no significant difference in the time course of arterial PCO₂ between the two groups ($p > 0.05$, 2-way repeated-measures ANOVA). * $p < 0.05$ versus group-Dextran[saline] at each time point, unpaired *t*-test. † $p < 0.05$ versus group-Dextran[saline] at each time point, Welch test.

Table 3. The time course of glucose metabolism during the experiments

Groups	Time point			
	T-1	T-2	T-3	T-4
Blood glucose levels (mg/dL)				
Dextran[saline]	129 ± 21	193 ± 89	139 ± 61	55 ± 16
Dextran[glucose]	130 ± 21	177 ± 70	625 ± 62*	252 ± 61†
Plasma insulin levels (ng/mL)				
Dextran[saline]	0.8 ± 0.2	3.0 ± 2.5	1.7 ± 1.0	0.6 ± 0.2
Dextran[glucose]	0.9 ± 0.4	2.2 ± 1.3	6.8 ± 5.3†	5.9 ± 4.9†
Blood lactate levels (mmol/L)				
Dextran[saline]	0.83 ± 0.11	4.53 ± 1.10	4.71 ± 1.56	8.38 ± 3.65
Dextran[glucose]	0.75 ± 0.09	4.09 ± 1.32	3.14 ± 0.82*	3.76 ± 1.07†

Data are shown as means ± S.D. There are significant differences in the time course of blood glucose levels, plasma insulin levels and blood lactate levels between the two groups ($p < 0.05$ in all comparisons, 2-way repeated-measures ANOVA). * $p < 0.05$ versus group-Dextran[saline] at each time point, unpaired t -test. † $p < 0.05$ versus group-Dextran[saline] at each time point, Welch test.

3.3. Glucose metabolism

The time course of blood glucose levels, plasma insulin levels and blood lactate levels are shown in Table 3.

There was a significant difference in the time course of glucose levels between the two groups ($p < 0.0001$, 2-way repeated-measures ANOVA); group-Dextran[glucose] showed significantly higher glucose levels than group-Dextran[saline] at T-3 ($p < 0.0001$, unpaired t -test) and T-4 ($p < 0.0001$, Welch test). There was a significant difference in the time course of insulin levels between the two groups ($p = 0.0002$, 2-way repeated-measures ANOVA); group-Dextran[glucose] showed significantly higher insulin levels than group-Dextran[saline] at T-3 and T-4 ($p = 0.0432$ and $p < 0.0001$, respectively, Welch test). There was a significant difference in the time course of lactate levels between the two groups ($p < 0.0001$, 2-way repeated-measures ANOVA); group-Dextran[glucose] showed significantly lower lactate levels than group-Dextran[saline] at T-3 ($p = 0.0243$, unpaired t -test) and T-4 ($p = 0.0086$, Welch test).

3.4. Correlation between base excess and blood lactate levels

Base excess at T-4 significantly correlated with lactate levels at T-4 ($p < 0.0001$, $R^2 = 0.8644$, simple linear regression analysis; Figure 1).

3.5. Relationship between glucose levels and lactate levels

The mean levels of glucose and lactate in all rats at T-4 were 111 mg/dL and 6.07 mmol/L, respectively. The relationship between glucose levels at T-4 and lactate levels at T-4 was assessed using these parameters: lower glucose levels with lower lactate levels (category-I), higher glucose levels with lower lactate levels (category-II), higher glucose levels with higher lactate levels (category-III) and lower glucose levels with higher lactate levels (category-IV). All data in group-Dextran[saline] were within category-I and category-IV, while all data in group-Dextran[glucose] were within category-II (Figure 2).

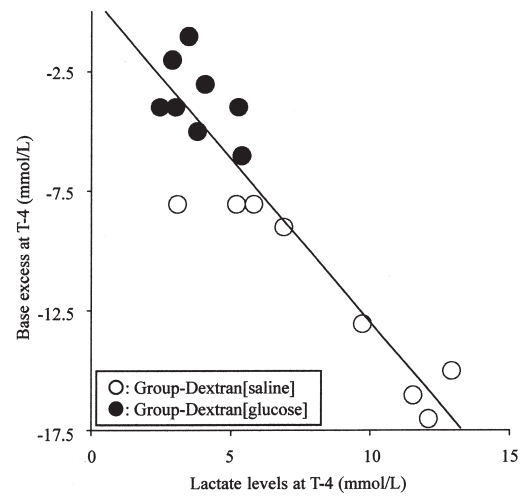


Figure 1. Correlation between base excess at T-4 and lactate levels at T-4. Simple linear regression analysis shows a significant correlation between base excess at T-4 and lactate levels at T-4 ($p < 0.0001$, $R^2 = 0.8644$).

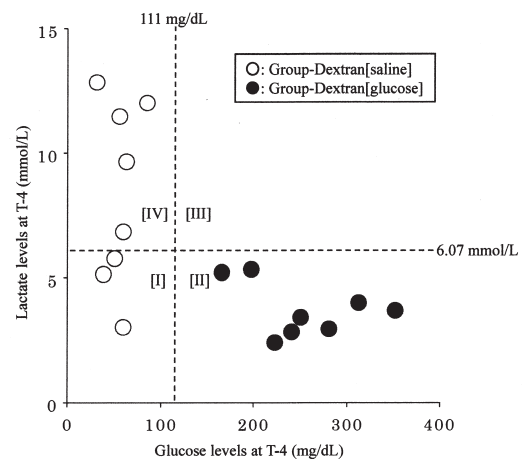


Figure 2. Relationship between glucose levels at T-4 and lactate levels at T-4. The mean glucose level at T-4 in all rats is 111 mg/dL, and the mean lactate level at T-4 in all rats is 6.07 mmol/L. The relationship between glucose levels at T-4 and lactate levels at T-4 was assessed using these parameters: lower glucose levels with lower lactate levels (category-I), higher glucose levels with lower lactate levels (category-II), higher glucose levels with higher lactate levels (category-III) and lower glucose levels with higher lactate levels (category-IV).

4. Discussion

Acid/base-imbalance after volume resuscitation from hemorrhagic shock in group-Dextran[glucose] was significantly less than that in group-Dextran[saline]. It is conceivable that metabolic acidosis is a cause of the difference in acid/base-balance between group-Dextran[saline] and group-Dextran[glucose], because there were no significant difference in arterial PCO₂ throughout the experimental period between the two groups. Lactate levels after volume resuscitation from hemorrhagic shock in group-Dextran[glucose] were significantly lower than those in group-Dextran[saline]. The significant correlation between base excess at T-4 and lactate levels at T-4 reflects the contribution of hyperlactatemia to acid/base-imbalance in group-Dextran[saline], although the blood concentration of other anions (*i.e.*, citrate and acetate), which have been reported to be responsible, to some extent, for metabolic acidosis after hemorrhagic shock, were not examined (8). Volume resuscitation, using a plasma substitute alone, from hemorrhagic shock is not practical in clinical settings; however, results in this study using fasted rats suggest the possible advantageous effect of glucose administration during volume resuscitation from hemorrhagic shock.

Increased lactate production *via* anaerobic glucose metabolism due to oxygen demand/supply-imbalance (9,10), increased lactate production *via* enhanced aerobic glycolysis coupled with Na⁺, K⁺-ATPase activities in skeletal muscle (11) and impaired lactate clearance in the liver can be considered as mechanisms underlying elevated lactate levels after volume resuscitation from hemorrhagic shock.

There was no significant difference in MAP between group-Dextran[saline] and group-Dextran[glucose] throughout the experimental period. There were no significant difference in HR between group-Dextran[saline] and group-Dextran[glucose] at T-1, T-2 and T-3; however, a significant difference was detected only at T-4 between the two groups. There were no significant difference in arterial PO₂ throughout the experimental period between group-Dextran[saline] and group-Dextran[glucose]. Dilutional anemia was observed after volume resuscitation from hemorrhagic shock in both group-Dextran[saline] and group-Dextran[glucose]; and there was no significant difference in hematocrit throughout the experimental period between the two groups. Taken together, we believe that oxygen demand/supply-balance after volume resuscitation from hemorrhagic shock in group-Dextran[glucose] was not considerably different from that in group-Dextran[saline].

Rats were fasted for 20 h prior to the experiments; it is, therefore, assumable that glycogen storage in the body was markedly reduced (12). Group-Dextran[saline] showed hypoglycemia (55 ± 16 mg/dL) without increases in insulin levels (0.6 ± 0.2 ng/

mL) at T-4, suggesting shortness of energy substrates after volume resuscitation from hemorrhagic shock. Hyperlactatemia was associated with hypoglycemia at T-4 in group-Dextran[saline]; therefore, we suppose that the enhanced aerobic glycolysis coupled with Na⁺, K⁺-ATPase activities in skeletal muscle was not the cause of hyperlactatemia after volume resuscitation from hemorrhagic shock in group-Dextran[saline].

Assurance of energy demand/supply-balance is definitely important for preventing organ failure in critical situations. In group-Dextran[glucose], glucose administration during volume resuscitation from hemorrhagic shock significantly increased glucose levels, but rapid decreases in glucose levels were observed at 30 min after volume resuscitation. The rapid decreases in glucose levels with significantly higher insulin levels reflect a sufficient energy supply after volume resuscitation from hemorrhagic shock in group-Dextran[glucose]. In contrast, hypoglycemia that was not accompanied by increases in insulin levels was observed at T-4 in group-Dextran[saline], suggesting that energy supply *via* stress-induced endogenous glucose production was insufficient after volume resuscitation from hemorrhagic shock.

Among the several types of glucose transporters (GLUTs), the target molecule for insulin is GLUT-4. Glucose use in the liver is dependent on both GLUT-2 and glucokinase enzyme activities; plasma insulin levels affect hepatic glucokinase enzyme activities, although glucose uptake *via* GLUT-2 is independent of insulin (13). It was reported that co-administration of glucose with insulin during resuscitation from hemorrhagic shock increases hepatic ATP (14). Lactate is metabolized by lactate dehydrogenase in the liver, and the metabolite (*i.e.*, pyruvate) is used as an energy substrate. We, therefore, suppose that glucose administration (*i.e.*, the exogenous energy supply) during volume resuscitation from hemorrhagic shock ameliorated energy insufficiency and maintained lactate clearance in the liver, resulting in the prevention of an acid/base-imbalance related to hyperlactatemia.

The importance of maintenance of energy demand/supply-balance is generally accepted. In addition, recent studies (15-19) reported that hyperglycemia increases morbidity and mortality and hypoglycemia associated with intensive insulin therapy increases mortality, suggesting that control of blood glucose levels is important in critically ill patients. Although results in this study using fasted rats suggest possible advantageous effects of glucose administration during volume resuscitation from hemorrhagic shock, we cannot simply extrapolate the finding in this animal study to clinical practice for several reasons. First, the significance of intraoperative glucose administration under general anesthesia has been controversial. Second, glucose administration during volume resuscitation from hemorrhagic shock is not considered as a clinically

standard procedure at this moment. Third, rats in group-Dextran[glucose] showed drastic hyperglycemia (625 ± 62 mg/dL) immediately after volume resuscitation from hemorrhagic shock in this study, and adverse effects associated with hyperglycemia are well known in clinical settings. We, thus, consider that further clinical investigation is required to elucidate the efficiency of glucose administration during volume resuscitation from hemorrhagic shock; furthermore, the appropriate dose of glucose administration should be determined.

In conclusion, glucose administration during volume resuscitation using dextran-40 from hemorrhagic shock ameliorates acid/base-imbalance related to hyperlactatemia in fasted rats under sevoflurane anesthesia, suggesting the importance of maintaining energy demand/supply-balance by the exogenous energy supply in critical situations.

Acknowledgements

This work was supported by a departmental fund (Department of Anesthesiology, Faculty of Medicine, The University of Tokyo).

References

1. Braz JRC, do Nascimento P Jr, Filho OP, Braz LG, Vane LA, Vianna PTG, Rodrigues GR Jr. The early systemic and gastrointestinal oxygenation effects of hemorrhagic shock resuscitation with hypertonic saline and hypertonic saline 6% dextran-70: A comparative study in dogs. *Anesth Analg*. 2004; 99:536-546.
2. Ferreira ELA, Terzi RGG, Silva WA, de Moraes AC. Early colloid replacement therapy in a near-fatal model of hemorrhagic shock. *Anesth Analg*. 2005; 101:1785-1791.
3. Knotzer H, Pajk W, Maier S, Dunser MW, Ulmer H, Schwarz B, Salak N, Hasibeder WR. Comparison of lactated Ringer's, gelatin and blood resuscitation on intestinal oxygen supply and mucosal tissue oxygen tension in haemorrhagic shock. *Br J Anaesth*. 2006; 97:509-516.
4. Haas T, Fries D, Holz C, Innerhofer P, Streif W, Klingler A, Hanke A, Velik-Salchner C. Less impairment of hemostasis and reduced blood loss in pigs after resuscitation from hemorrhagic shock using the small-volume concept with hypertonic saline/hydroxyethyl starch as compared to administration of 4% gelatin or 6% hydroxyethyl starch solution. *Anesth Analg*. 2008; 106:1078-1086.
5. Dubniks M, Persson J, Grande P-O. Comparison of the plasma volume-expanding effects of 6% dextran 70, 5% albumin, and 6% HES 130/0.4 after hemorrhage in the guinea pig. *J Trauma*. 2009; 67:1200-1204.
6. Ljungqvist O, Jansson E, Ware J. Effects of food deprivation on survival after hemorrhage in the rat. *Circ Shock*. 1987; 22:251-260.
7. Ljungqvist O, Alibegovic A. Hyperglycemia and survival after hemorrhage. *Eur J Surg*. 1994; 160:465-469.
8. Bruegger D, Kemming GI, Jacob M, Meisner FG, Wojtczyk CJ, Packert KB, Keipert PE, Faithfull NS, Habler OP, Becker BF, Rehm M. Causes of metabolic acidosis in canine hemorrhagic shock: Role of unmeasured ions. *Crit Care*. 2007; 11:R130-143.
9. Rixen D, Siegel JH. Bench-to bedside review: oxygen debt and its metabolic correlates as quantifiers of the severity of hemorrhagic and post-traumatic shock. *Crit Care*. 2005; 9:441-453.
10. Ronco JJ, Fenwick JC, Tweeddale MG, Wiggs BR, Phang PT, Cooper DJ, Cunningham KF, Russell JA, Walley KR. Identification of the critical oxygen delivery for anaerobic metabolism in critically ill septic and nonseptic humans. *JAMA*. 1993; 270:1724-1730.
11. McCarter FD, James JH, Luchette FA, Wang L, Friend LA, King J-K, Evans JM, George MA, Fischer JE. Adrenergic blockade reduces skeletal muscle glycolysis and Na^+ , K^+ -ATPase activity during hemorrhage. *J Surg Res*. 2001; 99:235-244.
12. Ljungqvist O, Boija PO, Esahili H, Larsson M, Ware J. Food deprivation alters liver glycogen metabolism and endocrine responses to hemorrhage. *Am J Physiol*. 1990; 22:E692-698.
13. Tiedge M, Lenzen S. Effects of glucose refeeding and glibenclamide treatment on glucokinase and GLUT2 gene expression in pancreatic B-cells and liver from rats. *Biochem J*. 1995; 388:139-144.
14. Chang CG, Van Way CW III, Dhar A, Helling T Jr, Hahn Y. The use of insulin and glucose during resuscitation from hemorrhagic shock increases hepatic ATP. *J Surg Res*. 2000; 92:171-176.
15. Gandhi GY, Nuttall GA, Abel MD, Mullany CJ, Schaff HV, Williams BA, Schrader LM, Rizza RA, McMahon MM: Intraoperative hyperglycemia and perioperative outcomes in cardiac surgery patients. *Mayo Clin Proc*. 2005; 80:862-866.
16. McGirt MJ, Woodworth GF, Brooke BS, Coon AL, Jain S, Buck D, Huang J, Clatterbuck RE, Tamargo RJ, Perler BA: Hyperglycemia independently increases the risk of perioperative stroke, myocardial infarction, and death after carotid endarterectomy. *Neurosurgery*. 2006; 58:1066-1073.
17. Ammori JB, Sigakis M, Englesbe MJ, O'Reilly M, Pelletier SJ: Effects of intraoperative hyperglycemia during liver transplantation. *J Surg Res*. 2007; 140:227-233.
18. Van den Berghe G, Wousters P, Weekers F, Verwaest C, Bruyininckx F, Schetz M, Vlasselaers D, Ferdinande P, Lauwers P, Bouillon R. Intensive insulin therapy in critically ill patients. *N Engl J Med*. 2001; 345:1359-1367.
19. NICE-SUGAR Study Investigators, Finfer S, Liu B, Chittock DR, Norton R, Myburgh JA, McArthur C, Mitchell I, Foster D, Dhingra V, Henderson WR, Ronco JJ, Bellomo R, Cook D, McDonald E, Dodek P, Hebert PC, Heyland DK, Robinson BG: Hypoglycemia and risk of death in critically ill patients. *N Engl J Med*. 2012; 367:1108-1118.

(Received June 8, 2013; Revised June 15, 2013; Accepted June 18, 2013)

Label-free quantification proteomics reveals novel calcium binding proteins in matrix vesicles isolated from mineralizing Saos-2 cells

Xiaoying Zhou^{1,2}, Yazhou Cui¹, Jing Luan¹, Xiaoyan Zhou¹, Genglin Zhang¹, Xiumei Zhang¹, Jinxiang Han^{1,*}

¹ Key Laboratory for Rare Disease Research of Shandong Province, Key Laboratory for Biotech Drugs of the Ministry of Health, Shandong Medical Biotechnological Center, Shandong Academy of Medical Sciences, Ji'nan, Shandong, China;

² School of Medicine and Life Sciences, University of Jinan-Shandong Academy of Medical Science, Ji'nan, Shandong, China.

Summary Matrix vesicles (MVs) involved in the initiation of mineralization by deposition of hydroxyapatite (HA) in their lumen are released by the budding of mineralization-competent cells during skeletogenesis and bone development. To identify additional mineralization-related proteins, MVs were isolated from non-stimulated and stimulated Saos-2 cells in culture *via* an Exoquick™ approach and the corresponding proteomes were identified and quantified with label-free quantitative proteome technology. The isolated MVs were confirmed by electron microscopy, alkaline phosphatase activity (ALP), biomarkers, and mineral formation analyses. Label-free quantitative proteome analysis revealed that 19 calcium binding proteins (CaBPs), including Grp94, calnexin, calreticulin, calmodulin, and S100A4/A10, were up-regulated in MVs of Saos-2 cells upon stimulation of mineralization. This result provides new clues to study the mechanism of the initiation of MV-mediated mineralization.

Keywords: Mineralization, matrix vesicles, Exoquick™, label-free LC-MS/MS, calcium-binding proteins

1. Introduction

Skeletogenesis and bone development occur by a series of physicochemical and biochemical processes. Together, these processes facilitate the mineralization of the extracellular matrix (ECM), in part by promoting the deposition of hydroxyapatite (HA) crystals in the sheltered interior of matrix vesicles (MVs). The MVs are membrane-invested bodies with diameters ranging from 30 to 400 nm that perform specialized roles in the initiation of matrix mineralization (1,2). These roles include transporting amorphous calcium phosphate (ACP), managing mineral nucleation, regulating

the Pi/PPi ratio in the intra- and extra-cellular fluid, controlling calcium ion and Pi homeostasis, and interacting with the surrounding ECM to direct HA localization and growth (3-7). MVs possess protein and lipid machinery, highly enriched in certain mineralization-related proteins, that is essential to carrying out these functions (8). Proteomic studies of MVs isolated from different mineralization-competent cells have recently been reported (1,2,9), but whole-proteome pattern analysis and quantification of changes in MVs during mineralization process have yet to be performed.

Human osteosarcoma Saos-2 cells undergo the entire osteoblastic differentiation sequence from proliferation to mineralization (10) and release mineralization-competent MVs (11). Therefore, Saos-2 cells serve as a model of pro-mineralizing cells and were selected to analyze the functions of MVs. MVs are traditionally isolated from conditioned media by serial ultracentrifugation (1,2). Recently, a rapid proprietary method of exosome isolation called Exoquick™,

*Address correspondence to:

Dr. Jinxiang Han, Key Laboratory for Rare Disease Research of Shandong Province, Key Laboratory for Biotech Drugs of the Ministry of Health, Shandong Medical Biotechnological Center, Shandong Academy of Medical Sciences, Ji'nan, Shandong 250062, China.
E-mail: samshjx@sina.com

became commercially available; this method is reported to be as effective as ultracentrifugation (12,13). The current study used Exoquick™ to isolate MVs from non-stimulated and stimulated Saos-2 cell cultures. Label-free quantitative liquid chromatography-tandem mass spectrometry (label-free LC-MS/MS) was used to analyze the protein expression of two MV preparations. Results revealed novel calcium-binding proteins (CaBPs), including Grp94 (endoplasmic/HSP90), calnexin, calreticulin (calregulin), calmodulin, S100A4/A10, and plastin-3. These proteins were found to be highly expressed in MVs isolated from stimulated Saos-2 cells. Their functions in relation to mineralization are discussed here in conjunction with existing knowledge of the mineralization process.

2. Materials and Methods

2.1. Cell culture and treatment

Human osteosarcoma Saos-2 cells, acquired from the Cell Bank of Type Culture Collection of the Chinese Academy of Sciences (Shanghai, China), were cultured in McCoy's 5A (Gibco, Carlsbad, CA, USA) supplemented with 15% (v/v) fetal bovine serum (Gibco, Carlsbad, CA, USA), 100 U/mL penicillin, and 100 µg/mL streptomycin (both from Invitrogen, Carlsbad, CA, USA). Mineralization was induced by treatment of confluent Saos-2 cells (6 days to reach confluence) for 6 days in growth medium supplemented with 7.5 mM β-glycerophosphate (β-GP) (Sigma-Aldrich, St. Louis, MO, USA) and 50 µg/mL ascorbic acid (AA) (Sigma-Aldrich) (14).

2.2. Isolation of MVs

MVs were harvested from non-stimulated and stimulated Saos-2 cell cultures after 6 days using Exoquick™ (System Biosciences Inc., Carlsbad, CA, USA) (13). Saos-2 cells were digested with 1 mg/mL collagenase Type IA (Sigma-Aldrich) in Hank's balanced salt mixture (Solabio, Shanghai, China) at 37°C for 3 h. Cells were then pelleted by centrifugation at 3,000 g for 30 min. The supernatant was filtered through a 100K Amicon Ultra filter (Millipore Corporation, Billerica, MA, USA) to the appropriate volume. The supernatant was then added to Exoquick™ and mixed well by inversion. After refrigeration overnight (at least 12 h), the Exoquick/biofluid mixture was centrifuged at 1,500 g for 30 min to collect MVs, and all traces of supernatant were removed by aspiration. The collected MVs appeared as a white pellet and were stored at -80°C.

2.3. Transmission electron microscopy

Freshly obtained MV pellets were fixed in situ with

2.5% glutaraldehyde in 0.1 M sodium cacodylate acidulated buffer at 4°C for 2 h; after fixation, pellets were incubated in a 1% osmium tetroxide phosphate buffer solution for 1 h. The samples were dehydrated in a graded ethanol series with acetone and then embedded in epoxy resin. Semithin sections of approximately 75 nm were prepared, mounted on copper grids, and stained with uranyl acetate and lead citrate solutions to enhance the contrast. Electron micrographs were taken with an H800 transmission electron microscope (TEM) (Hitachi Electronic Instruments, Japan).

2.4. Alkaline phosphatase activity analysis

The alkaline phosphatase (ALP) activity of MVs was determined using *p*-nitrophenyl phosphate (*p*-NPP) (Sigma-Aldrich) as a substrate and absorbance was recorded at 405 nm. An aliquot of MV pellets was lysed by addition of 100 µL buffer containing 25 mM Tris-HCl (pH = 7.4) and 0.5% Triton X-100 (15). Then, 1 µL of MVs lysate was mixed with 100 µL *p*-NPP. The reaction was stopped by addition of 50 µL NaOH (3 M) and absorbance was detected at 405 nm using Bio-Tek Synergy HT. ALP activity was normalized to total protein content using the Bradford method.

2.5. Mineralization analysis

Freshly collected MVs were suspended in mineralizing buffer (14) (100 mM NaCl, 12.7 mM KCl, 0.57 mM MgCl₂, 1.83 mM NaHCO₃, 0.57 mM Na₂SO₄, 3.42 mM NaH₂PO₄, 2 mM CaCl₂, 5.55 mM D-glucose, 63.5 mM sucrose, and 16.5 mM TES, pH = 7.5) and incubated for 12 h at 37°C. The calcium phosphate mineral complex was divided into two parts, centrifuged at 8,800 g for 15 min, and washed with water. One part of the resulting pellet was dried and incorporated by pressing it into KBr pellets. Mineral composition were determined in the range 400 – 4,000 cm⁻¹ using a Nicolet 6700 Fourier transform infrared (FTIR) spectrometer equipped with a deuterated triglycine sulfate (DTGS) detector. The mineral deposit produced a spectrum identical to that of the HA standard (Aladdin Industrial Inc., Shanghai, China). Another portion of the resulting pellet was solubilized with 0.1 M HCl for 3 h. The calcium content of the HCl supernatant was measured using a Calcium Assay Kit (Bioassay Systems, Carlsbad, CA, USA) (16) and normalized to total protein content using the Bradford method.

2.6. LC-MS/MS

Nano-flow LC-MS/MS was performed on a Thermo Easy-nLC 1000 equipped with a C18 reverse phase (RP) column (0.15 × 100 mm, Thermo EASY column SC200). The mobile phases were 2% acetonitrile

(ACN) with 0.1% formic acid (phase A and the loading phase) and 84% ACN with 0.1% formic acid (phase B). Samples were loaded onto a Thermo EASY column SC001 trap column (RP-C18, 0.15 × 2 mm) and equilibrated with 100% phase A. Samples were then subsequently separated with the C18 RP column at a flow rate of 400 nL/min. To achieve proper separation, a 120 min linear gradient elution was used: 0-100 min with 0% to 45% phase B; 100-108 min with 45% to 100% phase B; and 108-120 min with 100% phase B. Analysis of tryptic peptides was performed using a Q-Exactive mass spectrometer (Thermo Scientific). The mass spectrometer was operated in data-dependent mode and all analyses were performed using the positive nano-electrospray ion mode. The normalized collision energy value was set at 30%. Previously fragmented peptides were excluded for 25 s.

2.7. Protein database search and label-free quantification

Continuum LC-MS data were processed and searched using MaxQuant software (version 1.3.0.5). Proteins were searched against a "decoy database" based on the Homo sapiens protein sequence database (downloaded September 2012) from UniProt (<http://www.uniprot.org/>) and combined with common contaminants using the Andromeda search engine (17). Quantitative analyses were performed using a label-free approach, as previously described (18). A minimum of one quantification was required to establish the intensity value for each peptide. MaxQuant output files were subsequently uploaded into Perseus (version 1.2.0.17) for calculation of significance. The level of significance was determined with a 2-fold change. Analysis of data was completed using MAS 3.0 and <http://string.embl.de/> workstation.

2.8. Western blotting

MV pellets were homogenized in radio-immunoprecipitation assay (RIPA) buffer (Beyotime, Shanghai, China) supplemented with protease and phosphatase inhibitors on ice for 60 min and centrifuged at 12,500 g for 5 min at 4°C. The protein concentration of the MV lysate was determined using the Bradford method (BioRad Laboratories, Carlsbad, CA, USA). Samples (20 µg) were suspended in Laemmli loading buffer and incubated at 95°C for 6 min. Proteins were separated using 12% sodium dodecyl sulfate polyacrylamide gel electrophoresis (SDS-PAGE) gels and transferred onto a polyvinylidene fluoride (PVDF) membrane. After 1 h of blocking with 5% low fat milk in TBST (10 mM Tris, 100 mM NaCl, and 0.05% Tween-20), membranes were incubated with the following primary antibodies overnight at 4°C: rabbit polyclonal anti-human CD63,

CD9, and Hsp70 (1:1,000) from System Biosciences, Inc. (Carlsbad, CA, USA); mouse monoclonal anti-human ALP (B-10) (1:200), goat polyclonal anti-human Grp94 (C-19) (1:400), mouse monoclonal anti-human Calnexin (E-10) (1:1,000), and mouse monoclonal anti-human Calregulin (A-9) (1:100) from Santa Cruz Biotechnology (Carlsbad, CA, USA); mouse monoclonal anti-human Actin (1:1,000) from Beyotime (Shanghai, China); and rabbit polyclonal anti-human S100A10 (1:1,000) from Proteintech Group, Inc. (Wuhan, Hubei, China). Primary antibodies were immunostained with the appropriate peroxidase-conjugated secondary antibodies. Finally, the blots were visualized using ECL reagents (Millipore Corporation, Billerica, MA, USA) in accordance with the manufacturer's instructions.

2.9. Statistical analysis

For quantitative data, results are expressed as the mean ± S.D. of *n* observations. Statistical significance between groups was determined using an unpaired Student's *t* test. Statistical significance was defined as *p* < 0.05.

3. Results

3.1. AA and β-GP stimulated Saos-2 cell mineralization and the release of mineralization-competent MVs

AA and β-GP are two osteogenic factors known to accelerate osteoblastic differentiation and mineralization (14). As expected, mineralization was greatly enhanced by the concomitant addition of 50 mg/mL AA and 7.5 mM β-GP in Saos-2 cell cultures over 6 days. MVs were isolated from non-stimulated and stimulated Saos-2 cells after 6 days using Exoquick™. The intact MVs were confirmed by electron microscopy and assayed for ALP activity, expression of biomarkers, and mineral formation. As seen in TEM, freshly isolated MVs were recognized as spherical membrane-bounded vesicle structures with diameters ranging from 30 to 400 nm (Figures 1A and 1B). MVs isolated from stimulated cells contained electron-dense material (Figure 1B), which was previously reported to have mineralizing capabilities (1). As expected, MVs isolated from stimulated Saos-2 cells exhibited greater ALP activity than those from non-stimulated cells (Figure 1C). Moreover, after incubation in mineralizing buffer for 12 h MVs that were isolated from stimulated cells were able to continue Ca²⁺ uptake (Figure 1E) and form mineral HA, a finding that was confirmed using FTIR (Figure 1D). Proteins including CD63, CD9, and Hsp70, which are known to be reliable biomarkers of MVs and exosomes (6,19), were present in both types of MV preparations (Figure 2).

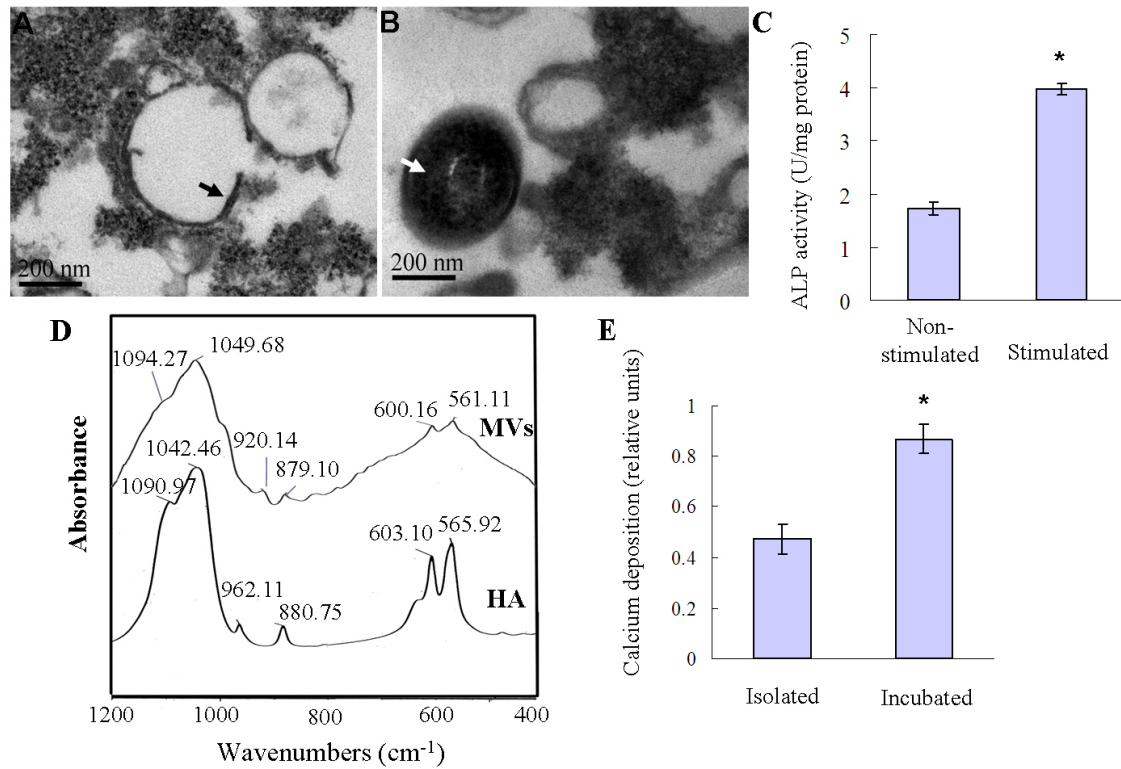


Figure 1. Ultrastructural studies, ALP activity, and functional studies of MVs. (A, B) TEM view of MVs isolated from non-stimulated and stimulated Saos-2 cells. The black arrow indicates MVs that were membrane-bounded bodies. The white arrow shows a vesicle containing electron-dense material, previously reported to be signs of calcification. (C) ALP activity of MVs isolated from non-stimulated and stimulated Saos-2 cells (Results are mean \pm SD, $n = 3$). * $p < 0.05$, vs. non-stimulated cells. (D, E) Mineralization assay of MVs. MVs isolated from stimulated Saos-2 cells were incubated at 37°C in mineralizing buffer for 12 h. Infrared spectra (D) indicated that the mineral formed by MVs was hydroxyapatite. Isolated MVs were able to continue taking up Ca^{2+} (E) when incubated in mineralizing buffer (Results are mean \pm SD, $n = 3$). * $p < 0.05$, vs. isolated group.

3.2. Results and classification of MV proteins identified by LC-MS/MS

In total, 255 different proteins were obtained from MVs from non-stimulated and stimulated Saos-2 cells according to software analysis (fold ≥ 2). Of these, 186 proteins increased and 69 proteins decreased. MV proteins that were previously reported to be related to mineralization, such as ALP and NPP1 (inorganic pyrophosphatase, ectonucleotide pyrophosphatase phosphodiesterase 1) (8), were highly expressed in the mineralized MVs, demonstrating the usefulness of this model for discovery of new proteins involved in the mineralization process. The different proteins were classified based on Gene Ontology (GO) and Kyoto Encyclopedia of Genes and Genomes (KEGG) pathway classification using the MAS 3.0 workstation.

Analysis of molecular function based on the GO classification indicated that 19 CaBPs and 4 calmodulin-binding proteins (CaMBPs) were up-regulated in MVs of Saos-2 cells upon stimulation of mineralization (Table S1, <http://www.biosciencetrends.com/docindex.php?year=2013&kanno=3>). Analysis based on KEGG pathway classification revealed that 7 proteins associated with calcium signaling pathways (CaSP) were highly expressed in mineralized MVs

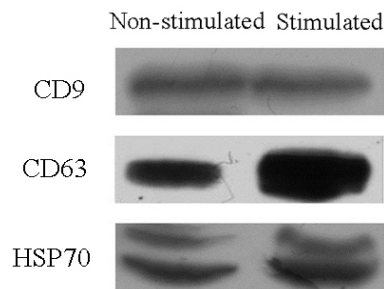


Figure 2. Presence of exosomal protein markers. CD9, CD63, and Hsp70 were present in both MV preparations.

(Table S1, <http://www.biosciencetrends.com/docindex.php?year=2013&kanno=3>).

3.3. Validation of MV proteins identified by Western blotting

To confirm both the accuracy of protein identification by mass spectrometry and label-free quantification, five proteins were selected for validation by Western blotting. Consistent with label-free quantification, four detected CaBPs (Grp 94, calnexin, calregulin, and S100A10) were more highly expressed in the MVs isolated from stimulated cells than those from non-

stimulated cells (Figure 3). Furthermore, ALP, used as a marker of mineralization and identifier of MVs (20), was also enriched in the mineralized MVs (Figure 3). Together, data from proteomics and Western blotting results suggest that the current study reliably identified MV proteomes of Saos-2 cells.

4. Discussion

This study confirmed that the Exoquick™ approach, used to isolate biofluid and cell culture-derived exosomes (12,13), was effective at isolating quality MVs from Saos-2 cells. The MVs isolated from stimulated cells can still take up Ca ions and form HA when incubated in mineralizing buffer, thus indicating that MVs have their own proteins to carry out mineralization. Label-free LC-MS/MS helped to shed light on subtle differences between MVs from non-stimulated and stimulated Saos-2 cells.

The intravesicular initiation of mineralization requires Ca^{2+} influx into MVs and formation of phosphatidylserine (PS) nucleation complexes (21). The CaBPs, which bind Ca ions in specific domains, are known to actively participate in numerous cellular functions such as Ca^{2+} homeostasis and Ca^{2+} signal pathways (22). The current results showed that 19 CaBPs were up-regulated in different ratios; this was partly confirmed by Western blotting (Figure 3). In addition, Grp94, calnexin, calreticulin, calmodulin, and plastin-3 were previously identified as MV proteins (1,2,9,23), but they have not been cited as important components of MV-mediated mineralization. Both Grp94 and calreticulin are reported to bind HA (24,25). A recent study determined that purified native Grp94 can directly bind both ACP and HA in the presence of excess calcium and phosphate but that its binding to ACP is inhibited by ATP, bisphosphonates, and pyrophosphate (24). That study also noted a novel Grp94-calreticulin-annexin A5-mineral complex generated after massive calcium influx in SiHa cells (24). Alternatively, abundant CaBPs including Grp94 and calreticulin are responsible for the storage of calcium to protect cells from massive calcium influx (26). Therefore, these CaBPs are presumed to be involved in the initiation of mineral nucleation. When mitochondrial Ca^{2+} is released *via* mitochondrial transition pores into the Pi-rich intracellular vesicles (7), the released Ca^{2+} interacts simultaneously with both Pi and PS, forming PS- Ca^{2+} -Pi complexes, and it interacts with PS and CaBPs to form PS- Ca^{2+} -CaBPs-Pi complexes. ACP is a major component of both PS- Ca^{2+} -Pi and PS- Ca^{2+} -CaBPs-Pi complexes (27). After that interaction, vesicles containing ACP are transported to the extracellular space and deposited on collagen fibrils. These vesicles continue to accumulate Ca and Pi, which stimulate the formation of HA crystals from the immature mineral present in the lumen, initiating

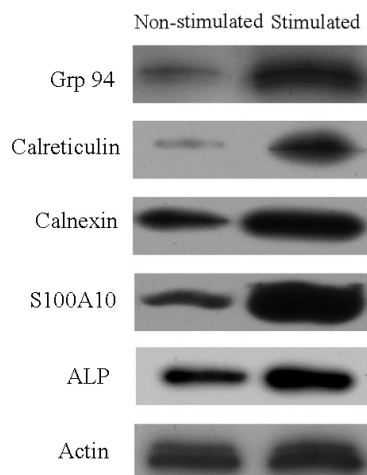


Figure 3. Enrichment of MVs with Grp 94, calnexin, calreticulin, S100A10, and ALP upon stimulation.

mineralization (7). During HA crystal propagation, CaBPs are also needed to bind the influx of free Ca^{2+} to the mineral. In addition, the increased regulation of calumenin is associated with mouse cartilage development (28) and healing of closed mid-diaphyseal fractures (29). Plastin-3 has a potential Ca^{2+} -binding site near the N terminus and may also contribute to the assembly and maintenance of plasma membrane protrusions. These protrusions, from which MVs appear to originate, are characteristic of growth plate chondrocytes *in vivo* (27) and MC3TC cells *in vitro* (1). This group of CaBPs may take part in the biogenesis of MVs, managing mineral nucleation, transporting Ca^{2+} , and controlling calcium homeostasis in the MVs. Moreover, further studies are needed to ascertain the possible function of each CaBP.

Calmodulin, one of the major calcium sensors and Ca^{2+} signal mediators, is not confined to its Ca^{2+} -bound form because the Ca^{2+} -free form can also recognize different target proteins including calmodulin kinase II, calcineurin, and many ion channel proteins (30). The calmodulin pathway is associated with regulation of osteoblast growth and differentiation (30,31). The inhibition of both calmodulin and calmodulin kinase II can decrease ALP activity and cell mineralization (31). Calmodulin can interact selectively and non-covalently with CaMBPs, both in its calcium-bound and calcium-free states. The current study identified 4 CaMBPs including MYO1C/1B, MARCKS, and IQGAP1, that were up-regulated in the mineralization process. Fortunately, all four have previously been identified as MV proteins (2,9,32), but their roles in mineralization are unknown. These CaMBPs may interact with calmodulin or regulate the calmodulin pathway to affect biomineralization.

In addition, the current study found that S100A4, A6, A10, A11, and A13 were expressed in two MV samples. Only S100A4 and A10 were significantly up-

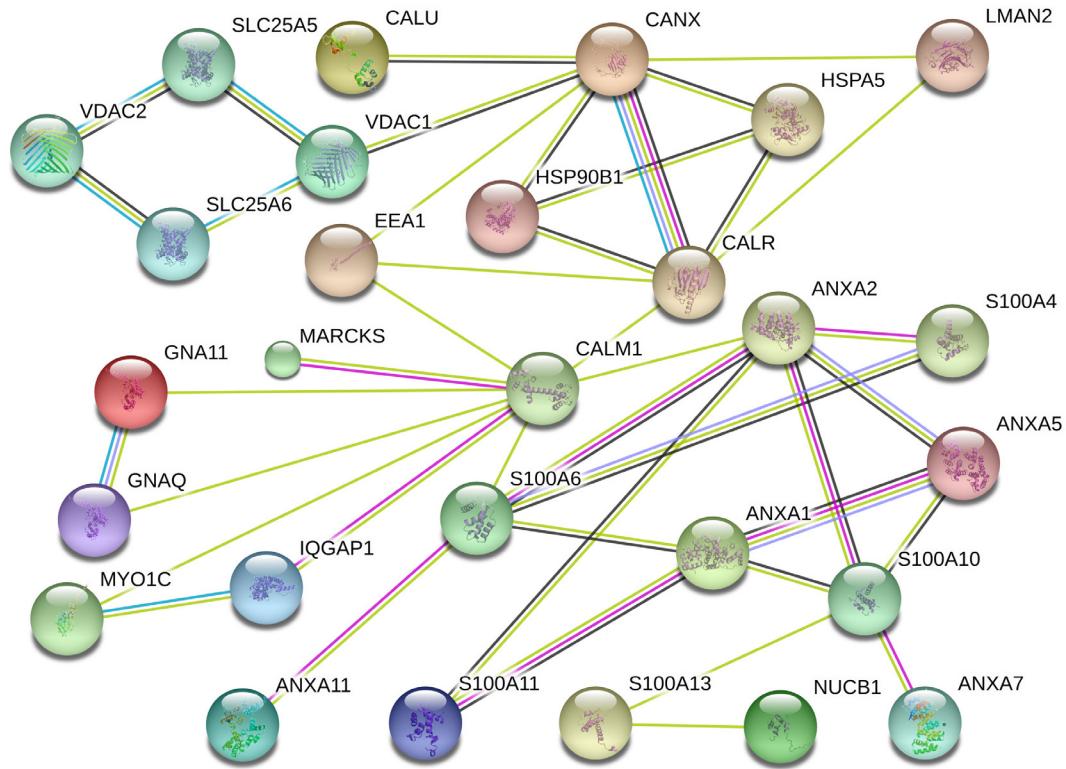


Figure 4. STRING analysis of direct (physical) or indirect (functional) associations among the calcium-associated proteins analyzed. The network nodes are proteins in the illustration shown. The lines in different colors represent the types of evidence for the associations.

regulated in MVs from stimulated cells. To date, there has been little evidence suggesting the enrichment of S100 families in mineralized MVs compared to non-mineralized MVs (11). In agreement with a previous study (11), the current results suggest that S100A10 may be associated with MV-mediated mineralization. However, determination of the specific function of S100A10 will require additional study.

The annexins have previously been described as important to MV function through channel-directed Ca ion uptake into MVs (11,33). Nevertheless, a recent study found that Annexin A5 and Annexin A6-deficient mice developed no abnormal mineralization (34). The same group also found that the depletion of Annexin A5 and Annexin A6 in mice caused no gross changes in MV-mediated mineralization (35). The current results revealed no significant differences in Annexin A1, 2, 4, 5, 6, 7, or 11 expression for MVs from non-stimulated and stimulated cells. Therefore, annexins may not be essential or directly linked to the MV-mediated mineralization process.

STRING workstation (36) was used to analyze the interaction among the calcium-associated proteins indicated earlier (Table S1, <http://www.biosciencetrends.com/docindex.php?year=2013&kanno=3>). Figure 4 shows that calnexin, calreticulin, and calmodulin act as connection centers. Thus, further studies are clearly needed to determine whether these CaBPs

play an important role in bone mineralization as MV components.

In conclusion, MVs were isolated from non-stimulated and stimulated Saos-2 cell cultures *via* an Exoquick™ approach and their proteomes were identified and quantified using label-free quantitative proteome technology. The proteomes analysis indicated that 19 CaBPs were up-regulated in MVs of Saos-2 cells upon stimulation of mineralization. Understanding the role of CaBPs and their potential partners in MV functions may provide novel insights into the mechanism of physiological bone mineralization.

Acknowledgements

This work was supported by the Key Project for Drug Research and Development of the Ministry of Science and Technology of China (Grant No. 2010ZX09401-302-5-07).

References

1. Xiao Z, Camalier CE, Nagashima K, Chan KC, Lucas DA, de la Cruz MJ, Gignac M, Lockett S, Issaq HJ, Veenstra TD, Conrads TP, Beck GR Jr. Analysis of the extracellular matrix vesicle proteome in mineralizing osteoblasts. *J Cell Physiol.* 2007; 210:325-335.
2. Thouverey C, Malinowska A, Balcerzak M, Strzelecka-Kiliszek A, Buchet R, Dadlez M, Pikula S. Proteomic

- characterization of biogenesis and functions of matrix vesicles released from mineralizing human osteoblast-like cells. *J Proteomics*. 2011; 74:1123-1134.
3. Anderson HC. Molecular biology of matrix vesicles. *Clin Orthop Relat Res*. 1995; 314:266-280.
 4. Golub EE. Biomineralization and matrix vesicles in biology and pathology. *Semin Immunopathol*. 2011; 33:409-417.
 5. Golub EE. Role of matrix vesicles in biomineralization. *Biochim Biophys Acta*. 2009; 1790:1592-1598.
 6. Xiao Z, Blonder J, Zhou M, Veenstra TD. Proteomic analysis of extracellular matrix and vesicles. *J Proteomics*. 2009; 72:34-45.
 7. Boonrungsiman S, Gentleman E, Carzaniga R, Evans ND, McComb DW, Porter AE, Stevens MM. The role of intracellular calcium phosphate in osteoblast-mediated bone apatite formation. *Proc Natl Acad Sci U S A*. 2012; 109:14170-14175.
 8. Zhou X, Cui Y, Zhou X, Han J. Phosphate/pyrophosphate and MV-related proteins in mineralisation: Discoveries from mouse models. *Int J Biol Sci*. 2012; 8:778-790.
 9. Balcerzak M, Malinowska A, Thouverey C, Sekrecka A, Dadlez M, Buchet R, Pikula S. Proteome analysis of matrix vesicles isolated from femurs of chicken embryo. *Proteomics*. 2008; 8:192-205.
 10. Hausser HJ, Brenner RE. Low doses and high doses of heparin have different effects on osteoblast-like Saos-2 cells *in vitro*. *J Cell Biochem*. 2004; 91:1062-1073.
 11. Cmoch A, Strzelecka-Kiliszek A, Palczewska M, Groves P, Pikula S. Matrix vesicles isolated from mineralization-competent Saos-2 cells are selectively enriched with annexins and S100 proteins. *Biochem Biophys Res Commun*. 2011; 412:683-687.
 12. King HW, Michael MZ, Gleadle JM. Hypoxic enhancement of exosome release by breast cancer cells. *BMC Cancer*. 2012; 12:421.
 13. Umezu T, Ohyashiki K, Kuroda M, Ohyashiki JH. Leukemia cell to endothelial cell communication *via* exosomal miRNAs. *Oncogene*. 2013; 32:2747-2755.
 14. Thouverey C, Strzelecka-Kiliszek A, Balcerzak M, Buchet R, Pikula S. Matrix vesicles originate from apical membrane microvilli of mineralizing osteoblast-like Saos-2 cells. *J Cell Biochem*. 2009; 106:127-138.
 15. Zhang YY, Cui YZ, Luan J, Zhou XY, Zhang GL, Han JX. Platelet-derived growth factor receptor kinase inhibitor AG-1295 promotes osteoblast differentiation in MC3T3-E1 cells *via* the Erk pathway. *Biosci Trends*. 2012; 6:130-135.
 16. Hernandez L, Park KH, Cai SQ, Qin L, Partridge N, Sesti F. The antiproliferative role of ERG K⁺ channels in rat osteoblastic cells. *Cell Biochem Biophys*. 2007; 47:199-208.
 17. Cox J, Neuhauser N, Michalski A, Scheltema RA, Olsen JV, Mann M. Andromeda: A peptide search engine integrated into the MaxQuant environment. *J Proteome Res*. 2011; 10:1794-1805.
 18. Lubber CA, Cox J, Lauterbach H, Fancke B, Selbach M, Tschopp J, Akira S, Wiegand M, Hochrein H, O'Keefe M, Mann M. Quantitative proteomics reveals subset-specific viral recognition in dendritic cells. *Immunity*. 2010; 32:279-289.
 19. Epple LM, Griffiths SG, Dechkovskaia AM, Dusto NL, White J, Ouellette RJ, Anchordoquy TJ, Bemis LT, Graner MW. Medulloblastoma exosome proteomics yield functional roles for extracellular vesicles. *PLoS One*. 2012; 7:e42064.
 20. Sekrecka-Belniak A, Balcerzak M, Buchet R, Pikula S. Active creatine kinase is present in matrix vesicles isolated from femurs of chicken embryo: Implications for bone mineralization. *Biochem Biophys Res Commun*. 2010; 391:1432-1436.
 21. Kapustin AN, Davies JD, Reynolds JL, McNair R, Jones GT, Sidibe A, Schurgers LJ, Skepper JN, Proudfoot D, Mayr M, Shanahan CM. Calcium regulates key components of vascular smooth muscle cell-derived matrix vesicles to enhance mineralization. *Circ Res*. 2011; 109:e1-12.
 22. Carafoli E. The Symposia on Calcium Binding Proteins and Calcium Function in Health and Disease: An historical account, and an appraisal of their role in spreading the calcium message. *Cell Calcium*. 2005; 37:279-281.
 23. Rosenthal AK, Gohr CM, Ninomiya J, Wakim BT. Proteomic analysis of articular cartilage vesicles from normal and osteoarthritic cartilage. *Arthritis Rheum*. 2011; 63:401-411.
 24. Ho WH, Lee DY, Chang GD. Proteomic Identification of a Novel Hsp90-Containing Protein-Mineral Complex Which Can Be Induced in Cells in Response to Massive Calcium Influx. *J Proteome Res*. 2012; 11:3160-3174.
 25. Baksh S, Burns K, Busaan J, Michalak M. Expression and purification of recombinant and native calreticulin. *Protein Expr Purif*. 1992; 3:322-331.
 26. Lee D, Michalak M. Membrane associated Ca²⁺ buffers in the heart. *BMB Rep*. 2010; 43:151-157.
 27. Wuthier RE, Lipscomb GF. Matrix vesicles: Structure, composition, formation and function in calcification. *Front Biosci*. 2011; 16:2812-2902.
 28. Wilson R, Norris EL, Brachvogel B, Angelucci C, Zivkovic S, Gordon L, Bernardo BC, Stermann J, Sekiguchi K, Gorman JJ, Bateman JF. Changes in the chondrocyte and extracellular matrix proteome during post-natal mouse cartilage development. *Mol Cell Proteomics*. 2012; 11:M111.014159.
 29. Nakazawa T, Nakajima A, Seki N, Okawa A, Kato M, Moriya H, Amizuka N, Einhorn TA, Yamazaki M. Gene expression of periostin in the early stage of fracture healing detected by cDNA microarray analysis. *J Orthop Res*. 2004; 22:520-525.
 30. Zayzafoon M. Calcium/calmodulin signaling controls osteoblast growth and differentiation. *J Cell Biochem*. 2006; 97:56-70.
 31. Zayzafoon M, Fulzele K, McDonald JM. Calmodulin and calmodulin-dependent kinase II alpha regulate osteoblast differentiation by controlling c-fos expression. *J Biol Chem*. 2005; 280:7049-7059.
 32. Hale JE, Chin JE, Ishikawa Y, Paradiso PR, Wuthier RE. Correlation between distribution of cytoskeletal proteins and release of alkaline phosphatase-rich vesicles by epiphyseal chondrocytes in primary culture. *Cell Motil*. 1983; 3:501-512.
 33. Chen NX, O'Neill KD, Chen X, Moe SM. Annexin-mediated matrix vesicle calcification in vascular smooth muscle cells. *J Bone Miner Res*. 2008; 23:1798-1805.
 34. Belluoccio D, Grskovic I, Niehoff A, Schlötzer-Schrehardt U, Rosenbaum S, Etich J, Frie C, Pausch F, Moss SE, Pöschl E, Bateman JF, Brachvogel B. Deficiency of annexins A5 and A6 induces complex changes in the transcriptome of growth plate cartilage but does not inhibit the induction of mineralization. *J*

- Bone Miner Res. 2010; 25:141-153.
35. Grskovic I, Kutsch A, Frie C, *et al.* Depletion of annexin A5, annexin A6, and collagen X causes no gross changes in matrix vesicle-mediated mineralization, but lack of collagen X affects hematopoiesis and the Th1/Th2 response. J Bone Miner Res. 2012; 27:2399-2412.
36. Chakraborty C, Roy SS, Hsu MJ, Agoramoorthy G.

Landscape mapping of functional proteins in insulin signal transduction and insulin resistance: A network-based protein-protein interaction analysis. PLoS One. 2011; 6:e16388.

(Received May 10, 2013; Revised May 29, 2013; Re-revised June 14, 2013; Accepted June 21, 2013)

Aberrant expression of Notch3 predicts poor survival for hepatocellular carcinomas

Lei Hu¹, Feng Xue¹, Minhua Shao², Anmei Deng^{3,*}, Gongtian Wei^{1,*}

¹ The second department of liver surgery, Eastern Hepatobiliary Hospital affiliated to the Second Military Medicine College, Shanghai, China;

² Department of Pulmonary Medicine, Shanghai Chest hospital, Affiliated to Jiaotong University, Shanghai, China;

³ Department of Laboratory Diagnostic, Changhai Hospital, Second Military Medical University, Shanghai, China.

Summary

Using a meta-analysis on gene expression data of hepatocellular carcinomas (HCC) from the Oncomine database, we identified that the Notch3 gene ranked as the highest up-regulated Notch pathway member in HCC tissues compared with normal liver tissues. We further detected the expression of Notch3 in 95 cases of HCC samples by immunohistochemistry, and evaluated its clinicopathological and prognostic significance. We confirmed that Notch3 is overexpressed in HCC tissues compared with normal liver tissues, and a high expression level of Notch3 was significantly associated with bigger tumor size ($p = 0.014$), multiple tumors ($p = 0.026$), late tumor-node-metastasis (TNM) stage ($p < 0.01$) and shorter overall survival ($p = 0.002$). Furthermore, high Notch3 expression emerged as a significant independent prognostic factor in multivariate analysis. In conclusion, we identified a positive association between Notch3 expression with more aggressive traits and shorter survival in HCC. Our findings suggest that Notch3 might be an important regulator in the development of HCC, and a potential therapeutic target for patients with HCC.

Keywords: Notch pathway, Notch3, hepatocellular carcinomas, immunohistochemistry, prognosis

1. Introduction

Hepatocellular carcinoma (HCC) is the fifth or sixth most prevalent cancer worldwide, including China (1). HCC has a relatively aggressive clinical course, even when receiving intensive treatment including curative resection, percutaneous ablation therapy, chemotherapy or liver transplantation, advanced HCC patients still have a poor prognosis. Therefore, there is an urgent need to develop novel prognostic biomarkers and therapeutic targets for HCC to improve its clinical

outcome.

The Notch signaling pathway is an evolutionarily highly conserved mechanism involved in cell fate determination during development (2). Aberrant Notch signaling activation has been highlighted as having a potential role in cancer stem cells (3). High Notch pathway activity correlates with more aggressive or treatment-resistant phenotypes, and poor prognosis in multiple cancers (4).

In this present study, we performed a meta-analysis on the gene expression datasets of HCC from the Oncomine database, and identified Notch3 as ranked at the top of significantly overexpressed Notch pathway genes in HCC. Several previous studies investigated the expression of Notch3 in HCC, however, the results were inconsistent (5,6). Especially, the clinicopathological and prognostic significance of Notch3 in HCC has seldom been investigated. Therefore, in this study, we examined the expression of Notch3 protein in human HCC tissues and adjacent normal liver tissues by immunohistochemistry, to clarify the possible roles of Notch3 in the malignant progress and prognosis of HCC.

Hu L and Xue F contributed equally to this work.

*Address correspondence to:

Dr. Anmei Deng, Department of Laboratory Diagnostic, Changhai Hospital, Second Military Medical University, NO.168 Changhai Road, Shanghai 200433, China.
E-mail: anmeideng@yahoo.com.cn

Dr. Gongtian Wei, The second department of liver surgery, Eastern Hepatobiliary Hospital affiliated to the Second Military Medicine College, No.225 Changhai Road, Shanghai, Shanghai 200438, China.
E-mail: weigongtian@163.com

2. Materials and Methods

2.1. Data mining

Oncomine cancer microarray database (<https://www.oncomine.org>) was used to mine the mRNA expression profile data of HCC tissue relative to normal liver tissue according to the methodology established by Oncomine (7). Six publicly available datasets of gene expression profiles (Chen Liver, Mas Liver, Roessler Liver, Roessler Liver 2, TCGA Liver and Wurmbach Liver) were selected for the meta-analysis. All the genes, in which mRNA levels increased by more than two fold in HCC tissue vs. normal liver tissue were selected. The gene ranks across 6 datasets were compared, and then a concept filter *Notch signaling pathway - KEGG Pathway* was used to identify known Notch signaling pathway members overexpressed in HCC at the mRNA level.

2.2. Patients

Archived formalin-fixed paraffin-embedded HCC specimens undergoing hepatectomy were obtained between January 2005 and January 2009. The diagnoses of HCC patients were confirmed by histopathology. All the HCC patients received curative liver resection which was defined previously (8). Patients with confirmed recurrence received further treatment including resection, transarterial chemoembolization (TACE) or radiofrequency ablation (RFA). None of the patients received neoadjuvant chemotherapies, radiation therapies or immunotherapies. Overall survival (OS) was calculated from the date of surgery until the date of death or last follow-up. Ethics approval to start this study was obtained from the local human research ethics committees. The clinicopathologic variables, such as gender, age, tumor size, histological grade, tumor-node-metastasis (TNM) stage, status of cirrhosis, tumor numbers, hepatitis status, capsular formation and vein invasion are seen in Table 1.

2.3. Immunohistochemistry

A total of 95 archived formalin-fixed paraffin-embedded HCC specimen tissues and 20 cases of adjacent normal liver tissue were included in the immunohistochemical study. Immunostaining was performed in accordance with the standard streptavidin-peroxidase (SP) procedures according to the manufacturer's protocol (Zymed Laboratories, South San Francisco, CA, USA). Antigen retrieval was performed using microwave heating in sodium citrate buffer. Immunostaining was performed with a rabbit polyclonal antibody against Notch3 (AbCam Biotechnology, Abcam China, Hong Kong). Immunostaining was visualized with 3,3'-Diaminobenzidine (DAB) substrate, and counterstained with hematoxylin. Non-specific rabbit IgG

was used as a negative control. The immunohistochemical results of Notch3 expression were assessed according to the criteria described previously (9,10). Because Notch3 staining was almost homogeneous within each tumor, Notch3 immunostaining intensity was used to evaluate immunohistochemical results and classified into three expression levels: none (no staining even at $\times 400$ field), low (weak staining, staining obvious only at $\times 400$ field), and high (moderate or strong staining, staining obvious at $\times 100$ or $\times 40$ field).

2.4. Statistics

The relationship between Notch3 and clinicopathological characteristics among different groups was compared using the χ^2 test or *t*-test when appropriate. Overall survival curves were made using the Kaplan-Meier method and evaluated using the Log-Rank test. Multivariate analysis of clinicopathological variables and Notch3 expression was performed using the Cox proportional hazard regression model. Statistical analyses were completed using SPSS 15.0 and a $p < 0.05$ was considered statistically significant.

3. Results

3.1. Data mining on Oncomine database

We systematically compared mRNA gene expression levels between HCC and normal liver tissue from 6 datasets from the Oncomine database, then the up-regulated genes in HCC tissues belonging to Notch pathway members were further filtered out. The top 20 up-regulated Notch pathway members in HCC are listed in Figure 1, among which Notch3 was the highest ranked gene (median rank = 674) with the most significant *P* value of 3.20×10^{-6} . In a previous study, Gramantieri *et al.* (5) also indicated that Notch3 mRNA was abnormally accumulated in a major proportion of HCC tumors, but was negative in normal liver and cirrhotic tissue. These findings support the hypothesis of an activation of Notch signalling by Notch3 in HCC. Therefore, we selected Notch3 for further validation in a cohort of HCC samples by immunohistochemistry.

3.2. Immunohistochemical results of Notch3 in HCC and normal liver tissue

Our immunohistochemical results indicated that Notch3 expression level was significantly higher than that in normal liver tissue, which is consistent with the finding in the meta-analysis on datasets from the Oncomine database. In all the HCC samples, 70 cases (73.7%) indicated Notch3 positive staining, including 44 cases (46.3%) with low expression and 26 cases (27.4%) with high expression according to the staining evaluation criteria we established, whereas only 5 cases of normal



Figure 1. OncoPrint heat map of up-regulated genes in clinical HCC samples compared to normal liver tissue filtered by Notch3 pathway concept. Notch3 ranked at the top of up-regulated Notch pathway members.

liver samples demonstrate even low Notch3 expression. Positive staining of Notch3 was located in the cytoplasm and nucleus of cancer cells. Representative immunostaining images are seen in Figure 2.

3.3. Association between Notch3 expression and clinicopathological features

The association between Notch3 expression and clinicopathological features of HCC are shown in Table 1. We found that Notch3 expression in HCC was significantly associated with tumor size ($p = 0.014$), TNM stage ($p < 0.01$) and tumor numbers ($p = 0.026$). High Notch3 expression was more frequently seen in bigger, multiple or later stage HCC tumors. No significant association was observed between Notch3 expression and other clinicopathological traits.

3.4. The prognostic significance of Notch3 for HCC patients

Survival curves were plotted using the Kaplan-Meier method (Figure 3). The results indicated that HCC tumors with high Notch3 expression had a significantly shorter survival time, compared with those with no or low expression (hazards ratio = 1.858, 95% confidence interval = 1.264-2.731, $p = 0.002$). All of the HCC

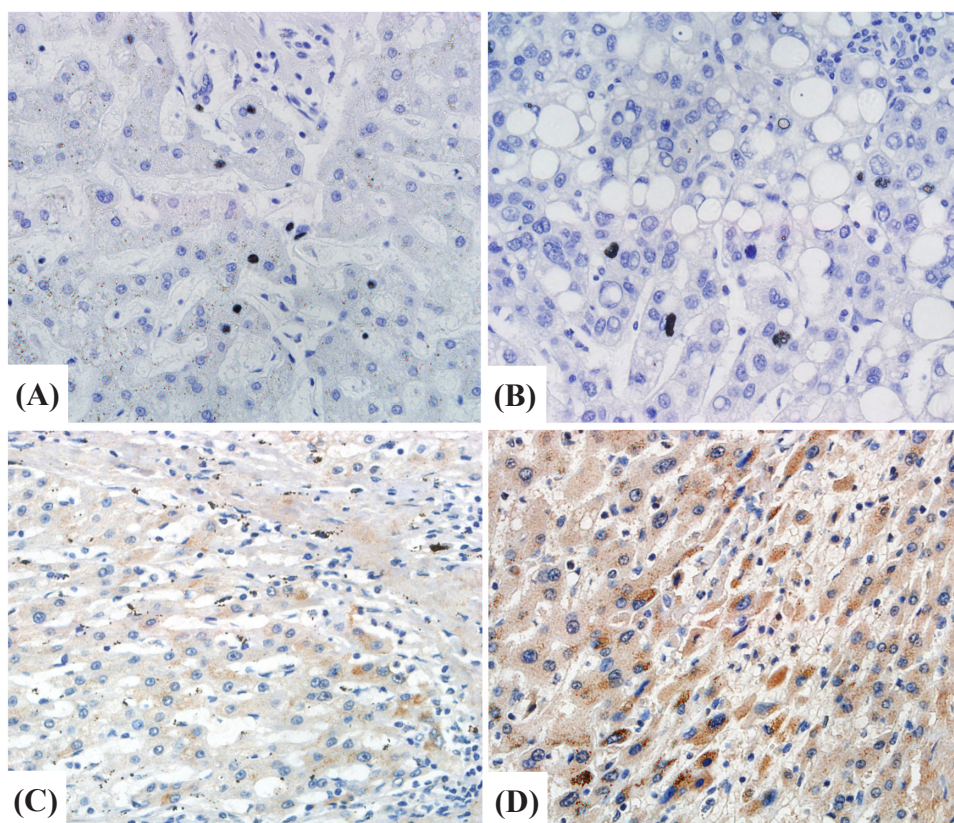


Figure 2. Representative images of Notch3 immunostaining in this study. (A) no Notch3 immunostaining in normal liver tissues; (B) no Notch3 immunostaining in HCC tissues; (C) low expression of Notch3 in HCC tissues; (D) high expression of Notch3 in HCC tissues.

Table 1. Association between Notch3 expression and clinicopathological characteristics in HCC samples

Variables (n)	Notch3 expression level			p value
	None (%)	Low (%)	High (%)	
Age (year)	54.0 ± 9.1	53.7 ± 8.2	55.5 ± 10.2	0.328
Gender				
Male (78)	20 (25.6)	37 (47.4)	21 (26.9)	0.894
Female (17)	5 (29.4)	7 (41.2)	5 (29.4)	
Tumor size				
T1-2 (74)	21 (28.4)	38 (51.5)	15 (20.3)	0.014
T3 (21)	4 (19.1)	6 (28.6)	11 (52.4)	
Histological grade				
1 (12)	3 (25.0)	6 (50.0)	3 (25.0)	0.445
2 (60)	13 (21.7)	29 (48.3)	18 (30.0)	
3 (21)	9 (42.9)	7 (33.3)	5 (23.8)	
TNM Stage				
I (58)	18 (31.0)	33 (56.9)	7 (12.1)	< 0.001
II (15)	1 (6.7)	6 (40.0)	8 (53.3)	
III (19)	6 (31.6)	5 (26.3)	8 (42.1)	
IV (3)	0 (0)	0 (0)	3 (100)	
Cirrhosis				
Presence (34)	8 (23.5)	18 (52.9)	8 (23.5)	0.624
Absence (61)	17 (27.9)	26 (42.6)	18 (29.5)	
Tumor nodules				
Single (81)	23 (28.4)	40 (49.4)	18 (22.2)	0.026
Multiple (14)	2 (14.3)	4 (28.6)	8 (57.1)	
Hepatitis				
Negative (32)	5 (15.6)	16 (50.0)	11 (34.4)	0.212
HBV/HCV (63)	20 (31.7)	28 (44.4)	15 (23.8)	
Capsular formation				
Presence (44)	13 (29.5)	22 (50.0)	9 (20.5)	0.369
Absence (51)	12 (23.5)	22 (43.1)	17 (33.3)	
Vein invasion				
Presence (25)	5 (20.0)	12 (48.0)	8 (32.0)	0.670
Absence (70)	20 (28.6)	32 (45.7)	18 (25.7)	

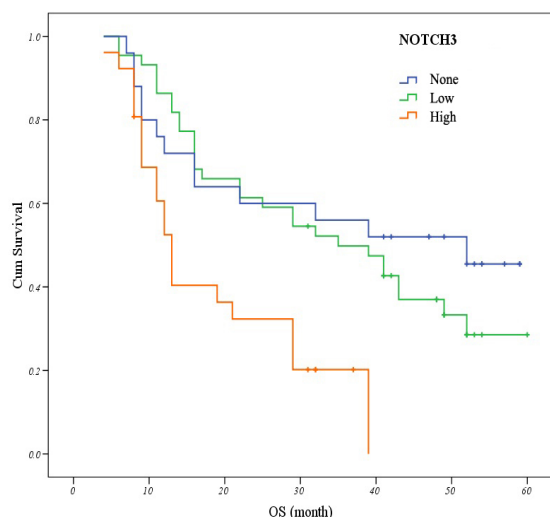


Figure 3. Kaplan-Meier survival curves based on expression of Notch3. Subgroups with high Notch3 expression had a significantly shorter survival time, compared to those with no or low Notch3 expression ($p = 0.002$, Log-Rank test).

clinical and pathological variables together with Notch3 expression status were included in a multivariate Cox regression model. Our data demonstrated that high Notch3 expression emerged as an independent

prognostic factor for HCC patients (Table 2).

4. Discussion

Aberrant activation of the Notch pathway has been demonstrated in the context of many cancers, and regarded as a novel potential therapeutic target for cancers (11). High Notch signaling pathway activity is caused by the deregulation of a list of pathway members at different levels (such as DNA, mRNA, protein). In this study, using a meta-analysis on gene expression microarray datasets, we identified that Notch3 ranked at the top of most up-regulated Notch pathway genes in HCC at the mRNA level. Consistent with our finding, in a previous study, Gramantieri et al. also reported an upregulation of Notch3 mRNA in 95% of HCCs vs. normal liver tissue by *in situ* hybridization (5). Notch3 and its ligand Jagged1 play a key role as Notch pathway members in the pathogenesis of multiple malignancies (12). It has been demonstrated that Notch3 signaling affects apoptosis and tumor growth in cancers by co-operating with the EGFR-MAPK and CSL (CBF-1/RBP-Jκ, Su(H) Lag-1) pathway (13,14). Therefore, these data promoted the assumption that Notch3 overexpression might partially account for the increased Notch pathway activation in HCC.

Next, by an immunohistochemistry method, we observed a high frequency (73.7%) of Notch3 expression in HCC, similar to the findings of Gramantieri's study in which Notch3 was not expressed in normal liver tissue, and displayed abnormal accumulation in 78% of HCC tissue (5). However, Gramantieri's and our data were not consistent with those of Gao *et al.*'s previous study in which cytoplasmic Notch3 expression showed no difference between HCC and adjacent non-cancerous liver samples (6).

In this study, we further extended the previous findings to identify a positive association between Notch3 and more aggressive phenotypes, and emphasized an independent predictor for poor prognosis in HCC. Several *in vitro* studies have revealed the relationship between Notch3 and malignant biological behavior in HCC, and the exact molecular mechanisms have also been explored. For example, Giovannini *et al.* (15) detected a high expression of the Notch3 intracellular domain in HepG2 cells, which suggests that Notch3 might be constitutively activated in human HCC. In another study, they demonstrated that down-regulation of Notch3 resulted in up-regulation of CDKN1C/P57, a cyclin-dependent kinase inhibitor in two HCC cell lines, accompanied by reduced cell growth (16). Giovannini *et al.* (17) indicated that Notch3 silencing enhances doxorubicin's chemotherapeutic effect by a p53-dependent mechanism in HCC cells, and could provide a novel strategy for HCC treatment. Together with these findings, we proposed that Notch3 plays an important regulatory role in the progression of

Table 2. Univariate and multivariate analysis for prognosis in HCC

Variables	Univariate survival analyses		Multivariate survival analysis	
	HR (95% CI)*	p Value	Adjusted HR (95% CI)	p Value
Age	0.982 (0.954-1.012)	0.240	0.853 (0.388-1.875)	0.693
Gender	0.684 (0.326-1.437)	0.316	0.988 (0.956-1.021)	0.465
Tumor size	2.025 (1.169-3.509)	0.012	0.962 (0.350-2.642)	0.940
Histological grade	0.769 (0.506-1.170)	0.220	0.864 (0.516-1.447)	0.579
TNM stage	1.530 (1.177-1.988)	0.001	1.397 (1.034-1.887)	0.030
Cirrhosis	1.110 (0.657-1.878)	0.696	1.065 (0.576-1.970)	0.840
Tumor nodules	2.697 (1.449-5.020)	0.002	1.491 (0.479-4.641)	0.491
Hepatitis	1.224 (0.713-2.100)	0.463	1.314 (0.746-2.314)	0.345
Capsular formation	1.289 (0.781-2.127)	0.321	1.031 (0.584-1.821)	0.916
Vein invasion	0.575 (0.337-0.981)	0.042	0.683 (0.382-1.221)	0.198
Notch3	1.858 (1.264-2.731)	0.002	1.578(1.036-2.402)	0.034

*: HR, Hazards ratios; CI: confidence interval.

HCC, and could be regarded as a candidate for potential therapeutic targets for this malignancy.

In conclusion, in this study, we identified Notch3 as ranked at the top of overexpressed Notch pathway-related genes on datasets from the Oncomine database. We validated an aberrantly increased Notch3 expression in HCC, and found an association between its expression with more progressive traits and short survival in HCC. In addition, we also confirmed Notch3 to be an independent prognostic factor for HCC. Such knowledge should also provide novel ideas to develop better targeted therapeutic strategies that could significantly enhance HCC treatment and patient survival in the future.

References

- Nordenstedt H, White DL, El-Serag HB. The changing pattern of epidemiology in hepatocellular carcinoma. *Dig Liver Dis.* 2010; 42(Suppl 3):S206-S214.
- Dang TP. Notch, apoptosis and cancer. *Adv Exp Med Biol.* 2012; 727:199-209.
- Ambler CA, Maatta A. Epidermal stem cells: Location, potential and contribution to cancer. *J Pathol.* 2009; 217:206-216.
- Purow B. Notch inhibition as a promising new approach to cancer therapy. *Adv Exp Med Biol.* 2012; 727:305-319.
- Gramantieri L, Giovannini C, Lanzi A, Chieco P, Ravaioli M, Venturi A, Grazi GL, Bolondi L. Aberrant Notch3 and Notch4 expression in human hepatocellular carcinoma. *Liver Int.* 2007; 27:997-1007.
- Gao J, Song Z, Chen Y, Xia L, Wang J, Fan R, Du R, Zhang F, Hong L, Song J, Zou X, Xu H, Zheng G, Liu J, Fan D. Deregulated expression of Notch receptors in human hepatocellular carcinoma. *Dig Liver Dis.* 2008; 40:114-121.
- Rhodes DR, Kalyana-Sundaram S, Mahavisno V, Varambally R, Yu J, Briggs BB, Barrette TR, Anstet MJ, Kincead-Beal C, Kulkarni P, Varambally S, Ghosh D, Chinnaiyan AM. Oncomine 3.0: Genes, pathways, and networks in a collection of 18,000 cancer gene expression profiles. *Neoplasia.* 2007; 9:166-180.
- Shah SA, Cleary SP, Wei AC, Yang I, Taylor BR, Hemming AW, Langer B, Grant DR, Greig PD, Gallinger S. Recurrence after liver resection for hepatocellular carcinoma: risk factors, treatment, and outcomes. *Surgery.* 2007; 141:330-339.
- Rahman MT, Nakayama K, Rahman M, Katagiri H, Katagiri A, Ishibashi T, Ishikawa M, Iida K, Nakayama S, Otsuki Y, Miyazaki K. Notch3 overexpression as potential therapeutic target in advanced stage chemoresistant ovarian cancer. *Am J Clin Pathol.* 2012; 138:535-544.
- Zhao C, Chen Y, Zhang W, Zhang J, Xu Y, Li W, Chen S, Deng A. Expression of protein tyrosine kinase 6 (PTK6) in nonsmall cell lung cancer and their clinical and prognostic significance. *Onco Targets Ther.* 2013; 6:183-188.
- Nickoloff BJ, Osborne BA, Miele L. Notch signaling as a therapeutic target in cancer: A new approach to the development of cell fate modifying agents. *Oncogene.* 2003; 22:6598-6608.
- Serafini V, Persano L, Moserle L, *et al.* Notch3 signalling promotes tumour growth in colorectal cancer. *J Pathol.* 2011; 224:448-460.
- Yamaguchi N, Oyama T, Ito E, *et al.* NOTCH3 signaling pathway plays crucial roles in the proliferation of ErbB2-negative human breast cancer cells. *Cancer Res.* 2008; 68:1881-1888.
- Haruki N, Kawaguchi KS, Eichenberger S, Massion PP, Olson S, Gonzalez A, Carbone DP, Dang TP. Dominant-negative Notch3 receptor inhibits mitogen-activated protein kinase pathway and the growth of human lung cancers. *Cancer Res.* 2005; 65:3555-3561.
- Giovannini C, Lacchini M, Gramantieri L, Chieco P, Bolondi L. Notch3 intracellular domain accumulates in HepG2 cell line. *Anticancer Res.* 2006; 26:2123-2127.
- Giovannini C, Gramantieri L, Minguzzi M, Fornari F, Chieco P, Grazi GL, Bolondi L. CDKN1C/P57 is regulated by the Notch target gene *Hes1* and induces senescence in human hepatocellular carcinoma. *Am J Pathol.* 2012; 181:413-422.
- Giovannini C, Gramantieri L, Chieco P, Minguzzi M, Lago F, Pianetti S, Ramazzotti E, Marcu KB, Bolondi L. Selective ablation of Notch3 in HCC enhances doxorubicin's death promoting effect by a p53 dependent mechanism. *J Hepatol.* 2009; 50:969-979.

(Received May 6, 2013; Revised June 2, 2013; Accepted June 9, 2013)

Perspectives on human clinical trials of therapies using iPS cells in Japan: Reaching the forefront of stem-cell therapies

Peipei Song¹, Yoshinori Inagaki^{1,2,*}, Yasuhiko Sugawara¹, Norihiro Kokudo¹

¹Hepato-Biliary-Pancreatic Surgery Division, Department of Surgery, Graduate School of Medicine, The University of Tokyo, Tokyo, Japan;

²Laboratory of Microbiology, Graduate School of Pharmaceutical Sciences, The University of Tokyo, Tokyo, Japan.

Summary

A research project involving sheets of retinal pigment epithelium constructed from iPS cells derived from patients with age-related maculopathy is one step closer to being approved for clinical trials by the Japanese Government. Now is the time to make therapies using iPS cells clinically available.

Keywords: Induced pluripotent stem cell, age-related maculopathy, clinical trial

In 2013, a therapy using induced pluripotent stem (iPS) cells progressed to the clinical trial stage in Japan. On February 28th, RIKEN and the Foundation for Biomedical Research and Innovation jointly applied for approval of a research project involving clinical trials of sheets of retinal pigment epithelium constructed from iPS cells derived from patients with age-related maculopathy. This project was reviewed by the committee of Health Science Council to review policies on clinical research involving human stem cells with an emphasis on safety and especially tumorigenesis. On June 26th, the Committee decided to approve this project with some provisos. If the Ministry of Health, Labor, and Welfare officially approves the project based on a decision by another committee on scientific technology, then the world's first clinical trial using material from patient-derived iPS cells may be conducted in the summer of 2014. This will bring Japan to the forefront of efforts to introduce a pioneering biomedical technology and benefit stem-cell therapies.

iPS cells were first generated from mouse mature skin cells by Prof. Shinya Yamanaka (Nobel laureate in 2012) of Kyoto University in Japan, and these cells have been used in basic studies worldwide. iPS cells have the ability to differentiate into various types of

somatic cells and can be used to construct functional cell sheets and tissue for transplantation. *In vivo* studies have raised concerns about the usage of iPS cells in that they may induce the formation of tumors, but improved gene transfer method has helped to increase the safety of this technology. In August 2012, Prof. Yamanaka proposed establishment of a standard assay system and cell bank of iPS cells (1). The RIKEN Bio-Resource Center began providing established iPS cells to non-profit researchers. This system helps to enhance the quality and speed of iPS cell research. Basic studies have been performed using the cell bank system. The cell bank system is a promising way to store and maintain iPS cells derived from individual patients.

A large program was launched in Japan starting in 2012 to support several long-term projects to facilitate the clinical use of iPS cell therapies (Table 1); the program is budgeted tens of millions of dollars every year. One of these long-term projects is studying age-related maculopathy, and the project is the first to apply to the government for approval of clinical trials. Age-related maculopathy is the leading cause of permanent blindness in the elderly and affects the central area of the retina, which is essential for central and color vision (2,3). The current treatment, administration of an anti-vascular endothelial growth factor receptor drug such as bevacizumab, alleviates symptoms but does not cure the condition. Retinitis pigmentosa is the main cause of blindness or visual impairment, so replacement of diseased retinal cells should be an effective treatment. Over the past few years, a research group led by Dr. Masayo Takahashi of the Center for Developmental

*Address correspondence to:

Dr. Yoshinori Inagaki, Hepato-Biliary-Pancreatic Surgery Division, Department of Surgery, Graduate School of Medicine, The University of Tokyo, 7-3-1 Hongo, Bunkyo-ku, Tokyo 113-8655, Japan.
E-mail: yinagaki-tky@umin.ac.jp

Table 1. Main projects to implement regenerative medicine in Japan

Research topic	Institute/facility responsible
Development of therapies for age-related maculopathy by transplantation of retinal pigment epithelial cells established from iPS cells	RIKEN
Regeneration of the knee meniscus using synovial stem cells	Tokyo Medical and Dental University
Achieving regenerative medicine for the corneal endothelium by transplantation of cultured human corneal endothelial cells	Kyoto Prefectural University of Medicine
Development of less invasive liver regeneration therapies using cultured human bone marrow cells	Yamaguchi University
Development of regenerative therapies for the cornea using iPS cells	Osaka University
Establishment of therapies for serious heart failure by transplantation of regenerated heart myocytes derived from autologous iPS cells	Keio University
Clinical study of drugs derived from human embryonic stem cells to treat congenital metabolic disorders with severe hyperammonemia	National Center for Child Health and Development Kyoto University
Development of stem cell transplantation therapies for Parkinson's disease	

Biology of RIKEN has developed a novel method to construct retinal cells from human iPS cells (4). The group's most recent study examined the Ca²⁺ response and electrophysiological properties of developing and grafted rods and it established a way to evaluate the activation of transplanted rods (5). The researchers concluded that grafted cells function as rods and that rods derived from iPS cells *in vitro* may provide a renewable source for cell replacement therapy. The long-term project on age-related maculopathy is seeking to conduct clinical trials on sheets of retinal pigment epithelium constructed from iPS cells derived from patients with the condition. This project should offer insights into iPS cells and their clinical use in the near future.

Another project to facilitate the clinical use of iPS cell therapies involves the development of therapies for Parkinson's disease with the support of the Japanese Government. A research group led by Prof. Jun Takahashi of Kyoto University showed that dopaminergic neurons differentiated from human iPS cells under feeder-free and serum-free conditions and that these neurons survived in a primate model of Parkinson's disease (6). Prof. Takahashi expressed his intent to apply for approval of a clinical trial of a novel therapy for Parkinson's disease involving transplantation of iPS cell-derived dopaminergic neurons in 2014, if all goes smoothly.

Advances in stem-cell therapies have been early awaited worldwide for several decades now. The large program launched in 2012 in Japan with the support of the Japanese Government will play a key role in facilitating the clinical use of iPS cell therapies. Currently, the Ministry of Health, Labor, and Welfare of

Japan is considering approval of clinical trials of sheets of retinal pigment epithelium constructed from iPS cells derived from patients with age-related maculopathy, and the Ministry's approval of clinical trials of a therapy for Parkinson's disease using iPS cell-derived neurons will soon be sought. "Now is the time to make therapies using iPS cells clinically available."

References

1. Cyranoski D. Stem-cell pioneer banks on future therapies. *Nature*. 2012; 488:139.
2. Jin ZB, Okamoto S, Mandai M, Takahashi M. Induced pluripotent stem cells for retinal degenerative diseases: A new perspective on the challenges. *J Genet*. 2009; 88:417-424.
3. Girmens JF, Sahel JA, Marazova K. Dry age-related macular degeneration: A currently unmet clinical need. *Intractable Rare Dis Res*. 2012; 1:103-114.
4. Osakada F, Takahashi M. Neural induction and patterning in Mammalian pluripotent stem cells. *CNS Neurol Disord Drug Targets*. 2011; 10:419-432.
5. Homma K, Okamoto S, Mandai M, Gotoh N, Rajasimha HK, Chang YS, Chen S, Li W, Cogliati T, Swaroop A, Takahashi M. Developing rods transplanted into the degenerating retina of crx-knockout mice exhibit neural activity similar to native photoreceptors. *Stem Cells*. 2013; 31:1149-1159.
6. Kikuchi T, Morizane A, Doi D, Onoe H, Hayashi T, Kawasaki T, Saiki H, Miyamoto S, Takahashi J. Survival of human induced pluripotent stem cell-derived midbrain dopaminergic neurons in the brain of a primate model of Parkinson's disease. *J Parkinson's Disease*. 2011; 1:395-412.

(Received June 27, 2013; Accepted June 29, 2013)

Guide for Authors

1. Scope of Articles

BioScience Trends is an international peer-reviewed journal. BioScience Trends devotes to publishing the latest and most exciting advances in scientific research. Articles cover fields of life science such as biochemistry, molecular biology, clinical research, public health, medical care system, and social science in order to encourage cooperation and exchange among scientists and clinical researchers.

2. Submission Types

Original Articles should be well-documented, novel, and significant to the field as a whole. An Original Article should be arranged into the following sections: Title page, Abstract, Introduction, Materials and Methods, Results, Discussion, Acknowledgments, and References. Original articles should not exceed 5,000 words in length (excluding references) and should be limited to a maximum of 50 references. Articles may contain a maximum of 10 figures and/or tables.

Brief Reports definitively documenting either experimental results or informative clinical observations will be considered for publication in this category. Brief Reports are not intended for publication of incomplete or preliminary findings. Brief Reports should not exceed 3,000 words in length (excluding references) and should be limited to a maximum of 4 figures and/or tables and 30 references. A Brief Report contains the same sections as an Original Article, but the Results and Discussion sections should be combined.

Reviews should present a full and up-to-date account of recent developments within an area of research. Normally, reviews should not exceed 8,000 words in length (excluding references) and should be limited to a maximum of 100 references. Mini reviews are also accepted.

Policy Forum articles discuss research and policy issues in areas related to life science such as public health, the medical care system, and social science and may address governmental issues at district, national, and international levels of discourse. Policy Forum articles should not exceed 2,000 words in length (excluding references).

Case Reports should be detailed reports of the symptoms, signs, diagnosis, treatment, and follow-up of an individual patient. Case reports may contain a demographic profile of the patient but usually describe an unusual or novel occurrence. Unreported or unusual

side effects or adverse interactions involving medications will also be considered. Case Reports should not exceed 3,000 words in length (excluding references).

News articles should report the latest events in health sciences and medical research from around the world. News should not exceed 500 words in length.

Letters should present considered opinions in response to articles published in BioScience Trends in the last 6 months or issues of general interest. Letters should not exceed 800 words in length and may contain a maximum of 10 references.

3. Editorial Policies

Ethics: BioScience Trends requires that authors of reports of investigations in humans or animals indicate that those studies were formally approved by a relevant ethics committee or review board.

Conflict of Interest: All authors are required to disclose any actual or potential conflict of interest including financial interests or relationships with other people or organizations that might raise questions of bias in the work reported. If no conflict of interest exists for each author, please state "There is no conflict of interest to disclose".

Submission Declaration: When a manuscript is considered for submission to BioScience Trends, the authors should confirm that 1) no part of this manuscript is currently under consideration for publication elsewhere; 2) this manuscript does not contain the same information in whole or in part as manuscripts that have been published, accepted, or are under review elsewhere, except in the form of an abstract, a letter to the editor, or part of a published lecture or academic thesis; 3) authorization for publication has been obtained from the authors' employer or institution; and 4) all contributing authors have agreed to submit this manuscript.

Cover Letter: The manuscript must be accompanied by a cover letter signed by the corresponding author on behalf of all authors. The letter should indicate the basic findings of the work and their significance. The letter should also include a statement affirming that all authors concur with the submission and that the material submitted for publication has not been published previously or is not under consideration for publication elsewhere. The cover letter should be submitted in PDF format. For example of Cover Letter, please visit <http://www.biosciencetrends.com/downcentre.php> (Download Centre).

Copyright: A signed JOURNAL PUBLISHING AGREEMENT (JPA) form must be provided by post, fax, or as a scanned file before acceptance of the article. Only forms with a hand-written signature are accepted. This copyright will ensure the widest possible dissemination of information. A form facilitating transfer of copyright can be downloaded by clicking the

appropriate link and can be returned to the e-mail address or fax number noted on the form (Please visit [Download Centre](#)). Please note that your manuscript will not proceed to the next step in publication until the JPA Form is received. In addition, if excerpts from other copyrighted works are included, the author(s) must obtain written permission from the copyright owners and credit the source(s) in the article.

Suggested Reviewers: A list of up to 3 reviewers who are qualified to assess the scientific merit of the study is welcomed. Reviewer information including names, affiliations, addresses, and e-mail should be provided at the same time the manuscript is submitted online. Please do not suggest reviewers with known conflicts of interest, including participants or anyone with a stake in the proposed research; anyone from the same institution; former students, advisors, or research collaborators (within the last three years); or close personal contacts. Please note that the Editor-in-Chief may accept one or more of the proposed reviewers or may request a review by other qualified persons.

Language Editing: Manuscripts prepared by authors whose native language is not English should have their work proofread by a native English speaker before submission. If not, this might delay the publication of your manuscript in BioScience Trends.

The Editing Support Organization can provide English proofreading, Japanese-English translation, and Chinese-English translation services to authors who want to publish in BioScience Trends and need assistance before submitting a manuscript. Authors can visit this organization directly at <http://www.iacmhr.com/iac-eso/support.php?lang=en>. IAC-ESO was established to facilitate manuscript preparation by researchers whose native language is not English and to help edit works intended for international academic journals.

4. Manuscript Preparation

Manuscripts should be written in clear, grammatically correct English and submitted as a Microsoft Word file in a single-column format. Manuscripts must be paginated and typed in 12-point Times New Roman font with 24-point line spacing. Please do not embed figures in the text. Abbreviations should be used as little as possible and should be explained at first mention unless the term is a well-known abbreviation (e.g. DNA). Single words should not be abbreviated.

Title Page: The title page must include 1) the title of the paper (Please note the title should be short, informative, and contain the major key words); 2) full name(s) and affiliation(s) of the author(s), 3) abbreviated names of the author(s), 4) full name, mailing address, telephone/fax numbers, and e-mail address of the corresponding author; and 5) conflicts of interest (if you have an actual or potential conflict of interest to disclose, it must be included as a footnote on the title page of the manuscript; if no conflict of

interest exists for each author, please state "There is no conflict of interest to disclose"). Please visit [Download Centre](#) and refer to the title page of the manuscript sample.

Abstract: The abstract should briefly state the purpose of the study, methods, main findings, and conclusions. For article types including Original Article, Brief Report, Review, Policy Forum, and Case Report, a one-paragraph abstract consisting of no more than 250 words must be included in the manuscript. For News and Letters, a brief summary of main content in 150 words or fewer should be included in the manuscript. Abbreviations must be kept to a minimum and non-standard abbreviations explained in brackets at first mention. References should be avoided in the abstract. Key words or phrases that do not occur in the title should be included in the Abstract page.

Introduction: The introduction should be a concise statement of the basis for the study and its scientific context.

Materials and Methods: The description should be brief but with sufficient detail to enable others to reproduce the experiments. Procedures that have been published previously should not be described in detail but appropriate references should simply be cited. Only new and significant modifications of previously published procedures require complete description. Names of products and manufacturers with their locations (city and state/country) should be given and sources of animals and cell lines should always be indicated. All clinical investigations must have been conducted in accordance with Declaration of Helsinki principles. All human and animal studies must have been approved by the appropriate institutional review board(s) and a specific declaration of approval must be made within this section.

Results: The description of the experimental results should be succinct but in sufficient detail to allow the experiments to be analyzed and interpreted by an independent reader. If necessary, subheadings may be used for an orderly presentation. All figures and tables must be referred to in the text.

Discussion: The data should be interpreted concisely without repeating material already presented in the Results section. Speculation is permissible, but it must be well-founded, and discussion of the wider implications of the findings is encouraged. Conclusions derived from the study should be included in this section.

Acknowledgments: All funding sources should be credited in the Acknowledgments section. In addition, people who contributed to the work but who do not meet the criteria for authors should be listed along with their contributions.

References: References should be numbered in the order in which they appear in the text. Citing of unpublished results, personal communications, conference abstracts, and theses in the reference list is not recommended but these sources may be mentioned in the text. In the reference list,

cite the names of all authors when there are fifteen or fewer authors; if there are sixteen or more authors, list the first three followed by *et al.* Names of journals should be abbreviated in the style used in PubMed. Authors are responsible for the accuracy of the references. Examples are given below:

Example 1 (Sample journal reference): Inagaki Y, Tang W, Zhang L, Du GH, Xu WF, Kokudo N. Novel aminopeptidase N (APN/CD13) inhibitor 24F can suppress invasion of hepatocellular carcinoma cells as well as angiogenesis. *Biosci Trends*. 2010; 4:56-60.

Example 2 (Sample journal reference with more than 15 authors): Darby S, Hill D, Auvinen A, *et al.* Radon in homes and risk of lung cancer: Collaborative analysis of individual data from 13 European case-control studies. *BMJ*. 2005; 330:223.

Example 3 (Sample book reference): Shalev AY. Post-traumatic stress disorder: diagnosis, history and life course. In: Post-traumatic Stress Disorder, Diagnosis, Management and Treatment (Nutt DJ, Davidson JR, Zohar J, eds.). Martin Dunitz, London, UK, 2000; pp. 1-15.

Example 4 (Sample web page reference): Ministry of Health, Labour and Welfare of Japan. Dietary reference intakes for Japanese. <http://www.mhlw.go.jp/houdou/2004/11/h1122-2a.html> (accessed June 14, 2010).

Tables: All tables should be prepared in Microsoft Word or Excel and should be arranged at the end of the manuscript after the References section. Please note that tables should not be image format. All tables should have a concise title and should be numbered consecutively with Arabic numerals. If necessary, additional information should be given below the table.

Figure Legend: The figure legend should be typed on a separate page of the main manuscript and should include a short title and explanation. The legend should be concise but comprehensive and should be understood without referring to the text. Symbols used in figures must be explained.

Figure Preparation: All figures should be clear and cited in numerical order in the text. Figures must fit a one- or two-column format on the journal page: 8.3 cm (3.3 in.) wide for a single column, 17.3 cm (6.8 in.) wide for a double column; maximum height: 24.0 cm (9.5 in.). Please make sure that the symbols and numbers appeared in the figures should be clear. Please make sure that artwork files are in an acceptable format (TIFF or JPEG) at minimum resolution (600 dpi for illustrations, graphs, and annotated artwork, and 300 dpi for micrographs and photographs). Please provide all figures as separate files. Please note that low-resolution images are one of the leading causes of article resubmission and schedule delays. All color figures will be reproduced in full color in the online edition of the journal at no cost to authors.

Units and Symbols: Units and symbols

conforming to the International System of Units (SI) should be used for physicochemical quantities. Solidus notation (*e.g.* mg/kg, mg/mL, mol/mm²/min) should be used. Please refer to the SI Guide www.bipm.org/en/si/ for standard units.

Supplemental data: Supplemental data might be useful for supporting and enhancing your scientific research and BioScience Trends accepts the submission of these materials which will be only published online alongside the electronic version of your article. Supplemental files (figures, tables, and other text materials) should be prepared according to the above guidelines, numbered in Arabic numerals (*e.g.*, Figure S1, Figure S2, and Table S1, Table S2) and referred to in the text. All figures and tables should have titles and legends. All figure legends, tables and supplemental text materials should be placed at the end of the paper. Please note all of these supplemental data should be provided at the time of initial submission and note that the editors reserve the right to limit the size and length of Supplemental Data.

5. Submission Checklist

The Submission Checklist will be useful during the final checking of a manuscript prior to sending it to BioScience Trends for review. Please visit [Download Centre](#) and download the Submission Checklist file.

6. Online Submission

Manuscripts should be submitted to BioScience Trends online at <http://www.biosciencetrends.com>. The manuscript file should be smaller than 5 MB in size. If for any reason you are unable to submit a file online, please contact the Editorial Office by e-mail at office@biosciencetrends.com.

7. Accepted Manuscripts

Proofs: Galley proofs in PDF format will be sent to the corresponding author via e-mail. Corrections must be returned to the editor (proof-editing@biosciencetrends.com) within 3 working days.

Offprints: Authors will be provided with electronic offprints of their article. Paper offprints can be ordered at prices quoted on the order form that accompanies the proofs.

Page Charge: Page charges will be levied on all manuscripts accepted for publication in BioScience Trends (\$140 per page for black white pages; \$340 per page for color pages). Under exceptional circumstances, the author(s) may apply to the editorial office for a waiver of the publication charges at the time of submission.

(Revised February 2013)

Editorial and Head Office:

Pearl City Koishikawa 603
2-4-5 Kasuga, Bunkyo-ku
Tokyo 112-0003 Japan
Tel: +81-3-5840-8764
Fax: +81-3-5840-8765
E-mail: office@biosciencetrends.com

JOURNAL PUBLISHING AGREEMENT (JPA)

Manuscript No.:

Title:

Corresponding Author:

The International Advancement Center for Medicine & Health Research Co., Ltd. (IACMHR Co., Ltd.) is pleased to accept the above article for publication in BioScience Trends. The International Research and Cooperation Association for Bio & Socio-Sciences Advancement (IRCA-BSSA) reserves all rights to the published article. Your written acceptance of this JOURNAL PUBLISHING AGREEMENT is required before the article can be published. Please read this form carefully and sign it if you agree to its terms. The signed JOURNAL PUBLISHING AGREEMENT should be sent to the BioScience Trends office (Pearl City Koishikawa 603, 2-4-5 Kasuga, Bunkyo-ku, Tokyo 112-0003, Japan; E-mail: office@biosciencetrends.com; Tel: +81-3-5840-8764; Fax: +81-3-5840-8765).

1. Authorship Criteria

As the corresponding author, I certify on behalf of all of the authors that:

- 1) The article is an original work and does not involve fraud, fabrication, or plagiarism.
- 2) The article has not been published previously and is not currently under consideration for publication elsewhere. If accepted by BioScience Trends, the article will not be submitted for publication to any other journal.
- 3) The article contains no libelous or other unlawful statements and does not contain any materials that infringes upon individual privacy or proprietary rights or any statutory copyright.
- 4) I have obtained written permission from copyright owners for any excerpts from copyrighted works that are included and have credited the sources in my article.
- 5) All authors have made significant contributions to the study including the conception and design of this work, the analysis of the data, and the writing of the manuscript.
- 6) All authors have reviewed this manuscript and take responsibility for its content and approve its publication.
- 7) I have informed all of the authors of the terms of this publishing agreement and I am signing on their behalf as their agent.

2. Copyright Transfer Agreement

I hereby assign and transfer to IACMHR Co., Ltd. all exclusive rights of copyright ownership to the above work in the journal BioScience Trends, including but not limited to the right 1) to publish, republish, derivate, distribute, transmit, sell, and otherwise use the work and other related material worldwide, in whole or in part, in all languages, in electronic, printed, or any other forms of media now known or hereafter developed and the right 2) to authorize or license third parties to do any of the above.

I understand that these exclusive rights will become the property of IACMHR Co., Ltd., from the date the article is accepted for publication in the journal BioScience Trends. I also understand that IACMHR Co., Ltd. as a copyright owner has sole authority to license and permit reproductions of the article.

I understand that except for copyright, other proprietary rights related to the Work (e.g. patent or other rights to any process or procedure) shall be retained by the authors. To reproduce any text, figures, tables, or illustrations from this Work in future works of their own, the authors must obtain written permission from IACMHR Co., Ltd.; such permission cannot be unreasonably withheld by IACMHR Co., Ltd.

3. Conflict of Interest Disclosure

I confirm that all funding sources supporting the work and all institutions or people who contributed to the work but who do not meet the criteria for authors are acknowledged. I also confirm that all commercial affiliations, stock ownership, equity interests, or patent-licensing arrangements that could be considered to pose a financial conflict of interest in connection with the article have been disclosed.

Corresponding Author's Name (Signature):

Date:

